Applications of the Phase Separation of Intrinsically Disordered Proteins in the Design of Intravenous Hemostatic Agents

Inauguraldissertation zur Erlangung der Würde eines Doktors der Philosophie vorgelegt der Philosophisch-Naturwissenschaftlichen Fakultät der Universität Basel

Von

Ivan Urosev

Basel, 2021

Originaldokument gespeichert auf dem Dokumentenserver der Universität Basel
edoc.unibas.ch

Genehmigt von der Philosophisch-Naturwissenschaftlichen Fakultät auf Antrag von

Prof. Dr. Michael Nash

Prof. Dr. Dennis Gillingham

Prof. Dr. Alexander Büll

Basel, 22.06.21

Prof. Dr. Marcel Mayor, Dean

Declaration

"I hereby declare that this doctoral dissertation "*Applications of the Phase Separation of Intrinsically Disordered Proteins in the Design of Intravenous Hemostatic Agents*" has been completed exclusively with the assistance mentioned herein and that it has not been submitted to any other university or to any other faculty at the University of Basel.

Ivan Urosev, 24.05.21, Basel

Acknowledgements

I would like to begin by thanking my supervisor, Dr. Michael Nash, for his support throughout my PhD, for his managerial style, which succeeds at being encouraging without being overbearing, and for his willingness to invest the energy in finding a project that suited me well. I would also like to thank the other members of my committee, Dr. Dennis Gillingham and Dr. Alexander Büll, for agreeing to review my thesis, and for offering their suggestions for improving it.

I would like to thank all of the members of the Nash Lab, past and present, whose scientific passion and excellence encouraged me to try to do the best work that I could as well, and whose friendly and jovial natures made doing that work every day so pleasant. Special thanks are conveyed to Dr. Duy Tien Ta for being my guide into the fascinating world of molecular biology, to Dr. Rosario Vanella, for his wise counsel in the realms of science, running, and life, and to Mariana De Sa Cardoso, for being a faithful friend and desk mate since the beginning.

Thanks as well to all of the friends that I have made in my time in Basel, who helped to make this city and this country feel like a second home to me, and who made it much easier to stay positive in my work. Thanks in particular to Miguel Veloso, for the many late nights of lively philosophical discussion during our Terrasse Talks®, to Jaime de Santiago de Chile, for always being willing to lend an understanding ear, and for his appreciation of the art of banter, to Rocio Castellanos Rueda, for great evenings spent sharing a rope and some conversation, to Vittoria Chimisso, for being the nonna I never had, to Giacomo Persiani, for bringing me to new heights, to Adrian Spiess, for brightening up the neighbourhood, to Yoshbert Hund, for being a good boy, and to Claudio Zambaldo, for encouraging my development as a scientist. Thanks as well to some old friends, especially Shawn Brar, Radu Suciu, Shaan Gupta, Ben Wilson, Shyamie Gopalan, and Lili Aslostovar, who have made the effort to stay close despite the large geographical distances separating us. I hope that is an effort that we will not give up on in the years to come.

I want now to give my thanks and love to my girlfriend, Shanta Baumberger, whose belief in me has encouraged me to try to be the person that she thinks I am. Thank you for helping me to grow into that person.

Thanks as well to my brothers Sebastian and Alexey Greer, and Luka Franceško, for always welcoming me home, wherever that may be.

And finally, thanks to my parents, my dad Stojan Urosev, my step-dad Kevin Greer, and my mom Vesna Urosev, who did all of the hard work of emigrating, or simply working day-in and day-out without complaint, so that I could have the sort of life where I could fail many times and still have the chance to pursue my goals. I'm sure I'll never be able to repay you for the time and treasure that you invested in giving me this privilege, so I hope that I can live up to your example by trying to pay it forward instead.

Table of Contents

Summary

Liquid-liquid phase separation of biological macromolecules such as proteins, RNA, and DNA, is now understood to be a critical mechanism for the organization of cellular processes. The ubiquity of this phenomenon points to phase separating proteins as both potential tools and targets for the treatment of various disorders. Here, we describe the design and implementation of a particular type of phase separating, intrinsically disordered protein – an elastin-like polypeptide – as an intravenous hemostatic agent for the treatment of uncontrolled bleeding. A plurality of trauma deaths are caused by hemorrhagic shock, and there are currently limited interventions available for patients with non-compressible injuries. The current standard of care involves the transfusion of blood products, which is hampered by drawbacks such as short shelf-life, high cost, and the potential for viral transmission. Furthermore, the development of artificial intravenous hemostats is hampered by the need to achieve high specificity for blood clots at wound sites, in order to avoid the risk of off-target thrombosis. The hemostatic elastin-like polypeptides (hELPs) described in this work overcome these issues, to yield a hemostat that is specific, stable, and that can functionally improve the hemostatic properties of blood clots. The following chapters elucidate the rationale behind the development of hELPs, describe their design and effect on the biophysical properties of clots *in vitro*, and highlight their validation in a rat model of acute bleeding. **Chapter I** gives a general introduction on the concepts of biological phase separation, intrinsically disordered proteins, and elastin-like polypeptides, as well as on hemostasis and currently available hemostatic interventions. **Chapter II** takes a deeper look at the importance of the structure and mechanical properties of the fibrin networks that form the scaffold of blood clots, and how those characteristics affect hemostatic efficacy. **Chapter III** describes the design of hELPs and their effect on fibrin clots *in vitro*, highlighting in particular how the phase separation of hELPs is critical to their being able to improve the functionality of blood clots. **Chapter IV** explores alternative hELP designs, and describes the validation of hELPs in a rat model of acute bleeding. Altogether, the results outlined herein, in addition to indicating that hELPs are a hemostatic technology that could potentially be applied in the clinic, also provide a proof-of-concept for the use of phase separation of intrinsically disordered proteins as an intervention

in disorders which lead to substandard mechanical properties in other tissues and extra-cellular matrix components (e.g. cartilage, bone, etc.).

Chapter I: Introduction

Phase separation as an organizer of cellular biochemistry

The idea of the cell as the basic unit of life is a time-tested paradigm of biology. Cells were first observed in a piece of cork under a microscope by Robert Hooke in 1655, and cell theory – which states that all living things are composed of cells – was proposed by Schleiden and Schwann in 1838.[1] The elucidation of important structural features of cells occurred contemporaneously to the proposition of cell theory; indeed, the 19th century saw the discovery of various organelles including the nucleus (named in 1831), the mitochondria (discovered in 1857 by von Kolliker), the Golgi complex (discovered by Golgi in 1898), and the endoplasmic reticulum (observed by Garnier in 1897, who called it the ergastoplasm).[2–5] The production of the first commercial transmission electron microscope in 1939 paved the way for more detailed observations of the inner workings of the cell, and from these experiments researchers were able to cobble together a complete picture of the macroscopic features of the cell's microscopic world: the eukaryotic animal cell was a lipid membrane-bound entity, and within its interior cytoplasm existed smaller membrane-bound organelles that served to sequester the cell's various functions (e.g. protein synthesis, metabolism, energy production) in time and space, in much the same way that the organs of the body separate bodily functions.[6] Outside of these organelles cellular processes took place in the undefined milieu of the cytoplasm, wherein freely-distributed proteins, RNA, and small molecules would occasionally come into contact to facilitate some biochemical reaction.[7] This has been an enduring concept of cellular structure, so much so, that if a student passed through a high school or early year university biology course anytime in the past 50 years, this is the principle of intracellular organization that they are likely to have been taught. However, it may be another paradigm of biology that living systems defy simple explanations, and emerging research seems to indicate that there exists another phenomenon that could be as important to cellular organization as the lipid membrane: Liquid-liquid phase separation.

The challenge that eukaryotic cells must overcome in order to carry out the business of surviving, reproducing, and performing their functions in tissues, is that these processes

involve myriad biochemical reactions that may occur best at particular conditions of pH or ionic strength, require reactants to come together at the same point in time and space, and which need to occur at a rate that is sufficient for their intended purpose. One solution to this problem is the lipid membrane-bound organelle. Another solution, the ubiquity of which has only recently begun to be appreciated, is liquid-liquid phase separation. This process is so-called because it involves the formation of two or more liquid phases in one solution, as when droplets of oil are dispersed in water. In cells, liquid-liquid phase separation forms biomolecular condensates (BMCs; also called membrane-less organelles, MLOs), which consist of a coacervate phase comprised of proteins, RNA, or small molecules, suspended in a solution (i.e. the cytoplasm, or an extra-cellular fluid) that is locally depleted of those same components.

The earliest observed and likely most well-known intracellular BMC is the nucleolus, which is a protein granule that is involved in ribosomal biogenesis and control of transcription in eukaryotic cells.[8] Observations of the variability in size, shape, and indeed presence of nucleoli in cells at different stages of the cell cycle, led to the understanding of this sub-nuclear structure as a coalescence of proteins and rRNA that lacked an organizing membrane; it was a structure that was dynamic in nature. However, it would take more than 160 years from the time that nucleoli were first discovered until the principle that drives their coalescence could be explained.[9,10] In the meantime, several assemblies with similar properties ("colloidal bodies") were observed in eukaryotic cells, including Cajal bodies and PML nuclear bodies in the nucleus, and stress granules and germline granules in the cytoplasm.[11,12] Early attempts at delineating a mechanism for the formation of these structures centered on known features of cellular biochemistry, such as local synthesis, active transport, or anchoring of proteins to cellular structures, none of which could adequately explain their properties.[13] In fact, a satisfactory answer to the question of how BMCs are formed would not be forthcoming until just over a decade before the time of this writing, and it would come from a study into cell lineage determination in the roundworm, *C. Elegans.*

In 2009, Brangwynne and colleagues were investigating the asymmetric localization of protein-RNA coacervates (known as P granules) in dividing cells of the *C. Elegans* embryo. Initially P granules are distributed uniformly in the unpolarized single-cell embryo, but following symmetry breaking of the embryo these BMCs localize to the posterior portion of the cell, ultimately leading to the formation of two distinct daughter cells: a somatic cell

lacking P granules, and a germ-line progenitor cell rich in P granules. At the time, the proposed mechanism for this asymmetric distribution was based on cytoplasmic flow and the subsequent degradation of P granules in the anterior portion of the anisotropic embryo. Brangwynne et al. used 3D particle tracking of fluorescently-tagged P granule components to prove that there was a negligible net flux of these molecules across the anterior-posterior axis of the cell, indicating that cytoplasmic flow was not an adequate explanation for the posterior localization of these BMCs. Instead, the researchers were able to show that P granules condense spontaneously from non-aggregated components in the cytoplasm, and they proposed that the threshold concentration for condensation was lowered in the posterior portion of the embryo. Furthermore, they studied the material properties of P granules, and found that they flowed off of nuclei, dripped, and that two granules would fuse together when they came into contact, all of which are prototypical behaviours of liquids. This led the researchers to propose the following mechanism for P granule localization, based on the concept of liquid-liquid phase separation (which was already well-known in the field of polymer chemistry): the differential distribution of proteins that promote the aggregation or degradation of P granules in the anterior and posterior portions of the embryo serve to respectively raise and lower the "dew point" of P granules, leading to their dissolution in one cell region and condensation in the other.[14]

In the years since this discovery, several other BMCs such as stress granules, DNA damage repair sites, and indeed, the nucleolus, were all confirmed to be formed by liquid-liquid phase separation.[11,12,15] This mechanism of organizing biochemical reactions seemed to provide several advantages for cells, insomuch as it allowed for the close association of reaction components, while also allowing for rapid exchange of these components with the surrounding cellular environment as needed. Cells seem to be making good use of the utility of liquid-liquid phase separation, as the phenomenon has now been implicated in diverse processes such as localized actin polymerization, sequestration of certain factors (e.g. signalling factors) in order to prevent off-target effects, regulation of gene expression, and RNA processing.[16–18] Furthermore, aberrant liquid-liquid phase separation is beginning to be understood as a key driver of the development of certain pathologies, particularly in relation to neurodegenerative diseases and ageing.[19,20] For example, the amyloid lateral sclerosis (ALS) associated protein FUS is known to form stress granules through liquid-liquid phase separation; over time, these stress granules can lose their ability to demix and instead form

insoluble aggregates (i.e. amyloids) that have deleterious effects on cells and tissues. A compelling piece of evidence for this theory of coacervate-related disease development, comes from the fact that ALS patients were found to have mutations in their FUS genes which promoted this aberrant aggregation.[21]

In summation, it has become clear that liquid-liquid phase separation plays a central role in the organization of intracellular biochemistry, both in the context of regular cellular functioning and in the development of pathologies related to protein aggregation. While the ubiquity of this phenomenon in cell biology has come to be appreciated in the last decade, much work remains to be done in understanding the functions of the myriad biomolecular condensates present within the cell. Critically, if we are to be able to utilize this property of biological macromolecules for practical applications, or to intervene effectively in the development of devastating neurological and age-related diseases, we will need a thorough understanding of the mechanisms that regulate the formation of BMCs.

Mechanisms regulating biological phase separation

Unlike phase separation of synthetic polymers in solution, phase separation in living system is not governed entirely by equilibrium thermodynamics, as cells actively consume energy to create non-equilibrium states.[22] Adenosine triphosphate (ATP) is a common energy "currency" of the cell, and its turnover can lead to the dissolution or formation of BMCs, like those formed by the Dead-Box ATPase DDX4.[23] Furthermore, kinetically trapped condensates can be formed when the rate of recruitment of biomolecules to coacervates exceeds the rate of coacervate dissolution. For example, the P granule associated protein MEX-5 has been shown to have variable rates of diffusivity depending on its phosphorylation mediated interaction with low and high diffusivity complexes; in this way, protein concentration gradients can be created that promote MEX-5 aggregation in particular regions of the cell.[24] Biological phase separation is therefore a complex non-equilibrium process, that cannot be explained entirely by equilibrium-based models that often suffice for synthetic polymer systems. However, relaxation towards equilibrium does play a significant role in LLPS in cells; that is, coacervates will tend to form when their aggregation represents the lowest energy state of a particular system, as determined by enthalpic and entropic contributions. In general, the entropy of a distributed solution is greater than that of a densely packed

aggregate, so the loss of entropy that occurs with phase separation can be counterbalanced by enthalpically favourable interactions between coacervating partners. A caveat should be made on this point, however: studies of synthetic polymers have established that the mixing entropy for polymers is less than that for small molecules, due to the connectivity of individual polymer subunits; as such, polymeric solutions are more likely to exhibit phase transition behaviour. The same holds true in a biological context, and therefore BMCs tend to be formed from biopolymers such as proteins, RNA, and DNA.[25]

The majority of BMCs are highly multicomponent systems, comprised of as many as dozens to hundreds of different proteins, as well as RNA or DNA; in the field of phase separation such systems are referred to as complex coacervates.[26] Simple coacervates, on the other hand, are bulk aggregates of a single species and are more commonly observed in phase separating synthetic polymers; there are however, certain proteins that aggregate in this fashion, particularly in cases of the self-assembly of extracellular matrix (ECM) components such as tropoelastin.[27] Aggregation of biopolymers is promoted by non-covalent interactions such as electrostatic interactions, dipole-dipole interactions, or π-π stacking between aromatic residues.[28] These are in turn promoted by structural features common to phase separating biopolymers, such as multivalency or the presence of intrinsically disordered regions (IDRs).[29] The following subsections will explore how each of these concepts contribute to regulating phase separation of biopolymers in greater detail.

Multivalency

The phase separation of biopolymers can be driven by relatively weak non-covalent interactions; in order to overcome the effects of mixing entropy, coacervating proteins tend to have multiple repeats of binding domains that allow them to form several non-covalent bonds with their coacervating partners, be these other proteins, or RNA or DNA.[30] Often these bonds are formed through hydrophobic interactions. For example, repeats of the SRC homology 3 (SH3) domain (which binds proline-rich motifs (PRMs)) are found in many proteins that are involved in the assembly of signalling complexes through phase separation. By studying the assembly of one such complex (the nephrin–NCK–N-WASP system from kidney podocytes), as well as recombinant proteins containing multiple SH3 or PRM domains, Li *et al.* were able to show that valency was a strong determinant of the ability of these biopolymers to phase separate in aqueous solution.[31] Another common class of binding

domain that is found repetitively on phase-separating proteins is the RNA-binding domain, which is perhaps unsurprising given the role that BMCs play in regulating RNA translation and degradation.[12] Among RNA-binding proteins, one of the most conserved of these domains is the RGG-box (defined as a sequence of closely spaced Arg-Gly-Gly repeats), which has a high net positive charge and is therefore electrostatically attracted to negatively charged RNA.[32] Examples of RNA-binding proteins with multiple arginine-rich repeats include hnRNPA1 (implicated in the development of ALS), and the nucleolar protein nucleophosmin (involved in nucleolus self-assembly).[31,33,34] Such repeats have even been used in the *de novo* design of synthetic MLOs with programmable phase behaviour.[35]

Electrostatic interactions warrant additional discussion, as many proteins that are involved in the formation of BMCs have multiple regions of varying charge density along their sequences. For example, Pak *et al.* found that the BMC-forming Nephrin intercellular domain (NICD) protein had several regions of high negative charge density interspersed with aromatic residues along its length; in the presence of a positively charged aggregating partner (in this case, supercharged GFP) NICD would form complex coacervates through electrostatic interactions, and these coacervates would be subsequently stabilized by hydrophobic interactions between aromatic residues. Interestingly, the researchers found that the most important driver of phase separation in this system was not the precise sequence of NICD, but the overall density and patterning of its highly-charged regions.[36] Electrostatic interactions can also be involved in simple coacervation, in cases where a particular protein might contain several segregated blocks of opposite, and high, charge density. Examples of such proteins include LAF-1, which is critical to the formation of P granules in *C. Elegans* that were described in the previous section, and DDX4 (of the family of proteins known as DEAD-Box ATPases), which forms BMCs that are involved in RNA processing.[12,23]

In summary, a highly conserved feature among phase separating proteins is the presence of multiple residues or domains along their sequences, that are able to participate in the non-covalent interactions that are key enthalpic drivers of biological coacervation. Often these domains are found within regions of these proteins that have little-to-no secondary or tertiary structure, and which are therefore called intrinsically disordered regions. These IDRs – or, when an entire protein is unstructured, intrinsically disordered proteins (IDPs) – are also ubiquitous features of phase-separating proteins, and therefore warrant further exploration.

Protein intrinsic disorder

Proteins have long been understood to adopt secondary and tertiary structures, whereby they are folded into precise shapes through interactions between residues along their length, and between those residues and whatever solution these proteins are distributed within. These higher order structures are known to often be critical to the ability of a protein to carry out its intended purpose, and denaturation of a protein tends to lead to its inactivation; in the case of proteins therefore, form really does seem to equal function.[37,38] However, the situation is somewhat simpler in the case of proteins that form BMCs, insomuch as these proteins often contain, or are entirely comprised of, conformationally heterogeneous regions that lack a defined 3D secondary or tertiary structure, and are therefore referred to as being intrinsically disordered.[25,39] IDRs/IDPs seem to be critical to the ability of many BMC-related proteins to undergo phase separation, and often the multivalent binding sites described in the previous section are found within IDRs.[29] In the case of biological coacervation, it seems that it may actually be a lack of form that equals function.

IDRs that drive phase separation are characterized by low complexity at the amino acid level, often being comprised of repetitive sequences that are enriched in polar (Gly, Gln, Asn, Ser), charged (Arg, Lys, Asp, Glu), and aromatic (Phe, Tyr) residues.[40] The common thread amongst the side-chains of these amino acids, is their ability to participate in the various non-covalent interactions (e.g. electrostatic, π-π stacking, etc.) that provide the enthalpic contribution to phase separation.[25] These interactions serve to stabilize IDRs in a particular conformational (low energy) state, when they are in the presence of a coacervating partner, under appropriate conditions of pH, temperature, salt, etc.[28]

One of the first IDPs to be confirmed as critical to biological coacervation was DDX4, which was briefly mentioned in the preceding section as being a protein involved in the formation of MLOs for RNA processing. In 2015, Nott *et al.* were investigating the intrinsically disordered N-terminal tail of DDX4, and found that it was able to drive the formation of BMCs both *in vitro* and *in vivo*, whether it was attached to the remainder of DDX4, or expressed as a truncated polypeptide. Furthermore, they established that the key driver of aggregation amongst these IDRs was the presence of patterned charge regions along their length, lending further support to the importance of the interplay between intrinsic disorder and

multivalency in coacervating proteins. Similar sequence characteristics where also found within the IDRs of other proteins known to be involved in the formation BMCs.[41]

The IDRs of several other well-known coacervating proteins, such as the LAF-1 and hnRNPA1 proteins that were discussed previously, were subsequently established as key factors in the ability of these proteins to phase separate.[28,42] The potential clinical relevance of IDRs is also highlighted by the case of hnRNPA1, in that persistent stress granules formed by these proteins due to IDR interactions can become pathological when those assemblies turn into non-resoluble amyloids, which ultimately can lead to the development of ALS.[20,21] Other IDRs/IDPs have been implicated in a wide range of neurodegenerative and age-related diseases, such as Parkinson's disease, Huntington's disease, and Alzheimer's disease, further underscoring the importance of studying how it is that IDRs contribute to protein aggregation, and how disfunction or mutation in IDRs can cause normally functional coacervation to turn pathological.[43]

Understanding of the structure and functionality of IDRs has also allowed for the *de novo* synthesis of artificial disordered proteins, which are able to exhibit phase separation behaviour under conditions outside of those typically encountered by natural proteins (e.g. non-physiological temperature, pH, etc.).[44] For example, Simon *et al.* produced libraries of IDPs, based on the hydrophobic sequence of tropoelastin, with varying amino acid compositions and lengths; by combining proteins from these libraries in solution, the researchers were able to program the self-assembly of a variety of unique architectures, some of which are not typically seen among natural BMCs.[45] In another example, Chang *et al.* produced disordered polypeptides consisting of patterned repeats of charged glutamate or lysine residues, and then induced these to coacervate by combining them in solutions of appropriate ionic strength. Crucially, they were able to control the propensity of their synthetic IDPs to coacervate by changing the density of charges that repeated along their length.[46]

This work focuses on one particular type of artificially produced IDP, which is derived from the hydrophobic domains of human tropoelastin. An in-depth review of these constructs is given in the following section.

Elastin-like polypeptides

IDRs are not only biologically significant intracellularly; they in fact also play a role in the organization of extracellular proteins, such as those that constitute the extracellular matrix. A prototypical example is the protein tropoelastin, which is the soluble precursor to elastin. Since as early as the 1970s, it has been known that tropoelastin phase separates in response to increasing temperature (among other potential stimuli), and that this constitutes the first step of elastic fibre assembly.[47,48] Subsequent studies confirmed that the interaction between hydrophobic domains lead to an increase in the entropy of water around these molecules through a reduction in contacts between water molecules and hydrophobic domains ; these domains also turned out to be intrinsically disordered, but this was not an established concept in molecular biology at the time of their initial discovery.[27,49,50] By creating artificial polypeptides from repeating sequences of these hydrophobic domains, researchers could produce synthetic biomaterials that recapitulated the phase separating and temperature responsive behaviour of tropoelastin.[51–53] In time, these types of IDPs came to be known as elastin-like polypeptides (ELPs).

ELPs are comprised of pentapeptide repeats with the general sequence Val-Pro-Gly-Xaa-Gly, where Xaa can be any amino acid other than proline. One of the more unique characteristics of the IDPs based on these five amino acids, is that they exhibit a lower critical solution temperature (LCST). This property – more commonly associated with synthetic polymers like poly(N-isopropylacrylamide) – means that ELPs will phase separate into densely packed coacervates when they are heated above a particular temperature in solution, and then revert back to solvated individual chains if that solution is subsequently cooled below their LCST.[54] From a physical chemistry perspective, the temperature responsiveness of ELPs is explained as follows: Below their LCST, ELPs exist as IDP chains that are well solvated by water; above their LCST, ELPs adopt more ordered secondary structures mainly in the form of β-strands, with an associated increase in the number of peptide-peptide intramolecular interactions at the expense of peptide-solvent interactions, ultimately causing ELPs to phase separate from the surrounding solvent.[55,56] This temperature-dependant adoption of transient secondary structures has also been reported for several other IDPs.[57–59]

One of the more useful aspects of the phase separation behaviour of ELPs, is that the precise transition temperature (T_t) at which it occurs can be tuned for any particular ELP by

controlling three critical parameters: ELP length, concentration, and composition at the guest residue (Xaa) position.[60] By creating ELP libraries wherein any two of these parameters are fixed, the contributions of the third, variable parameter to the T_t of an ELP can be determined and modelled. For example, Meyer and Chilkoti created libraries of variable length based on three different ELP compositions, and used these to create a model for predicting the T_t of ELPs as a function of length or concentration (Eq. 1-1):[61]

$$T_t = T_{t,c} + \frac{k}{L} Ln(\frac{C_c}{C}) \quad \text{Eq. 1-1}$$

Where $T_{t,c}$, C_c, and k are the critical transition temperature, critical concentration, and a constant for a particular ELP composition, and L is the chain length in number of pentapeptide repeats. The practical implications of this model are that for an ELP of a given guest residue composition, the T_t will be inversely proportional to both chain length and concentration.

Similar investigations have been undertaken to determine the precise effect of guest residue composition on ELP T_t. In 1991, Urry *et al.* established that mean hydrophobicity at the Xaa position was an important determinant of the T_t of an ELP; specifically, as the mean hydrophobicity increased, the T_t decreased.[62] McDaniel *et al.* subsequently applied this concept in a predictive model for determining the transition temperature of ELPs with variable fractions of alanines or valines at the Xaa position (Eq. 1-2):[63]

$$T_t = Ae^{BfAlanine} + \frac{Ce^{DfAlanine}}{length} ln \frac{Ee^{FfAlanine}}{conc} \quad \text{Eq. 1-2}$$

where A – F are experimentally determined constants, and *fAlanine* is the proportion of alanine relative to valine at the guest residue position. A caveat should be made regarding the utility of the two models just described, in that they both rely on the experimental determination of constants for particular ELP compositions, thus precluding their use for the complete *de novo* prediction of the *Tt* of ELPs with compositions other than the ones used in the creation of the models. Nonetheless, such studies do provide, at a minimum, heuristics for the tuning of ELP transition temperature through manipulation of their length, composition, and concentration.

Given this understanding of the phase separation behaviour of ELPs, they have come to represent a platform for the synthesis of monodisperse IDPs with tuneable T_t, whose composition can be controlled at the amino acid level through genetic manipulation. This versatility has led to their use in a wide variety of biomedical applications, the most prominent of which will be described in the following section.

Applications of ELPs

The sequence and size of ELPs can be controlled at the genetic level, with a precision that cannot be matched by synthetic polymers. These factors, combined with the low immunogenicity of ELPs, have led to their widespread use as biomaterials for applications such as drug delivery and tissue engineering.[64] Furthermore, their low sequence complexity, ability to phase separate, and their elastic properties make them a simple model IDP, and so ELPs have also been used as a platform for the study of IDP biophysics and phase separation behaviour.[60]

An example of an early application of ELPs comes from Meyer and Chilkoti, who used them as a thermally-responsive purification tag that they attached to other recombinant proteins. These researchers found that ELPs retained their ability to phase separate, even when bound to other proteins; they made use of this by cycling cell lysates through buffers that either promoted ELP aggregation (i.e. high temperature or high ionic strength), or solubilization (low temperature or low ionic strength) in order to selectively precipitate or solubilize ELP-protein fusions.[65] By additionally taking advantage of the ability of ELP-protein fusions to be expressed at high levels without forming insoluble inclusion bodies, the researchers showed that they could purify proteins at much higher yields than those typically achieved using more well-established methods of protein purification, such as chromatography.[66]

In the sphere of tissue engineering ELPs represent an attractive material, owing to their aforementioned tuneable properties, and their ability to be produced in the gram quantities that are often needed for bulk tissue engineering applications. The use of ELPs in tissue engineering generally involves the formation of a hydrogel scaffold by one of two primary methods: (1) Coacervation of ELPs in response to ionic strength or temperature, or (2) chemical cross-linking of ELPs through functional residues included along their sequence. An example of the former method comes from Betre *et al.*, who used ELP aggregates as

scaffolds for cartilaginous tissue repair, and showed that these materials could maintain chondrocyte proliferation or drive their differentiation from human adipose-derived stem cells.[67,68] The major drawback of non-covalently cross-linked ELP scaffolds is that they tend to have poor mechanical stiffness, which precludes their use in many tissue engineering applications. This disadvantage can be overcome by introducing chemical cross-links into ELP gels. For example, McHale *et al.* improved the mechanical stiffness of ELPs for cartilaginous tissue repair by introducing lysines or glutamines at the guest residue position, which could be cross-linked through the formation of a γ-glutamyl–ε-lysyl bond catalysed by tissue transglutaminase (tTg).[69] Other strategies for improving ELP hydrogel mechanical strength involve the use of non-cytotoxic cross-linkers such as β-[tris(hydroxymethyl)phosphino] propionic acid, or the integration of ELPs into hybrid gels containing other scaffold components such as poly(ethylene glycol) or lipids.[70,71] In addition to the potential for inclusion of amino acids with functional side chains (e.g. cysteine, lysine) at the ELP guest residue position, it is also possible to insert cell adhesive motifs or enzyme-recognition sequences at ELP termini, or between VPGXG repeats, without comprising their ability to phase separate.[64]

The advantages of using ELPs for drug delivery applications, stem from the fact that it is possible to site-specifically insert therapeutic proteins or peptides at points along the ELP sequence, which can in turn confer benefits to the efficacy of these therapeutics in terms of extended *in vivo* half-lives or targeted delivery. One of the major challenges in the delivery of peptide-based therapeutics is that they are readily cleared from circulation owing to their small size; by conjugating these peptides to soluble ELP unimers, their circulation time, and in turn their therapeutic efficacy can in theory be extended.[72] ELPs can also be used to produce drug delivery vehicles with varying architectures. For example, diblock ELPs having different guest residue compositions with different hydrophobicities can be induced to self-assemble into protein-based micelles. In this configuration, they can take advantage of the enhanced permeability and retention effect (EPR) present in certain tumours to specifically localize to their intended site of action.[73] Alternatively, ELPs can be designed to have a *Tt* between room and physiological temperature, such that they can be injected through a syringe, but phase transition to form a depot of ELP + therapeutic *in vivo*. Liu *et al.* applied such a design in the delivery of radionuclides to tumours in mice, and found that long term release of the nuclide improved its anti-tumour efficacy.[74]

More recently, ELPs have been used in the design of synthetic membraneless organelles, owing to their low complexity, and the ease with which they can be produced. By fusing an RGG-box domain with an ELP, Simon *et al.* produced synthetic RNA binding IDPs, which could be used to selectively sequester RNA in granules in response to temperature, and thereby inhibit mRNA translation. In this way, these engineered ribonucleoprotein granules operated analogously to other RNA-regulating MLOs that are found naturally within the cell.[75]

In summary, the tuneable phase transition temperature, precise sequence control, functional versatility, and low immunogenicity of ELPs have led to their use in myriad tissue engineering and drug delivery applications, and as model IDPs for the design of synthetic membraneless organelles. These features suggested ELPs as an ideal platform for this work, with the aim of designing a therapeutic targeting a critically unmet need in the clinic: a hemostatic agent that could be intravenously delivered in order to minimize blood loss in cases of trauma or during surgery. The subsequent section will outline this problem, and the rational for targeting it with ELPs in greater detail.

Trauma and uncontrolled bleeding

Severe trauma due to injury is a leading cause of death worldwide, accounting for up to 5.4 million deaths in 1990, and projected by one study to account for as many as 8.4 million deaths in 2020.[76] Strikingly, trauma is the leading cause of death amongst individuals under the age of 45.[77] A plurality of these deaths can be attributed to uncontrolled bleeding, whereby a patient's natural clotting response and currently available clinical interventions are together unable to achieve hemostasis.[78,79] Current standards of care depend upon the nature and location of uncontrolled bleeding on or within a patient: For accessible and compressible wounds, there exists a wide variety of interventions in the form of compression bandages, torniquets, glues, fibrin sealants and others that have been applied in the clinic.[80] For internal and non-compressible injuries, on the other hand, the available interventions are fewer, and those that do exist still rely heavily on the transfusion of whole blood or blood components (platelets, fibrinogen, coagulation factors, etc.), which carries with it issues of contamination, short shelf-life, high cost, and sometimes uncertain efficacy.[81,82] The problem of uncontrolled bleeding is further exacerbated by the local depletion of clotting factors at the site of injury; this creates a positive feedback loop whereby a patient who was originally

unable to achieve hemostasis becomes even less able to do so, leading to a condition known as trauma-induced coagulopathy (TIC) in approximately 25% of trauma patients.[83] Given this, it is clear that there exists a significant clinical need for the development of hemostatic agents – particularly those that can be administered intravenously - which are safe, effective, inexpensive, and can be easily stored for long periods of time. Furthermore, the clinical importance of hemostatic agents is reinforced by economics: The global hemostatic agents market was worth US $3.3 billion in 2017, and it is estimated to be worth US $5.4 billion by 2025.[84]

These factors motivated the undertaking of this work, which sought to develop a novel hemostatic agent that could be intravenously delivered, and which would integrate into and support the clotting cascade. Critical to the success of this project, was a thorough understanding of how hemostasis occurs *in vivo,* outlined in the next sections.

Hemostasis

The mechanism of hemostasis exists, as the name suggests, in order to prevent excessive blood loss following injury to the vasculature. Hemostasis involves the interaction of a complex system of cells (such as platelets), proteins (such as fibrinogen and many coagulation factors), and other molecules (e.g. Ca^{2+}), that act in sequence, and in parallel, in order to drive the conversion of liquid blood into a gel (i.e. a clot) at the site of injury, and thereby stem bleeding.[85] The formation, properties, and degradation of clots are exquisitely controlled, and indeed they must be, as the consequences of off-target clot formation (i.e. thrombosis) can be fatal.[86]

One aspect of this control is maintained by temporally dividing the major events of hemostasis, known as the primary and secondary phase, wherein platelets or fibrinogen play the dominant role, respectively.[85] The following subsections will explore each of these phases in more detail.

Primary hemostasis

Primary hemostasis is the body's first response to bleeding, with the main aim of this process being the formation of a platelet plug at the site of injury. Platelets are anuclear cells – the smallest human blood cells (3.6 x 0.7 μm) – that are derived from the cytoplasm of megakaryocytes in the bone marrow. They play a role in myriad biological and pathological processes including inflammation, wound healing, tumour metastasis, and of course hemostasis.[87]

Prior to injury, platelets circulate through the blood at concentrations ranging from 150 000 to 350 000 cells/μL (in healthy patients) in a non-activated state.[88] In this "dormant" form platelets are not able to bind to one another due to the conformation of surface integrins (GPIIb-IIIa), and they are also prevented from binding to the endothelial layer due to repulsive electrostatic charges on endothelial and platelet cell surfaces, and to the release of inhibitors of platelet activation such as prostacyclin and nitric oxide.[85,89] Damage to the endothelium exposes the subendothelium, which is composed in part of collagen to which the multimeric protein von Willebrand factor (vWF) is bound; both of these constitute important substrates for platelet adhesion.[89] The mechanism of platelet adhesion to the subendothelium is in part dependant on the shear forces exerted by flowing blood, and involves a number of molecular interactions. Under low shear conditions, activation of platelets proceeds through binding of collagen, fibronectin, and laminin, and through the release of thromboxane A2 (TXA_2) from platelets, which is able to recruit other platelets to the nascent platelet plug.[90] In high shear conditions, platelet binding to the subendothelium occurs primarily through vWF, and there are a number of shear-associated changes to vWF that facilitate this, including conformational changes that expose platelet-binding domains, self-association of vWF molecules, and increases in the binding affinity between vWF and surface integrins on platelets.[91]

Whether platelets adhere to the subendothelium under low or high shear conditions, the end result is that they become activated, which involves their changing shape from homogenous discoid to an irregular shape with many pseudopodia extending from their surface. Note that is also possible for platelets to become activated in the presence of activated thrombin (which is largely generated during secondary hemostasis; see below) without adhering to the subendothelium or other platelets. Activation also involves

conformational changes in GPIIb-IIIa integrins, allowing them to bind circulating fibrinogen. Platelets then aggregate by binding the same fibrinogen molecule to form fibrinogen "bridges"; interestingly, once a fibrinogen molecule is bound to a platelet at one end, both activated and non-activated platelets can bind the same molecule at the other, thus activating the previously non-activated platelets and leading to an amplification of the rate of plug formation. Ultimately, the platelets aggregate in sufficient quantities to bridge the exposed gap between endothelial cells, which then release prostacyclin in order to inhibit platelet aggregation, in a negative feedback loop that prevents overgrowth of the platelet plug.[87,90]

Together, these events constitute the major, albeit simplified, steps of primary hemostasis. The platelet plug formed by this process provides an initial stopgap to stem the flow of blood from a wound site. However, this plug is not stable and will persist only for some hours, unless it is supported by the formation of a fibrin scaffold during secondary hemostasis.[92]

Secondary hemostasis

This phase of hemostasis involves the conversion of soluble fibrinogen into insoluble fibrin through the action of the clotting cascade; the resulting fibrin clot serves first to seal wounds in concert with the platelet plug that was formed during primary hemostasis, and subsequently to promote wound healing. Fibrinogen is a 340 kDa glycoprotein that circulates in the blood at a concentration of 2 – 3 mg mL^{-1}, and which is comprised of three polypeptide chains – Aα, Bβ, and γ – that are joined together by five symmetrical disulfide bridges.[93] The conversion of fibrinogen into fibrin involves the cleavage of a set of 14 – 16 residue fibrinopeptides from the Aα and Bβ chains (fibrinopeptide A (fpA) and fibrinopeptide B (fbB), respectively) by the serine protease thrombin, which is itself activated in the final stages of the clotting cascade.[94] This cascade consists of a series of zymogens, which are converted into active serine proteases by other members of the cascade in concert with a number of cofactors. The cascade itself can be initiated through one of two pathways: the extrinsic pathway (also known as the tissue factor (TF) pathway), or the intrinsic pathway (also known as the contact pathway).[95]

The extrinsic pathway is so named because it is activated by something not contained within blood plasma, namely TF (also known as factor III). Following injury to the endothelium,

cells are exposed which present TF on their membranes, and TF serves to activate the next member of the pathway, factor VII (FVII), through limited proteolysis. FVII is present at low concentrations in the blood plasma, but it functions most efficiently when it forms a complex with TF; this TF:FVIIa complex then activates FIX and FX. FXa is able to convert a small amount of circulating prothrombin into thrombin, which can begin cleaving fibrinopeptides from fibrinogen; however, at these low concentrations thrombin's primary function is to activate FVIII and FV, and to expose phosphatidylserines on the surfaces of activated platelets.[96] The latter serve as binding sites for factors IXa, VIIIa, X, Xa, Va, and prothrombin, which is critical to the propagation of the clotting cascade in the intrinsic pathway.[95]

The intrinsic pathway is also known as the contact pathway because it can be initiated through the contact of blood with an artificial surface.[97] However, it can also serve to amplify the formation of thrombin, and therefore fibrin, that was initiated by the extrinsic pathway. This occurs because thrombin is able to activate FXI, in addition the previously mentioned FVIII and FV, all of which are members of the intrinsic pathway; this results in the creation of a positive feedback loop that ultimately leads to a burst of thrombin activation.[96]

As mentioned, one of the primary functions of thrombin is to cleave fpA and fpB from fibrinogen to convert it into fibrin. But how does fibrin then go about forming the actual scaffold of the blood clot? The answer is that cleavage of those fibrinopeptides exposes knob A and knob B on the central E domain of fibrin; these can then non-covalently bind to constitutively exposed hole A and hole B on the distal D domains of other fibrin molecules. In this way fibrin monomers arrange themselves in a half-staggered conformation to form a growing protofibril. These protofibrils also interact laterally through αC domains to form fibrin fibres.[93] Subsequent to the cleavage of fpA and fpB, thrombin also activates one more enzyme in the clotting cascade, FXIII; FXIIIa is a transglutaminase that is able to catalyse the formation of γ-glutamyl-ϵ-lysyl cross-links between glutamine and lysine residues on adjacent fibrin monomers, thereby stabilizing the fibrin clot.[98] Following the cessation of bleeding, the clot is degraded through the enzymatic activity of plasmin, which is activated from its precursor, plasminogen, by tissue plasminogen activator and urokinase. This step is critical in order to prevent the unnecessary intravascular accumulation of fibrin, and to allow the removal of clots which might otherwise become dislodged from the site of injury and lead to thrombotic events.[99,100]

Together, these events constitute the major steps in secondary hemostasis, which results ideally in the stabilization of bleeding at a wound site. There are, however, many circumstances in which the natural clotting response is insufficient to achieve hemostasis, due to for example the size of an injury, the presence of inherited coagulation disorders (e.g. hemophilia), or the development of acute coagulopathies such as TIC. In these cases, artificial hemostats can be applied in the clinic or in the field in order to stem bleeding in a patient.

Hemostatic agents

Hemostatic agents, or hemostats, are used to augment the natural hemostatic response, either by direct physical occlusion of wounds through the application of sealants or pressure, or by supporting aspects of primary or secondary hemostasis. Certain practices for the clinical management of bleeding represent some of the most ancient medical interventions that are still being applied today; for example, there is evidence of the use of the tourniquet for hemorrhagic control in ancient Rome as early as the 1st century CE.[101] More modern innovations seek to leverage the properties of both synthetic and natural materials to create hemostatic agents that meet several design goals: (i) applicability to a variety of wound types, (ii) ability to rapidly achieve hemostasis, and to maintain it for sufficient time for wound healing to occur, (iii) easy and economical to produce, and ability to be stored under ambient conditions for extended periods of time, (iv) easy to apply, in the clinic or in the field, and (v) biocompatible, biodegradable, and having limited risk of transmission of pathogens.[81] Hemostatic agents are often classified by their method of application, topical or intravenous, as there are particular considerations for designing hemostats for each intended use. The following subsections will explore the major developments in both topical and intravenous hemostats in greater detail.

Topical hemostats

This category of hemostats comprises those treatments that can be applied to externally accessible injuries ranging from lacerations, to puncture wounds, and blunt traumas. A majority of hemostats that are in use in the clinic are topically applied, and they have proven to be quite effective in the treatment of bleeding at accessible injury sites.[102] Topical hemostats also have the advantage of being deliverable as diverse modalities,

including as glues, sprays, gels, gauze strips, or powders. Furthermore, they can be classified as active, when they work by promoting the formation of a fibrin clot at the end of the clotting cascade, or passive, when they are not biologically active and instead serve to mechanically inhibit bleeding or to promote platelet aggregation.[80]

Early examples of adjuvants used for hemostasis served to physically seal wounds, such as for example the "antiseptic wax" (beeswax, salicylic acid, and almond oil) used by surgeon Sir Victor Horsley in 1886. A version of this formulation is still sold today under the trade name Bone Wax (Ethicon, Sommerville, NJ), and as the name suggests, its use is particularly indicated in cases of bleeding originating from bone.[103] More modern iterations of these mechanical hemostats employed materials such as gelatin or oxidized cellulose in order to achieve similar passive hemostatic effects. Today there is a veritable cornucopia of passive mechanical hemostats on the market, including products such as GELFOAM (porcine gelatin, Baxter), SURGICEL (oxidized regenerated cellulose, Ethicon), Helistat (bovine collagen, Integra LifeSciences), VITASURE (polysaccharide spheres, Stryker).[104] These types of hemostats have the advantage of being easy to use and having minimal storage requirements, but as they act outside of the coagulation cascade, they are not appropriate for patients with acute or chronic coagulopathies.[102]

Following the development of techniques for fractionating proteins from plasma in the 1970s, active topical hemostats could be developed that were able to integrate into and support the natural hemostatic response. Thrombin for example, could be derived from bovine sources (THROMBIN-JMI, Pfizer), human pooled plasma (EVITHROM, Ethicon), or expressed recombinantly (RECOTHROM, Mallinckrodt Pharmaceuticals), and delivered as a formulation in combination with the mechanical hemostats described above (GELFOAM PLUS, for example, consists of a porcine gelatin sponge moistened with a solution of thrombin).[104] Active hemostats can also be delivered in liquid form to wound sites. Such formulations often involve the use of a double-barrel syringe, with one barrel containing active thrombin, Ca^{2+}, and other clotting or antifibrinolytic components (e.g. FXIII, tranexamic acid), and the other barrel containing high concentrations of fibrinogen (i.e. from 20 – 100 g L^{-1}). Upon mixing of these components in the nozzle of the syringe, the active thrombin is able to convert fibrinogen into fibrin, leading to the formation of a clot at the site of injury.[102] Products based on this design, such as TISSEEL (Baxter), represent some of the most widely used active topical hemostats on the market.[105] This type of system has the advantage of being able to function

even in patients with upstream coagulopathies, and has proven effective in the management of bleeding in European trauma centres for over 25 years. However, the use of blood derived products presents challenges in terms of the potential for viral transmission or immunogenicity, as well as issues with sourcing and stringent storage conditions.[81]

In summary, there are a number of topically applied interventions available in the clinic for the management of exposed wounds, and these treatments have demonstrated significant efficacy in the treatments of the particular types of injuries that they are indicated for over many decades of use. However, they all share the common drawback that they can only be used on accessible and/or compressible injury sites. For wounds that are not accessible, or where the site of injury cannot be found, a hemostatic agent that can be delivered systematically is required.

Intravenous hemostats

The ideal intravenous hemostat would be one that can be administered to a patient even in the field, after which it would be able to localize to the site of injury, support coagulation, and then be cleared from circulation without adverse immunological or inflammatory side effects. Critically, such a hemostat would have to exert its effects in a very specific manner, as the risk of off-target thrombus formation is significantly greater with this delivery method, as compared to the aforementioned topical hemostats.[85] Owing to this technical challenge, there have been comparatively fewer intravenous hemostats described in the literature, and fewer still have been translated to the clinic.[106] However, the goal of being able to intervene in cases of bleeding from internal or non-accessible wounds – and especially to be able to limit pre-hospital mortality in such patients by stabilizing them in the field – continues to motivate intensive research into these technologies.[107]

Current standards of care for the treatment of bleeding from non-compressible wounds involve the administration of blood products such as fresh frozen plasma, or platelets. In European trauma centres, fibrinogen concentrates are also sometimes administered.[108] As with the use of blood products in topical hemostats, these types of intravenous hemostatic interventions carry the risk of viral transmission or immunogenicity, and they have stringent storage requirements and short shelf-lives (platelets for example must be used within 3 – 7 days of extraction) which precludes their use in the field.[81,109] Furthermore, while there is some evidence to indicate that these types of transfusions

improve short-term patient outcomes, their effect on the longer-term survival of critically injured patients is less clear.[82,110]

Artificial intravenous hemostats fall broadly into two categories: platelet analogues and fibrin modulators. The former category represents the majority of intravenous hemostats described in the literature. These technologies seek to recapitulate one or more of the properties of native platelets, - such as binding to the subendothelium or aggregation to form a plug - and they could prove especially beneficial in patients who are suffering from reduced natural platelet counts (thrombocytopenia), as is the case with patients undergoing certain types of chemotherapy, for example.[111] Early examples of platelet substitutes sought to constitutively display platelet substrates on the surface of erythrocytes, including fibrinogen and arginine-glycine-aspartic acid (RGD) containing peptides, in order to promote platelet aggregation.[112,113] Later iterations of this approach sought to use phospholipids or synthetic polymers as the scaffold onto which these, and other platelet substrates such as the H12 domain of fibrinogen were bound.[114,115] For example, Bertram *et al.* functionalized poly(lactic-co-glycolic acid)-poly-L-lysine (PLGA-PLL) nanospheres with RGD peptides, to create synthetic platelets that were able to halve bleeding times in rat models of major trauma (**Figure 1-1**).[116] Other reported examples of synthetic platelets added additional functionalities, such as the ability to bind both platelets and the subendothelium, or the delivery of the platelet activator adenosine diphosphate (ADP).[117,118]

As mentioned, there are comparatively fewer artificial intravenous hemostats that are designed to bind to fibrin directly. One reason for this may be the high degree of structural homology between fibrin and circulating fibrinogen, and the need to therefore bind fibrin with a very high degree of specificity.[85] A notable example of a hemostat that is able to specifically bind fibrin comes from Brown *et al.*, who designed a hybrid hemostat that was able to exert a contractile force on fibrin networks in order to improve their mechanical properties, in a manner similar to natural platelets (for a more in-depth explanation of this phenomenon see the subsequent chapter). The researchers achieved this by evolving single variable domain-like recognition motifs (sdFv) with high affinities for fibrin through phage-display, and then using them to functionalize ultra-low cross-linked poly(N-isopropylacrylamide-co-acrylic acid) (pNIPAm-AAc) microgels. Upon binding to fibrin networks, the low modulus of these materials caused them to collapse, whereby they would exert their contractile force on the network. Ultimately these microgels were shown to

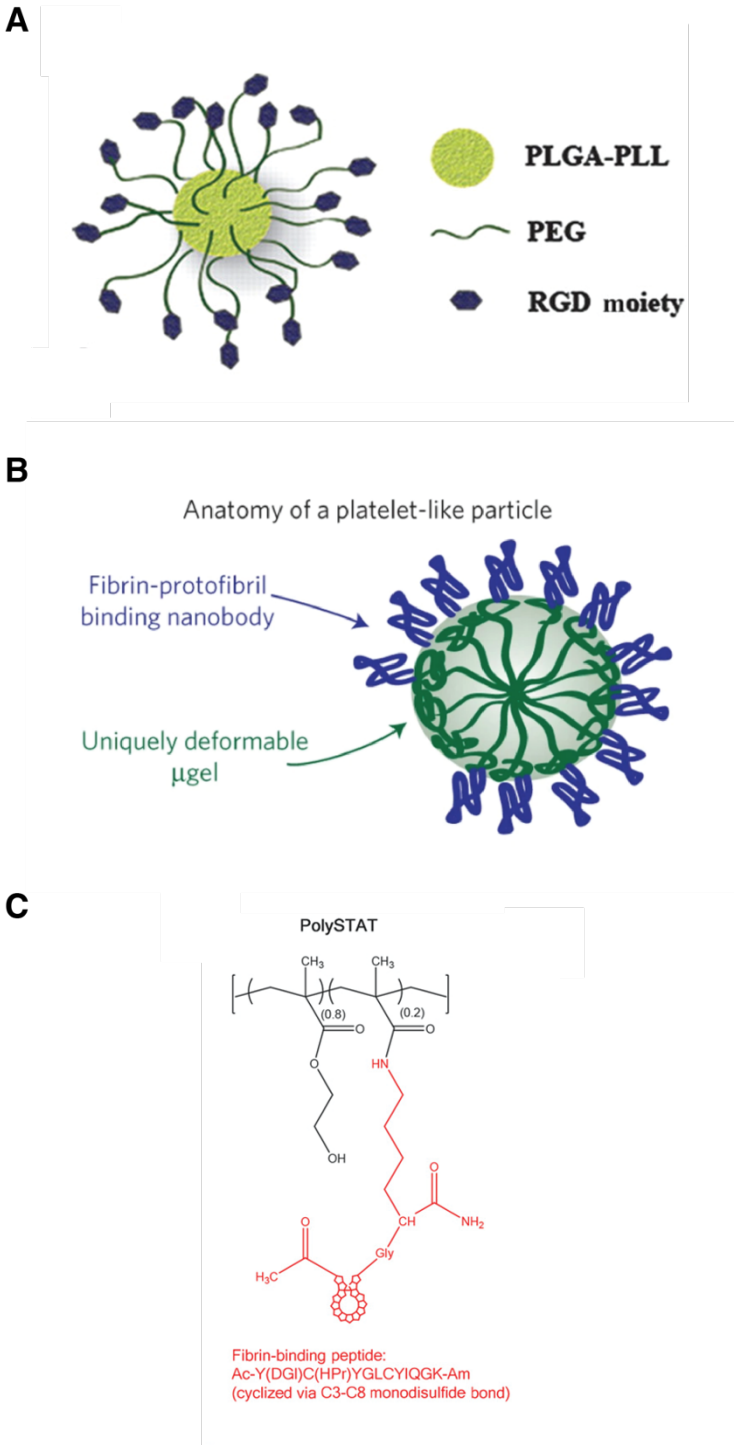

Figure 1-1. A selection of intravenous hemostats described in the literature. A) An intravenous nanoparticle functionalized with RGD for binding and aggregation of activated platelets.[116] B) A synthetic platelet comprised of an ultra-low cross-linked poly(N-isopropylacrylamide) core functionalized with fibrin-binding nanobodies.[119] C) PolyStat, a synthetic poly(hydroxyethyl)methacrylate backbone functionalized with circular peptides that have a high affinity for fibrin.[121] All figures reproduced with permission.

reduce bleeding times in rat models of injury.[119,120] Another example of a synthetic polymer that binds to fibrin bio-orthogonally comes from the Pun group. Their design consisted of a (hydroxyethyl)methacrylate (HEMA)-N-hydroxysuccinimide methacrylate (NHSMA) polymer backbone p(HEMA-co-NHSMA), which they functionalized with a cyclic peptide that had been isolated from phage display libraries, and which had high affinity and specificity for fibrin. They were able to show that administration of the functionalized polymer (which they called polySTAT), resulted in 100% survival of treated rats in a rat femoral artery injury model of bleeding.[107,121]

In summary, there a number of platelet analogues and several fibrin modulating intravenous hemostats that have shown promising efficacy *in vitro* and in animal models of traumatic injury. However, none of these systems have, as-of-yet, seen clinical application, and work remains to be done in order to render them sufficiently safe, cost efficient, and effective for human use. In the case of fibrin modulators, one key aspect of their efficacy has to do with how they alter the mechanical and structural properties of fibrin clots; this was critical in the development of the hemostat described in this work as well, and so the following section will investigate how the structural features of fibrin clots are affected by both endogenous influences (i.e. proteins, shear forces, platelets), as well as by certain artificial hemostatic agents.

References

1. Mazzarello, P. A unifying concept: The history of cell theory. *Nat. Cell Biol.* **1**, E13–E15 (1999).
2. Pederson, T. The nucleus introduced. *Cold Spring Harb. Perspect. Biol.* **3**, 1–16 (2011).
3. Ernster, L. & Schatz, G. Mitochondria: A historical review. *Journal of Cell Biology* **91**, (1981).
4. Bentivoglio, M. The discovery of the Golgi apparatus. *Journal of the History of the Neurosciences* **8**, 202–208 (1999).
5. Schuldiner, M. & Schwappach, B. From rags to riches - The history of the endoplasmic reticulum. *Biochimica et Biophysica Acta - Molecular Cell Research* **1833**, 2389–2391 (2013).
6. Big, E. J. A Short History of the Electron Microscope. *Bios* **27**, 33–37 (1956).
7. Minton, A. P. The Influence of Macromolecular Crowding and Macromolecular Confinement on Biochemical Reactions in Physiological Media. *Journal of Biological Chemistry* **276**, 10577–10580 (2001).
8. Mélèse, T. & Xue, Z. The nucleolus: an organelle formed by the act of building a ribosome. *Curr. Opin. Cell Biol.* **7**, 319–324 (1995).
9. Handwerger, K. E., Cordero, J. A. & Gall, J. G. Cajal bodies, nucleoli, and speckles in

the Xenopus oocyte nucleus have a low-density, sponge-like structure. *Mol. Biol. Cell* **16**, 202–211 (2005).
10. Boeynaems, S. *et al.* Protein Phase Separation: A New Phase in Cell Biology. *Trends in Cell Biology* **28**, 420–435 (2018).
11. Feric, M. *et al.* Coexisting Liquid Phases Underlie Nucleolar Subcompartments. *Cell* **165**, 1686–1697 (2016).
12. Banani, S. F., Lee, H. O., Hyman, A. A. & Rosen, M. K. Biomolecular condensates: Organizers of cellular biochemistry. *Nature Reviews Molecular Cell Biology* **18**, 285–298 (2017).
13. Alberti, S. Phase separation in biology. *Current Biology* **27**, R1097–R1102 (2017).
14. Brangwynne, C. P. *et al.* Germline P granules are liquid droplets that localize by controlled dissolution/condensation. *Science (80-.).* **324**, 1729–1732 (2009).
15. Brangwynne, C. P., Mitchison, T. J. & Hyman, A. A. Active liquid-like behavior of nucleoli determines their size and shape in Xenopus laevis oocytes. *Proc. Natl. Acad. Sci. U. S. A.* **108**, 4334–4339 (2011).
16. Su, X. *et al.* Phase separation of signaling molecules promotes T cell receptor signal transduction. *Science (80-.).* **352**, 595–599 (2016).
17. Takahara, T. & Maeda, T. Transient Sequestration of TORC1 into Stress Granules during Heat Stress. *Mol. Cell* **47**, 242–252 (2012).
18. Wang, Q. *et al.* Cajal bodies are linked to genome conformation. *Nat. Commun.* **7**, 1–17 (2016).
19. Alberti, S., Gladfelter, A. & Mittag, T. Considerations and Challenges in Studying Liquid-Liquid Phase Separation and Biomolecular Condensates. *Cell* **176**, 419–434 (2019).
20. Molliex, A. *et al.* Phase Separation by Low Complexity Domains Promotes Stress Granule Assembly and Drives Pathological Fibrillization. *Cell* **163**, 123–133 (2015).
21. Patel, A. *et al.* A Liquid-to-Solid Phase Transition of the ALS Protein FUS Accelerated by Disease Mutation. *Cell* **162**, 1066–1077 (2015).
22. Berry, J., Brangwynne, C. P. & Haataja, M. Physical principles of intracellular organization via active and passive phase transitions. *Reports on Progress in Physics* **81**, 046601 (2018).
23. Hondele, M. *et al.* DEAD-box ATPases are global regulators of phase-separated organelles. *Nature* **573**, (2019).
24. Griffin, E. E., Odde, D. J. & Seydoux, G. Regulation of the MEX-5 gradient by a spatially segregated kinase/phosphatase cycle. *Cell* **146**, 955–968 (2011).
25. Brangwynne, C. P., Tompa, P. & Pappu, R. V. Polymer physics of intracellular phase transitions. *Nat. Phys.* **11**, 899–904 (2015).
26. Uversky, V. N. Protein intrinsic disorder-based liquid–liquid phase transitions in biological systems: Complex coacervates and membrane-less organelles. *Advances in Colloid and Interface Science* **239**, 97–114 (2017).
27. Vrhovski, B. & Weiss, A. S. Biochemistry of tropoelastin. *Eur. J. Biochem.* **258**, 1–18 (1998).
28. Berry, J., Brangwynne, C. P. & Haataja, M. Physical principles of intracellular organization via active and passive phase transitions. *Reports Prog. Phys.* **81**, 046601 (2018).
29. Shin, Y. & Brangwynne, C. P. Liquid phase condensation in cell physiology and disease. *Science* **357**, (2017).

30. Dignon, G. L., Best, R. B. & Mittal, J. Biomolecular Phase Separation: From Molecular Driving Forces to Macroscopic Properties. *Annu. Rev. Phys. Chem.* **71**, 53–75 (2020).
31. Li, P. *et al.* Phase transitions in the assembly of multivalent signalling proteins. *Nature* **483**, 336–340 (2012).
32. Kiledjian, M. & Dreyfuss, G. Primary structure and binding activity of the hnRNP U protein: binding RNA through RGG box. *EMBO J.* **11**, 2655–2664 (1992).
33. Mitrea, D. M. *et al.* Nucleophosmin integrates within the nucleolus via multi-modal interactions with proteins displaying R-rich linear motifs and rRNA. *Elife* **5**, (2016).
34. Molliex, A. *et al.* Phase Separation by Low Complexity Domains Promotes Stress Granule Assembly and Drives Pathological Fibrillization. *Cell* **163**, 123–133 (2015).
35. Schuster, B. S. *et al.* Controllable protein phase separation and modular recruitment to form responsive membraneless organelles. *Nat. Commun.* **9**, 1–12 (2018).
36. Pak, C. W. *et al.* Sequence Determinants of Intracellular Phase Separation by Complex Coacervation of a Disordered Protein. *Mol. Cell* **63**, 72–85 (2016).
37. Comstock, M. J. *et al.* Direct observation of structure-function relationship in a nucleic acid -processing enzyme. *Science (80-.).* **348**, 352–354 (2015).
38. Littlechild, J. A. Enzymes from extreme environments and their industrial applications. *Frontiers in Bioengineering and Biotechnology* **3**, 161 (2015).
39. Vucetic, S., Brown, C. J., Dunker, A. K. & Obradovic, Z. Flavors of protein disorder. *Proteins Struct. Funct. Bioinforma.* **52**, 573–584 (2003).
40. Uversky, V. N., Kuznetsova, I. M., Turoverov, K. K. & Zaslavsky, B. Intrinsically disordered proteins as crucial constituents of cellular aqueous two phase systems and coacervates. *FEBS Lett.* **589**, 15–22 (2015).
41. Nott, T. J. *et al.* Phase Transition of a Disordered Nuage Protein Generates Environmentally Responsive Membraneless Organelles. *Mol. Cell* **57**, 936–947 (2015).
42. Elbaum-Garfinkle, S. *et al.* The disordered P granule protein LAF-1 drives phase separation into droplets with tunable viscosity and dynamics. *Proc. Natl. Acad. Sci. U. S. A.* **112**, 7189–7194 (2015).
43. Uversky, V. N. Intrinsically disordered proteins and their (disordered) proteomes in neurodegenerative disorders. *Front. Aging Neurosci.* **7**, 18 (2015).
44. Dzuricky, M., Rogers, B. A., Shahid, A., Cremer, P. S. & Chilkoti, A. De novo engineering of intracellular condensates using artificial disordered proteins. *Nat. Chem.* 1–12 (2020). doi:10.1038/s41557-020-0511-7
45. Simon, J. R., Carroll, N. J., Rubinstein, M., Chilkoti, A. & López, G. P. Programming molecular self-assembly of intrinsically disordered proteins containing sequences of low complexity. *Nat. Chem.* **9**, 509–515 (2017).
46. Chang, L. W. *et al.* Sequence and entropy-based control of complex coacervates. *Nat. Commun.* **8**, 1–8 (2017).
47. Cox, B. A., Starcher, B. C. & Urry, D. W. Coacervation of α-elastin results in fiber formation. *BBA - Protein Struct.* **317**, 209–213 (1973).
48. Cox, B. A., Starcher, B. C. & Urry, D. W. Coacervation of tropoelastin results in fiber formation. *J. Biol. Chem.* **249**, 997–998 (1974).
49. Yeo, G. C., Keeley, F. W. & Weiss, A. S. Coacervation of tropoelastin. *Advances in Colloid and Interface Science* **167**, 94–103 (2011).
50. Tarakanova, A., Yeo, G. C., Baldock, C., Weiss, A. S. & Buehler, M. J. Molecular model of human tropoelastin and implications of associated mutations. *Proc. Natl. Acad. Sci. U. S. A.* **115**, 7338–7343 (2018).

51. Urry, D. W., Haynes, B., Zhang, H., Harris, R. D. & Prasad, K. U. Mechanochemical coupling in synthetic polypeptides by modulation of an inverse temperature transition. *Proc. Natl. Acad. Sci. U. S. A.* **85**, 3407–3411 (1988).
52. Urry, D. W., Mitchell, L. W., Ohnishi, T. & Long, M. M. Proton and carbon magnetic resonance studies of the synthetic polypentapeptide of elastin. *J. Mol. Biol.* **96**, 101–117 (1975).
53. Castiglione Morelli, M. A., Debiasi, M., Destradis, A. & Tamburro, A. M. An aggregating elastin-like pentapeptide. *J. Biomol. Struct. Dyn.* **11**, 181–190 (1993).
54. Zhao, B., Li, N. K., Yingling, Y. G. & Hall, C. K. LCST Behavior is Manifested in a Single Molecule: Elastin-Like polypeptide (VPGVG)n. *Biomacromolecules* **17**, 111–118 (2016).
55. Urry, D. W. Physical chemistry of biological free energy transduction as demonstrated by elastic protein-based polymers. *Journal of Physical Chemistry B* **101**, 11007–11028 (1997).
56. Li, N. K., Quiroz, F. G., Hall, C. K., Chilkoti, A. & Yingling, Y. G. Molecular Description of the LCST Behavior of an Elastin-Like Polypeptide. *Biomacromolecules* **15**, 3522–3530 (2014).
57. Wuttke, R. *et al.* Temperature-dependent solvation modulates the dimensions of disordered proteins. *Proc. Natl. Acad. Sci. U. S. A.* **111**, 5213–5218 (2014).
58. Soranno, A. Physical basis of the disorder-order transition. *Archives of Biochemistry and Biophysics* **685**, 108305 (2020).
59. Kjaergaard, M. *et al.* Temperature-dependent structural changes in intrinsically disordered proteins: Formation of α-helices or loss of polyproline II? *Protein Sci.* **19**, 1555–1564 (2010).
60. Roberts, S., Dzuricky, M. & Chilkoti, A. Elastin-like polypeptides as models of intrinsically disordered proteins. *FEBS Lett.* **589**, 2477–2486 (2015).
61. Meyer, D. E. & Chilkoti, A. Quantification of the effects of chain length and concentration on the thermal behavior of elastin-like polypeptides. *Biomacromolecules* **5**, 846–851 (2004).
62. Urry, D. W. *et al.* Temperature of Polypeptide Inverse Temperature Transition Depends on Mean Residue Hydrophobicity. *J. Am. Chem. Soc.* **113**, 4346–4348 (1991).
63. McDaniel, J. R., Radford, D. C. & Chilkoti, A. A Unified Model for De Novo Design of Elastin-like Polypeptides with Tunable Inverse Transition Temperatures. *Biomacromolecules* **14**, 2866–2872 (2013).
64. Varanko, A. K., Su, J. C. & Chilkoti, A. Elastin-Like Polypeptides for Biomedical Applications. *Annu. Rev. Biomed. Eng.* **22**, 343–369 (2020).
65. Meyer, D. E. & Chilkoti, A. Purification of recombinant proteins by fusion with thermally-responsive polypeptides. *Nat. Biotechnol.* **17**, 1112–1115 (1999).
66. Trabbic-Carlson, K., Liu, L., Kim, B. & Chilkoti, A. Expression and purification of recombinant proteins from Escherichia coli: Comparison of an elastin-like polypeptide fusion with an oligohistidine fusion. *Protein Sci.* **13**, 3274–3284 (2004).
67. Betre, H., Setton, L. A., Meyer, D. E. & Chilkoti, A. Characterization of a genetically engineered elastin-like polypeptide for cartilaginous tissue repair. *Biomacromolecules* **3**, 910–916 (2002).
68. Betre, H. *et al.* Chondrocytic differentiation of human adipose-derived adult stem cells in elastin-like polypeptide. *Biomaterials* **27**, 91–99 (2006).
69. McHale, M. K., Setton, L. A. & Chilkoti, A. Synthesis and in vitro evaluation of

enzymatically cross-linked elastin-like polypeptide gels for cartilaginous tissue repair. *Tissue Eng.* **11**, 1768–1779 (2005).
70. Mozhdehi, D. *et al.* Genetically encoded lipid-polypeptide hybrid biomaterials that exhibit temperature-Triggered hierarchical self-Assembly. *Nat. Chem.* **10**, 496–505 (2018).
71. Wang, H., Cai, L., Paul, A., Enejder, A. & Heilshorn, S. C. Hybrid Elastin-like Polypeptide–Polyethylene Glycol (ELP-PEG) Hydrogels with Improved Transparency and Independent Control of Matrix Mechanics and Cell Ligand Density. *Biomacromolecules* **15**, 3421–3428 (2014).
72. Liu, W. *et al.* Tumor accumulation, degradation and pharmacokinetics of elastin-like polypeptides in nude mice. *J. Control. Release* **116**, 170–178 (2006).
73. McDaniel, J. R., Callahan, D. J. & Chilkoti, A. Drug delivery to solid tumors by elastin-like polypeptides. *Adv. Drug Deliv. Rev.* **62**, 1456–1467 (2010).
74. Liu, W. *et al.* Injectable intratumoral depot of thermally responsive polypeptide-radionuclide conjugates delays tumor progression in a mouse model. *J. Control. Release* **144**, 2–9 (2010).
75. Simon, J. R., Eghtesadi, S. A., Dzuricky, M., You, L. & Chilkoti, A. Engineered Ribonucleoprotein Granules Inhibit Translation in Protocells. *Mol. Cell* **75**, 66-75.e5 (2019).
76. Murray, C. J. & Lopez, A. D. Alternative projections of mortality and disability by cause 1990–2020: Global Burden of Disease Study. *Lancet* **349**, 1498–1504 (1997).
77. Trauma Facts - The American Association for the Surgery of Trauma. Available at: https://www.aast.org/resources/trauma-facts. (Accessed: 14th April 2021)
78. Curry, N. *et al.* The acute management of trauma hemorrhage: a systematic review of randomized controlled trials. *Crit. Care* **15**, R92 (2011).
79. Cothren, C. C., Moore, E. E., Hedegaard, H. B. & Meng, K. Epidemiology of Urban Trauma Deaths: A Comprehensive Reassessment 10 Years Later. *World J. Surg.* **31**, 1507–1511 (2007).
80. Emilia, M. *et al.* Topical hemostatic agents in surgical practice. *Transfus. Apher. Sci.* **45**, 305–311 (2011).
81. Hickman, D. A., Pawlowski, C. L., Sekhon, U. D. S., Marks, J. & Gupta, A. Sen. Biomaterials and Advanced Technologies for Hemostatic Management of Bleeding. *Adv. Mater.* **30**, 1700859 (2018).
82. Wafaisade, A. *et al.* Administration of fibrinogen concentrate in exsanguinating trauma patients is associated with improved survival at 6 hours but not at discharge. *J. Trauma Acute Care Surg.* **74**, 387–395 (2013).
83. Davenport, R. *et al.* Functional definition and characterization of acute traumatic coagulopathy. *Crit. Care Med.* **39**, 2652–2658 (2011).
84. Hemostats Market Size, Share, Growth | Global Report, 2026. Available at: https://www.fortunebusinessinsights.com/industry-reports/hemostatic-agents-market-100084. (Accessed: 31st March 2020)
85. Chan, L. W., White, N. J. & Pun, S. H. Synthetic Strategies for Engineering Intravenous Hemostats. *Bioconjug. Chem.* **26**, 1224–1236 (2015).
86. Esmon, C. T. Inflammation and thrombosis. *J. Thromb. Haemost.* **1**, 1343–1348 (2003).
87. Jurk, K. & Kehrel, B. E. Platelets: Physiology and biochemistry. in *Seminars in Thrombosis and Hemostasis* **31**, 381–392 (Copyright © 2005 by Thieme Medical Publishers, Inc., 333 Seventh Avenue, New York, NY 10001, USA., 2005).

88. Marx, R. E. Platelet-Rich Plasma (PRP): What Is PRP and What Is Not PRP? *Implant Dent.* **10**, (2001).
89. Ruggeri, Z. M. Von Willebrand factor, platelets and endothelial cell interactions. *J. Thromb. Haemost.* **1**, 1335–1342 (2003).
90. McMichael, M. Primary hemostasis. *Journal of Veterinary Emergency and Critical Care* **15**, 1–8 (2005).
91. Gogia, S. & Neelamegham, S. Role of fluid shear stress in regulating VWF structure, function and related blood disorders. *Biorheology* **52**, 319–335 (2016).
92. Broos, K., Feys, H. B., De Meyer, S. F., Vanhoorelbeke, K. & Deckmyn, H. Platelets at work in primary hemostasis. *Blood Rev.* **25**, 155–167 (2011).
93. Mosesson, M. W. Fibrinogen and fibrin structure and functions. in *Journal of Thrombosis and Haemostasis* **3**, 1894–1904 (John Wiley & Sons, Ltd, 2005).
94. Kattula, S., Byrnes, J. R. & Wolberg, A. S. Fibrinogen and Fibrin in Hemostasis and Thrombosis. *Arterioscler. Thromb. Vasc. Biol.* **37**, (2017).
95. Smith, S. A., Travers, R. J. & Morrissey, J. H. How it all starts: Initiation of the clotting cascade. *Crit. Rev. Biochem. Mol. Biol.* **50**, 326–36 (2015).
96. Wolberg, A. S. & Campbell, R. A. Thrombin generation, fibrin clot formation and hemostasis. *Transfus. Apher. Sci.* **38**, 15–23 (2008).
97. Müller, F., Gailani, D. & Renné, T. Factor XI and XII as antithrombotic targets. *Curr. Opin. Hematol.* **18**, 349–355 (2011).
98. Muszbek, L., Bereczky, Z., Bagoly, Z., Komáromi, I. & Katona, É. Factor XIII: A Coagulation Factor With Multiple Plasmatic and Cellular Functions. *Physiol. Rev.* **91**, 931–972 (2011).
99. Chapin, J. C. & Hajjar, K. A. Fibrinolysis and the control of blood coagulation. *Blood Rev.* **29**, 17–24 (2015).
100. Cesarman-Maus, G. & Hajjar, K. A. Molecular mechanisms of fibrinolysis. *Br. J. Haematol.* **129**, 307–321 (2005).
101. Kragh, J. F., Swan, K. G., Smith, D. C., Mabry, R. L. & Blackbourne, L. H. Historical review of emergency tourniquet use to stop bleeding. *American Journal of Surgery* **203**, 242–252 (2012).
102. Chiara, O. *et al.* A systematic review on the use of topical hemostats in trauma and emergency surgery. *BMC Surgery* **18**, (2018).
103. Moo, I. H., Chen, J. Y. Q., Pagkaliwaga, E. H., Tan, S. W. & Poon, K. B. Bone Wax Is Effective in Reducing Blood Loss After Total Knee Arthroplasty. *J. Arthroplasty* **32**, 1483–1487 (2017).
104. Tompeck, A. J. *et al.* A comprehensive review of topical hemostatic agents: The good, the bad, and the novel. *Journal of Trauma and Acute Care Surgery* **88**, E1–E21 (2020).
105. Fibrin Sealants Market Size & Share | Industry Report, 2017-2025. Available at: https://www.transparencymarketresearch.com/fibrin-sealants-market.html. (Accessed: 20th April 2021)
106. Lashof-Sullivan, M., Shoffstall, A. & Lavik, E. Intravenous hemostats: Challenges in translation to patients. *Nanoscale* **5**, 10719–10728 (2013).
107. Lamm, R. J. *et al.* Optimizing the Polymer Chemistry and Synthesis Method of PolySTAT, an Injectable Hemostat. *ACS Biomater. Sci. Eng.* **6**, 7011–7020 (2020).
108. Spahn, D. R. *et al.* Management of bleeding and coagulopathy following major trauma: an updated European guideline. *Crit. Care* **17**, R76 (2013).
109. Lambert, M. P., Sullivan, S. K., Fuentes, R., French, D. L. & Poncz, M. Challenges and

promises for the development of donor-independent platelet transfusions. *Blood* **121**, 3319–3324 (2013).
110. Yang, L., Stanworth, S., Hopewell, S., Doree, C. & Murphy, M. Is fresh-frozen plasma clinically effective? An update of a systematic review of randomized controlled trials (CME). *Transfusion* **52**, 1673–1686 (2012).
111. Modery-Pawlowski, C. L. *et al.* Approaches to synthetic platelet analogs. *Biomaterials* **34**, 526–541 (2013).
112. Coller, B. S. *et al.* Thromboerythrocytes. In vitro studies of a potential autologous, semi-artificial alternative to platelet transfusions. *J. Clin. Invest.* **89**, 546–555 (1992).
113. AGAM, G. & LIVNE, A. A. Erythrocytes with covalently bound fibrinogen as a cellular replacement for the treatment of thrombocytopenia. *Eur. J. Clin. Invest.* **22**, 105–112 (1992).
114. Modery, C. L. *et al.* Heteromultivalent liposomal nanoconstructs for enhanced targeting and shear-stable binding to active platelets for site-selective vascular drug delivery. *Biomaterials* **32**, 9504–9514 (2011).
115. Okamura, Y. *et al.* Hemostatic effects of phospholipid vesicles carrying fibrinogen γ chain dodecapeptide in vitro and in vivo. *Bioconjug. Chem.* **16**, 1589–1596 (2005).
116. Bertram, J. P. *et al.* Intravenous Hemostat: Nanotechnology to Halt Bleeding. *Sci. Transl. Med.* **1**, (2009).
117. Anselmo, A. C. *et al.* Platelet-like nanoparticles: Mimicking shape, flexibility, and surface biology of platelets to target vascular injuries. *ACS Nano* **8**, 11243–11253 (2014).
118. Okamura, Y. *et al.* Development of fibrinogen γ-chain peptide-coated, adenosine diphosphate-encapsulated liposomes as a synthetic platelet substitute. *J. Thromb. Haemost.* **7**, 470–477 (2009).
119. Brown, A. C. *et al.* Ultrasoft microgels displaying emergent platelet-like behaviours. *Nat. Mater.* **13**, 1108–1114 (2014).
120. Nandi, S. *et al.* Platelet-like particles dynamically stiffen fibrin matrices and improve wound healing outcomes. *Biomater. Sci.* (2019). doi:10.1039/C8BM01201F
121. Chan, L. W. *et al.* A synthetic fibrin cross-linking polymer for modulating clot properties and inducing hemostasis. *Sci. Transl. Med.* **7**, 277ra29 (2015).

Chapter II: Structure and Mechanical Properties of Fibrin Networks

Fibrin network structure

The formation of the fibrin network that constitutes the main scaffold component of blood clots is a complex process, whereby the final structure and functionality of that network is determined by the interplay of a variety of factors, including clotting factor concentration, ionic strength, platelet contraction, and fluid flow conditions, among several others.[1–4] Aberrations in the physiological concentrations or functionality of clotting factors are associated with a number of pathologies in which fibrin networks are formed with substandard mechanical properties, and consequently, insufficient hemostatic capacity. Below is an outline describing common techniques used in the measurement of clot mechanical properties, how both natural clotting factors and fibrin-binding synthetic hemostats affect fibrin network properties, including mechanical strength, fibre thickness, density, and degree of branching, porosity, and persistence, and a discussion of the implications of these effects on the ability of blood clots to achieve adequate hemostasis.

Measuring mechanical and structural properties of clots

Several techniques can be used to study structural properties of clots, including atomic force microscopy (AFM), turbidimetry, and rheology.[5,6] The clinical gold standard for these investigations is thromboelastography, which measures the clotting capacity of a patient's blood across a number of parameters in order to guide health care professionals in administering an appropriate treatment.[7] The following subsections will outline the principles of AFM studies of clot mechanics, rheology, and thrombelastography.

Atomic force microscopy studies of clot mechanics

AFM can be used to probe the properties of many biological materials. The earliest uses of AFM in a biological context involved imaging of the topography of cells, membrane proteins, DNA,

RNA, etc.[8] In the specific case of fibrin clots, AFM can be used to study morphological changes in clots formed under different environmental conditions (e.g. pH, [Ca^{2+}], etc.), with various concentrations of clotting factors (e.g. thrombin, fibrinogen, etc.), or in the presence of proteins that inhibit/promote clot formation (e.g. heparin) or degradation (e.g. plasmin).[9,10] Outside of direct imaging of clot structure, AFM can also be used to probe the mechanical properties of clots. A typical setup for such an experiment involves the use of a cantilever with a large diameter rounded tip to indent fibrin clots across a set area. From this, the young's modulus – a measure of clot stiffness – can be obtained through the fitting of the force response of the cantilever to the appropriate model.[11] Additionally, fibrin fibre mechanics can be studied by immobilizing fibres between cantilever tips and AFM surfaces; such studies have been used to determine the origins of the high extensibility of fibrin.[12] AFM therefore provides a tool for the high resolution measurement of clot structure and mechanical properties.

Rheology

Rheology is the study of how materials deform when a force is applied, taking into account the geometry of the applied force, its magnitude, and the length of time for which it is applied. In rheology, there are two ideal categories of materials which are defined by their particular force response: ideal solids that display elastic force response behaviour, and ideal liquids, which display viscous force response behaviour. When a force is applied to a perfectly elastic material, it deforms immediately, remains deformed until the applied force is removed, and then reverts back to its original state following the removal of force. Alternatively, when force is applied to a perfectly viscous material, it will deform without limit until the applied force is removed, after which it will remain in the deformed state. Two more key rheological concepts also help in differentiating these materials: stress, which is defined as force applied to a material per unit area, and strain, which is the relative deformation of a material under an applied force. In elastic materials, stress is proportional to strain, whereas in viscous materials, stress is proportional to the rate of strain (i.e. in the case of liquids, the liquid flow rate). In reality, most materials – including biological materials such as cells, tissue, or ECM - are neither perfectly elastic nor viscous; their behaviour can be described as a mixture of the two ideals, and so they are therefore referred to as being viscoelastic.[13]

One of the most commonly used instruments for measuring rheological properties is the rheometer, which is able to apply strain to materials in a variety of

geometries, and to quantify the material's response (in rheology, strain is a proportional measure of the degree to which a material is being deformed, relative to its initial state). For viscoelastic materials, a constantly applied strain will result in a condition of zero flow, and so such measurements are of limited use in characterizing the properties of these materials. Furthermore, constant strains can damage delicate biological materials, interfering with the ability to study their rheological characteristics under native conditions. For these reasons, rheometers most often use small amplitude oscillatory shear to investigate viscoelastic materials. In such a system, the oscillatory stress (force per unit area, in N/m^2) is related to the strain by the following formula (Eq. 2-1):

$$\sigma(t) = \sigma_0 \sin(\omega t + \delta) \qquad \text{Eq. 2-1}$$

where $\sigma(t)$ is the shear stress at time t, σ_0 is the stress amplitude, ω is the angular frequency of the applied strain, and δ is the phase shift between the applied strain and the resulting stress (0˚ for a perfectly elastic material, 90˚ for a perfectly viscous one).[13] Stress can be related to strain by the following formula (Eq. 2-2):

$$\sigma(t) = \gamma_0(G' sin\omega t + G'' cos\omega t) \qquad \text{Eq. 2-2}$$

where G' is referred to as the shear storage modulus, and G'' is referred to as the loss modulus. Materials are classified as solids when G' exceeds G''.

The significance of rheology in a biological context is becoming ever more apparent, as understanding grows as to how the mechanical properties of cells and their environment influences diverse phenomenon such as stem cell differentiation, cell proliferation, or cellular migration.[11,14,15] In the specific case of coagulation, rheological studies can provide a wealth of information on, for example, the structure and mechanical strength of clots, or how cells affect fibrin networks that they are bound to.[2,16] In turn, some of these properties can be indicators of the overall stability or robustness of clots; however, the timescale of rheological experiments, and the requirement of complex instrumentation and specialized operator knowledge precludes the use of rheology for measuring clot health in a clinical setting. In clinical applications, another, a more suitable technique is often used: thromboelastography.

Thromboelastography

Thromboelastography (TEG) is a technique to study the viscoelastic properties of clotting blood. It was first described by a German physician at the University of Heidelberg, Helmut Hartet, in 1948.[17] The first documented clinical use of TEG was by Kang *et al.* in 1985, who used it in liver transplantation; subsequently TEG was also applied in cardiac surgery.[18,19] Both of these procedures can involve major blood loss, and the use of TEG allows for the appropriate administration of coagulation promoters or inhibitors, and helps to avoid the unnecessary transfusion of blood products, which could have the negative effects of exacerbating coagulopathies, and result in the depletion of precious blood stores.[7] Today, the technology is sold under two different trade names, TEG (Haemoscope Corporation, IL, USA) and ROTEM (Sysmex, Milton Keynes, UK), each operating using slightly different mechanisms.[20] However, the underlying principle behind both systems is the same, and as TEG was the tool used in this work, the details of its operation will be outlined here.

A TEG instrument contains two cups, heated to 37 ˚C, into which blood samples from a patient can be filled. Once samples are in the measurement cups, clotting can be initiated through the addition of various factors, depending on how the blood was previously stored (for example, excess Ca^{2+} can be added to blood which has been stored in a sodium citrate solution). A free-standing pin connected to a mechanical or electrical transducer is then suspended in the clotting blood, while the cup oscillates 4° 45’ every 4.5 s. As the clot begins to gel, the free-standing pin begins to be displaced along with the motion of the cup, and this displacement can be recorded in a TEG trace. From this trace, information about time to clot initiation, the rate of clot formation, clot strength, rate of fibrinolysis, etc. can be deduced (**Figure 2-1**).

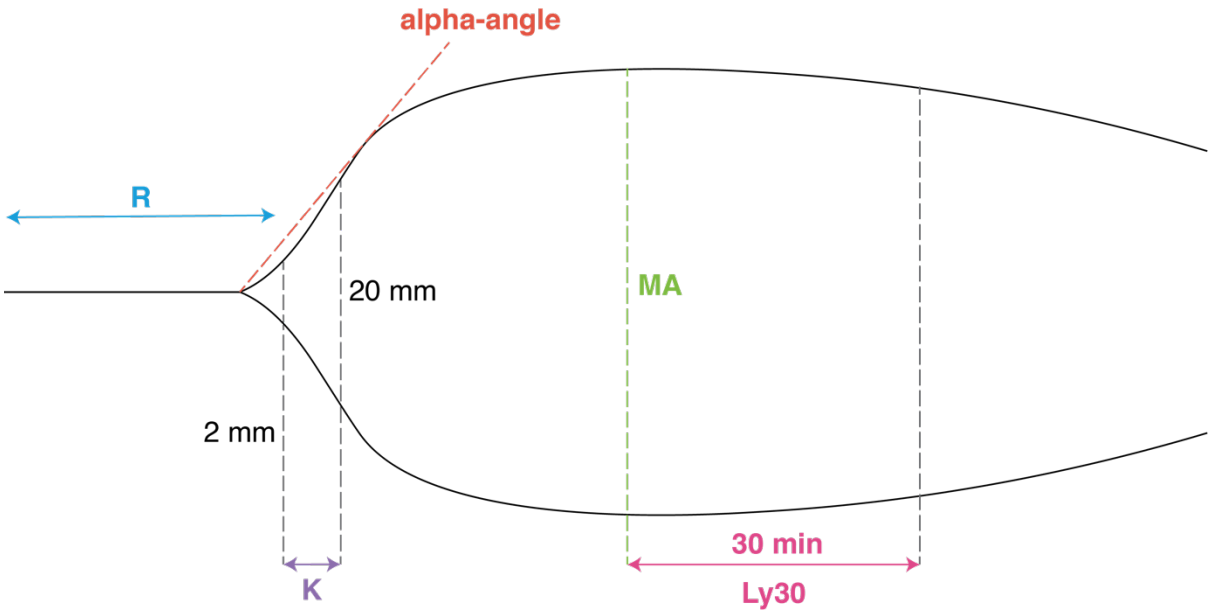

Figure 2-1. A schematic representation of a typical TEG trace, showing clot onset time (R), rate of clot growth (K, alpha-angle), the maximum amplitude (MA) achieved by the clot, and the Ly30 time, which is a measure of the rate of fibrinolysis following after a clot reaches MA.

Endogenous mediators of fibrin network structure

Thrombin

As discussed in the previous chapter, thrombin is a protease that is central to several aspects of the clotting cascade. Prior to activation, it exists as a 70 kDa zymogen known as prothrombin, which consists of a light chain bearing two kringle domains, and a heavy chain containing the serine protease domain. Cleavage of prothrombin at two sites leads to the release of the heavy chain, and activation of its proteolytic function. Active thrombin consists of a 36 residue A (or light) chain and a 259 residue B (or heavy) chain connected by disulfide bridges; the B chain consists of several loops that are involved in recognition of thrombin targets, and a catalytic cleft that constitutes thrombin's primary active site.[21,22] Structurally, proteolytic cleavage of prothrombin causes certain rearrangements in the catalytic cleft (e.g. the formation of a salt bridge) that lead to the formation of a catalytic triad of His, Asp, and Ser residues. The particular arrangement of these residues in thrombin gives this protease a preference for cleavage sites that follow basic residues. Unlike more promiscuous serine proteases such as trypsin, thrombin shows an additional specificity, due in part to the presence of large loops that partially occlude the binding cleft (**Figure 2-2**).[22]

Given the central role of thrombin in coagulation, disorders that affect its functionality or concentration in blood can have profound pathological implications. For example,

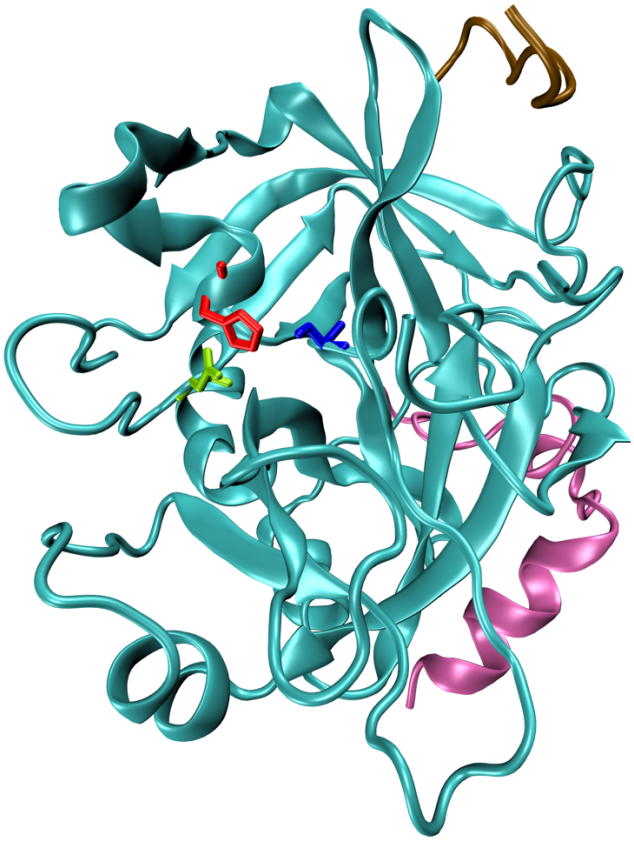

Figure 2-2. Crystal structure of activated thrombin in complex with hirudin inhibitor. The structure shows the thrombin heavy chain (green), light chain (orange), catalytic triad of histidine (yellow), aspartate (magenta), serine (red), the 60 loop and γ-loop which occlude the binding cleft (purple), and hirudin (cyan); PDB 2ZC9.

Hemophilia A and B are a result of disfunction in coagulation factors upstream of thrombin in the clotting cascade, and so the end result of these disorders is reduced thrombin generation, and therefore reduced clotting capacity. On the other hand, disorders such as Hyperprothrombinemia (caused by a mutation in the 3' untranslated region of the prothrombin gene) produce an overabundance of thrombin or its precursors in the blood, which can lead to increased risks of thrombosis. Other conditions that cause an increase in blood thrombin concentration include coronary artery disease and diabetes.[23]

The concentration of thrombin at the time of clotting is known to profoundly influence clot structure: clots formed at low thrombin concentrations have thicker, less dense fibres that are prone to fibrinolysis, while those formed at high thrombin concentrations have thinner, denser fibres that are resistant to proteolytic degradation.[23]

In vitro assays of the effects of thrombin concentration on clot structure typically involve adding a fixed amount of activated thrombin to a fibrinogen solution, which may not reflect the dynamic nature of thrombin generation *in vivo*, where free thrombin concentrations can range from 1 - 500 nM during coagulation depending on environmental conditions.[23] Modulation of these environmental conditions can produce changes in active thrombin concentration, and in the structure of resulting clots, in a manner that is similar to directly changing the concentration of thrombin present during coagulation. For example, Ca^{2+} is required for the assembly of procoagulant complexes and the generation of thrombin, and as such clotting onset times are shorter in the presence of Ca^{2+}, and these clots have thicker fibres than clots formed in the presence of thrombin alone.[24]

The mechanism by which varying thrombin concentration and/or activation rates drive changes in fibrin network structures was investigated by Domingues *et al.* using a number of non-destructive techniques such as turbidimetry and AFM, whereby fibrin networks were more likely to be representative of a native arrangement. The researchers found that increasing thrombin concentrations led to a significant decrease in the average number of fibrin protofibrils per fibre, but only a minor reduction in the size of those fibres, indicating that compaction of protofibrils was significantly reduced under these conditions.[6] This is in contrast to previous results gathered from SEM studies, which showed significant reduction in fibre diameter in the presence of higher thrombin concentrations, a result that the researchers attributed to the dehydration of fibre strands during sample preparation for SEM imaging.[23] The researchers further found that this reduced protofibril density resulted in weaker fibrin clot architectures.[6]

Factor XIII

Factor XIII (FXIII) is a tetrameric zymogen consisting of two catalytic (FXIII-A) and two inhibitory (FXIII-B) subunits. The roughly 320 kDa protein circulates through the blood in association with fibrinogen, at concentrations of 14 – 28 mg L^{-1}. FXIII-A is also present in platelets, macrophages and monocytes, although still in zymogen form.[25] Structurally, FXIII-A is comprised of 5 domains: an N-terminal activation peptide (AP-FXIII), a β-sandwich domain, a catalytic domain (with the catalytic triad of Cys, His, and Asp), and two β-barrel domains (**Figure 2-3**). In the plasma, FXIII is converted to its active form (FXIIIa) by the

concerted action of thrombin and Ca^{2+}; first, thrombin cleaves AP-FXIII from the zymogen N-terminus,

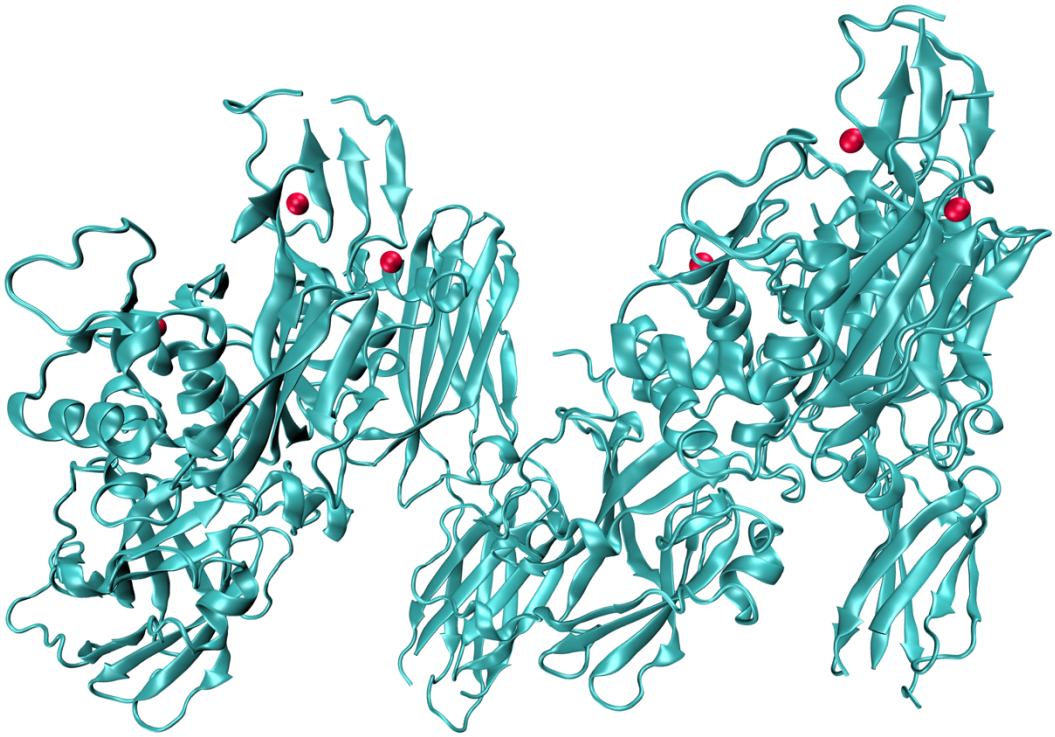

Figure 2-3. Crystal structure of activated Factor XIII (FXIII-A_2) homodimer (MW = 189 kDa) showing bound Ca^{2+} (red); PDB 5MHO.

and then Ca^{2+} causes the dissociation of the FXIII-B subunits, allowing FXIII-A_2 to adopt an active confirmation.[26] Like other transglutaminases, FXIIIa can catalyze an acyl-transfer reaction between the carboxamide group of glutamine and a primary amine; typically, the ε-amino group of lysine. The first step of this reaction involves the formation of a thioester between glutamine and the cysteine of the FXIIIa catalytic triad, after which ammonia is released and an acyl-enzyme intermediate is formed. Subsequently, this acyl group can be transferred to a primary amine when one is present, and the thiol group of the FXIIIa cysteine is recovered.[25] The primary plasma substrates of FXIIIa are fibrin and α_2-plasmin inhibitor (which it cross-links to fibrin to inhibit plasminolysis); given that FXIIIa is a transglutaminase that circulates in the blood, and given the danger of thrombosis posed by clot formation away from wound sites, FXIII activity must be tightly regulated, and it does indeed exhibit greater substrate specificity than other transglutaminases.[27] Furthermore, the release of proteases

from polymorphonuclear granulocytes in clots degrade both FXIII and inactivated FXIIIa, preventing the migration of the active form of the enzyme away from the site of injury.[27]

Inherited deficiencies in FXIIIa functionality, though rare, invariably lead to severe and persistent bleeding disorders.[28] Acquired deficiencies can also occur in patients with inflammatory diseases such as rheumatoid arthritis, ulcerative cholitis, or Crohn's disease.[29,30] On the other hand, certain FXIII polymorphisms are associated with increased FXIIIa activity, and a corresponding increase in the risk of thrombosis.[25]

The γ-glutamyl-ϵ-lysyl covalent cross-links between fibrin fibres that are catalyzed by FXIIIa serve to significantly improve the mechanical stability of clots, and to increase their resistance to proteolysis (**Figure 2-4**).[25] The improvements in clot properties that are observed in the presence of FXIIIa are believed to derive from the structural changes that are induced in fibrin networks by the catalytic action of this enzyme. Hethershaw *et al.* conducted turbidity measurements on fibrin clots formed with or without FXIII, in order to elucidate what effect the presence of FXIII had on fibrin fibre thickness and density.[31] Absorbance-based assays are an established method for investigating the structural properties of fibrin networks, and networks formed from thinner, more densely packed fibres tend to be less optically dense than those formed from larger diameter, loosely packed fibres.[32] The researchers found that clots formed in the presence of FXIII had significantly lower turbidity than those formed without FXIII; follow-up SEM studies confirmed that fibre diameter was significantly smaller (by approx. 10 nm) and density significantly higher (by approx. 0.6 fibres/μm) in the former case (**Figure 2-5**). Kurniawan and colleagues also applied absorbance-based assays to study the gelation of fibrin clots with and without inhibition of FXIII. They found that there was little effect of FXIII inhibition on the initial phase of clot formation (approx. 10 minutes under their conditions) during which fibrin protofibrils are aggregating laterally, but that inhibition did lead to the elimination of the secondary phase of gelation (lasting several hours), during which compaction of the fibrin network occurs.[1] Subsequent rheological studies showed that FXIII significantly increased the linear elastic modulus of clots, but that it did not affect the stiffness of these clots at higher strains. Given these results, the researchers proposed a multiscale structural model of fibrin networks, whereby FXIII cross-links and compacts protofibrils within a fibre, the thermal fluctuations of which are believed to dominate the elastic response of clots at low-strains. According to this model, at higher strains the elastic response becomes driven by the stretching of individual

protofibrils, and therefore FXIII-mediated compaction no longer influences the stiffness of these networks.

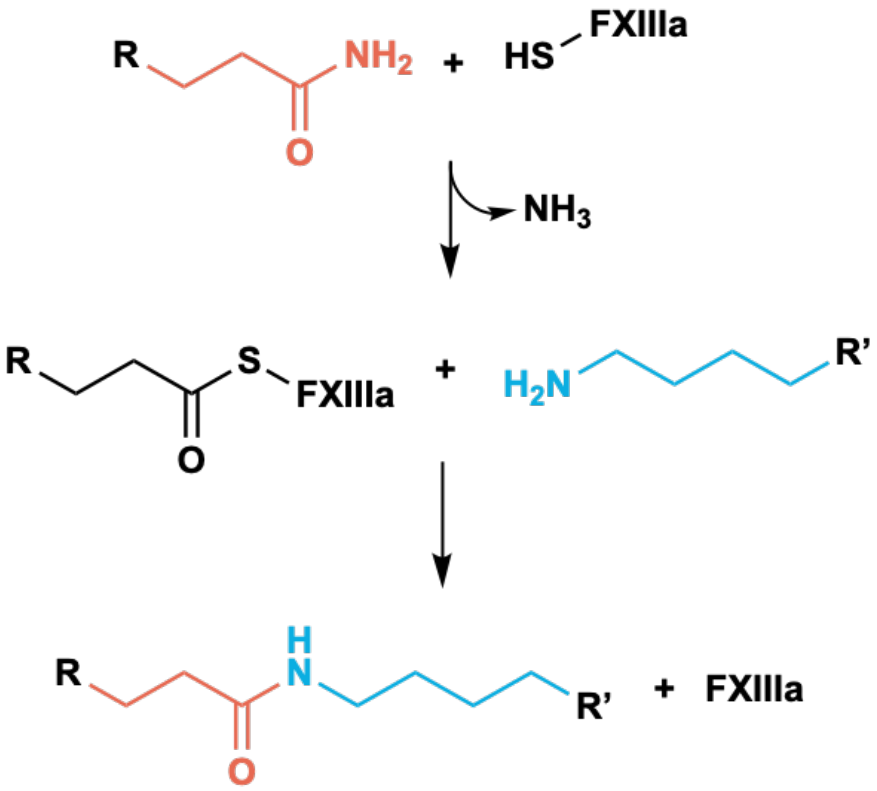

Figure 2-4. Schematic of the acyl-transfer reaction catalyzed by FXIIIa, showing glutamine in orange and lysine in blue.[33]

Dynamic stiffening through contractile stress generated by cells

Cells that bind to fibrin networks, such as platelets and fibroblasts, are able to alter the structural and mechanical properties of these networks by exerting stresses through the contraction of their cytoskeletons. Platelets are the main components of the primary hemostatic response, during which they become activated at wound sites and form a platelet plug, which is subsequently supported by the fibrin network that forms during secondary hemostasis.[34] Fibroblasts are recruited into a clot from the surrounding ECM primarily during the proliferation phase of wound healing, and they then work to promote the formation of new ECM at the site of injury through the release of collagen, fibronectin, and proteoglycans.[35]

Fibrin-bound platelets substantially decrease the size of clots (through an increase in the density of fibrin fibres) and increase their elastic modulus as much as tenfold through

actomyosin-based contraction of their cytoskeletal network.[36,37] In a landmark study, Lam *et al*. used atomic-force microscopy (AFM) to investigate the contractile forces generated by individual platelets that were bound to fibrinogen coated cantilevers and surfaces. The researchers found that each individual platelet can exert a contractile force of up to 29 nN, and that it was adhered to fibrinogen with a force of up to 70 nN. Furthermore, they found that the force of contraction was higher in platelets when they were bound to stiffer cantilevers that mimicked regions of higher stiffness in fibrin networks. Based on these results they proposed a mechanism of platelet contraction of fibrin, whereby platelets exert higher contractile forces on regions of higher fibre density, such that the contraction of the clot as a whole is more uniform and the overall elasticity of the clot is increased (**Fig 2-5**).[36]

Fibroblasts migrate into the clot during the proliferation stage of wound healing following the release of fibroblast growth factor (FGF) from macrophages, and their key functions are then regulated through the secretion of TGF-β from macrophages, platelets, and lymphocytes.[35] Through their binding to fibrin, fibroblasts can also exert contractile forces on fibrin networks, in a manner that is theorized to relate to the non-linear elasticity of those networks. Winer *et al.* proposed this theory after conducting AFM and rheological experiments on fibroblasts embedded within fibrin gels. They found that these embedded fibroblasts reached maximal spreading even in fibrin networks with low elastic moduli, in contrast to their behaviour in low stiffness linearly elastic gels, where they maintain a more rounded morphology.[38] Jansen *et al.* investigated this idea further using a similar model of fibroblasts embedded in fibrin gels, and found that fibroblasts exert myosin-II driven contractile forces on fibrin networks while spreading, which lead to local alignment of fibrin fibres around cells. They proposed that these forces push the surrounding fibrin gel into the nonlinear viscoelastic region, and thereby drive the strain-stiffening of these materials.[2,39]

Hydrodynamic shear stress

In vivo, blood clots are constantly exposed to hydrodynamic shear stress from the flow of blood through veins (10 - 100 s^{-1}) and arteries (500 - 1500 s^{-1}), and of course during extravasation of blood from vessels following injury.[40] Given this, it may be unsurprising that fluid flow can have profound effects on the structure and mechanical properties of fibrin networks. Campbell *et al.* investigated this by studying the formation of clots from platelet-

free plasma (PFP) in the presence of immortalized human dermal fibroblasts (NHF_1-hTert) under static and flow conditions. They found that clots formed under hydrodynamic flow had significantly larger, and more densely-packed, fibres than clots formed under static conditions.[40] Mechanistically, this can be explained by the fact that, for a given blood concentration of fibrin, a greater amount of fibrin will be deposited on a forming clot under flow than under static conditions, and therefore clots formed under the former condition will have a greater protein content.[41] Additionally, SEM studies conducted by the researchers showed that fibrin networks formed under flow had significantly greater fibre alignment as compared to those formed under static conditions (**Fig. 2-5**).

The consequences of such flow-induced changes in fibrin network structure on the mechanical properties of clots are manifold. Badiei and colleagues conducted controlled stress parallel superposition (CSPS) rheological experiments on incipient fibrin clots, whereby an oscillatory shear stress is superimposed on top of a steady state shear stress, in order to study the effect of unidirectional flow shear stress on their formation, fractal microstructure, and stiffness. They found that clots formed under conditions of unidirectional shear stress exhibited greater network compaction, which was then correlated with an increase in their shear storage moduli (G').[4]

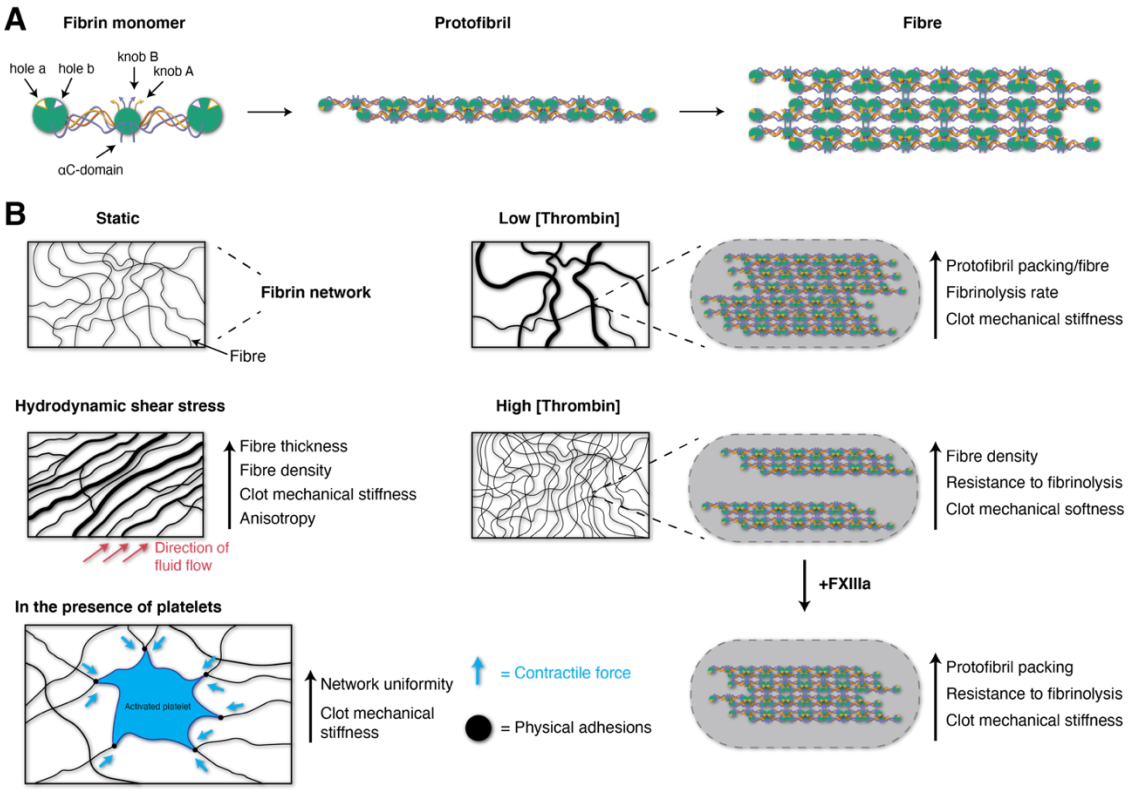

Figure 2-5. Endogenous mediators of fibrin network structure and mechanics. A) Assembly of fibrin monomers into fibres. B) Various mediators of fibrin network structure, and their effect on clot properties.

Hemostatic agents affecting fibrin network structure

Synthetic platelets

As described above, a key function of platelets in coagulation is to bind and compact fibrin fibres through the actin-myosin mediated contraction of their cytoskeletons. Synthetic platelets or platelet substitutes seeking to recapitulate this function must meet two important criteria: (A) they must be able to bind fibrin with high specificity (as opposed to homologous proteins such as fibrinogen), and (B) they must promote compaction of fibrin fibres, through the application of some contractile force, or through aggregation of the synthetic platelets. Brown *et al.* achieved this through the design of ultrasoft microgel particles coated with fibrin-binding nanobodies, which they called platelet-like particles (PLPs). Using a precipitation polymerization method, the researchers were able to synthesize ultra-low crosslinked poly(N-isopropylacrylamide-co-acrylic acid) microgels, which they then decorated with variable domain-like recognition motifs (sdFv) that had been evolved to show high specificity for fibrin through phage-display biopanning.[42,43] Not only were PLPs able to

promote the formation of fibrin clots in a manner akin to platelet-rich plasma (PRP), but upon binding to fibrin the ultra-soft particles would collapse, causing each PLP to exert a contractile force of approximately 6.5 ± 5.5 pN. While this is significantly lower than the contractile forces individual platelets were found to be able to exert (from 1.5 to 79 nN)[36], PLPs were still able to stiffen clots significantly and compact their local fibrin network. Ultimately, this resulted in clots that were more resistant to degradation, promoted wound healing, and reduced bleeding times in murine models of vascular injury.[11,42]

Fibrin-binding polymers

Synthetic polymers have been designed with the ability to bind fibrin both through engagement of fibrin's natural polymerization mechanism, and orthogonally, with the use of circular peptides with high affinity for fibrin. Considering the former case, extensive investigations have been conducted into how polyethylene glycol (PEG) bearing knob A and B mimics affect the structure of fibrin clots. "Knob A:hole a" associations are the main non-covalent bond forming interactions that drive the end-to-end aggregation of fibrin monomers to form protofibrils. The role of "knob B:hole b" interactions is more elusive, but they are believed to be involved in the lateral aggregation of protofibrils to form fibres. A summary of how knob A and B mimics and other fibrin network modulators affect fibrin-based biomaterials can be found in an extensive review by Brown and Barker.[44] One particularly unintuitive result was observed when Stabenfeldt *et al.* introduced PEG functionalized with knob B mimics to polymerizing fibrin gels. Engagement of hole b by knob b-PEG led to the formation of fibrin networks with greater porosity, but also, surprisingly, increased mechanical stiffness and greater resistance to fibrinolysis.[45] Through this method the researchers were able to improve the mechanical robustness of clots without sacrificing mass transport through the network, as evidenced by the ability of the modified clots to support angiogenesis at a level equivalent to control clots.

Another example of a synthetic polymer that binds to fibrin bio-orthogonally is polySTAT, which was introduced in the previous chapter.[46] It consists of a poly((hydroxyethyl)methacrylate) backbone, which is functionalized with cyclic peptides that had been evolved to bind fibrin with high specificity through phage display. When polySTAT was added to forming fibrin gels, it drove a number of structural changes in fibrin networks,

including reduced porosity, the formation of denser fibres, and increased mechanical stiffness, as compared to clots formed in the presence of non-fibrin-binding polymers or FXIII. Follow-up neutron scattering studies indicated that polySTAT likely enhanced clot properties by increasing the radius of fibres through recruitment of additional fibrin to those fibres.[47] Ultimately, these improved clot characteristics translated to reduced bleeding times and improved survivability in animal models of hemorrhage.

References

1. Kurniawan, N. A., Grimbergen, J., Koopman, J. & Koenderink, G. H. Factor XIII stiffens fibrin clots by causing fiber compaction. *J. Thromb. Haemost.* **12**, 1687–1696 (2014).
2. Jansen, K. A., Bacabac, R. G., Piechocka, I. K. & Koenderink, G. H. Cells actively stiffen fibrin networks by generating contractile stress. *Biophys. J.* **105**, 2240–2251 (2013).
3. Mihalko, E. & Brown, A. C. Clot Structure and Implications for Bleeding and Thrombosis. *Semin. Thromb. Hemost.* **46**, 96–97 (2020).
4. Badiei, N. *et al.* Effects of unidirectional flow shear stresses on the formation, fractal microstructure and rigidity of incipient whole blood clots and fibrin gels. *Clin. Hemorheol. Microcirc.* **60**, 451–464 (2015).
5. Storm, C., Pastore, J. J., MacKintosh, F. C., Lubensky, T. C. & Janmey, P. A. Nonlinear elasticity in biological gels. *Nature* **435**, 191–194 (2005).
6. Domingues, M. M. *et al.* Thrombin and fibrinogen γ' impact clot structure by marked effects on intrafibrillar structure and protofibril packing. *Blood* **127**, 487–495 (2016).
7. Reikvam, H. *et al.* Thrombelastography. *Transfus. Apher. Sci.* **40**, 119–123 (2009).
8. Dufrêne, Y. F. *et al.* Imaging modes of atomic force microscopy for application in molecular and cell biology. *Nature Nanotechnology* **12**, 295–307 (2017).
9. Jung, H., Tae, G., Kim, Y. H. & Johannsmann, D. Change of viscoelastic property and morphology of fibrin affected by antithrombin III and heparin: QCM-Z and AFM study. *Colloids Surfaces B Biointerfaces* **68**, 111–119 (2009).
10. Domingues, M. M. *et al.* Thrombin and fibrinogen γ' impact clot structure by marked effects on intrafibrillar structure and protofibril packing. *Blood* **127**, 487–495 (2016).
11. Nandi, S. *et al.* Platelet-like particles dynamically stiffen fibrin matrices and improve wound healing outcomes. *Biomater. Sci.* (2019). doi:10.1039/C8BM01201F
12. Brown, A. E. X., Litvinov, R. I., Discher, D. E. & Weisel, J. W. Forced unfolding of coiled-coils in fibrinogen by single-molecule AFM. *Biophys. J.* **92**, L39–L41 (2007).
13. Janmey, P. A., Georges, P. C. & Hvidt, S. Basic Rheology for Biologists. *Methods Cell Biol.* **83**, 1–27 (2007).
14. Park, J. S. *et al.* The effect of matrix stiffness on the differentiation of mesenchymal stem cells in response to TGF-β. *Biomaterials* **32**, 3921–3930 (2011).
15. Wang, Y., Wang, G., Luo, X., Qiu, J. & Tang, C. Substrate stiffness regulates the proliferation, migration, and differentiation of epidermal cells. *Burns* **38**, 414–420 (2012).
16. Ryan, E. A., Mockros, L. F., Weisel, J. W. & Lorand, L. Structural Origins of Fibrin Clot Rheology. *Biophys. J.* **77**, 2813–2826 (1999).
17. Hartert, H. Blutgerinnungsstudien Mit Der Thrombelastographie, Einem Neuen

Untersuchungsverfahren. *Klin. Wochenschr.* **26**, 577–583 (1948).
18. Kang, Y. G. *et al.* Intraoperative Changes in Blood Coagulation and Thrombelastographic Monitoring in Liver Transplantation. *Anesth. Analg.* **64**, (1985).
19. Spiess, B. D., Gillies, B. S. A., Chandler, W. & Verrier, E. Changes in transfusion therapy and reexploration rate after institution of a blood management program in cardiac surgical patients. *J. Cardiothorac. Vasc. Anesth.* **9**, 168–173 (1995).
20. Luddington, R. J. Thrombelastography/thromboelastometry. *Clin. Lab. Haematol.* **27**, 81–90 (2005).
21. De Cristofaro, R. & De Candia, E. Thrombin domains: Structure, function and interaction with platelet receptors. *Journal of Thrombosis and Thrombolysis* **15**, 151–163 (2003).
22. Davie, E. & Kulman, J. An Overview of the Structure and Function of Thrombin. *Semin. Thromb. Hemost.* **32**, 003–015 (2006).
23. Wolberg, A. S. Thrombin generation and fibrin clot structure. *Blood Rev.* **21**, 131–142 (2007).
24. Carr, M. E., Gabriel, D. A. & McDonagh, J. Influence of Ca2+ on the structure of reptilase-derived and thrombin-derived fibrin gels. *Biochem. J.* **239**, 513–516 (1986).
25. Bagoly, Z., Koncz, Z., Hársfalvi, J. & Muszbek, L. Factor XIII, clot structure, thrombosis. *Thrombosis Research* **129**, 382–387 (2012).
26. Muszbek, L., Yee, V. C. & Hevessy, Z. Blood coagulation factor XIII: Structure and function. *Thrombosis Research* **94**, 271–305 (1999).
27. Muszbek, L., Bereczky, Z., Bagoly, Z., Komáromi, I. & Katona, É. Factor XIII: A Coagulation Factor With Multiple Plasmatic and Cellular Functions. *Physiol. Rev.* **91**, 931–972 (2011).
28. Muszbek, L. & Katona, É. Diagnosis and Management of Congenital and Acquired FXIII Deficiencies. *Semin. Thromb. Hemost.* **42**, 429–439 (2016).
29. Levy, J. H. & Greenberg, C. Biology of Factor XIII and clinical manifestations of Factor XIII deficiency. *Transfusion* **53**, 1120–1131 (2013).
30. Karimi, M., Bereczky, Z., Cohan, N. & Muszbek, L. Factor XIII deficiency. *Seminars in Thrombosis and Hemostasis* **35**, 426–438 (2009).
31. Hethershaw, E. L. *et al.* The effect of blood coagulation factor XIII on fibrin clot structure and fibrinolysis. *J. Thromb. Haemost.* **12**, 197–205 (2014).
32. Sproul, E. P., Hannan, R. T. & Brown, A. C. Controlling Fibrin Network Morphology, Polymerization, and Degradation Dynamics in Fibrin Gels for Promoting Tissue Repair. in 85–99 (Humana Press, New York, NY, 2018). doi:10.1007/978-1-4939-7741-3_7
33. Factor XIII | Oncohema Key. Available at: https://oncohemakey.com/factor-xiii/. (Accessed: 22nd May 2021)
34. Chan, L. W., White, N. J. & Pun, S. H. Synthetic Strategies for Engineering Intravenous Hemostats. *Bioconjug. Chem.* **26**, 1224–1236 (2015).
35. Chester, D. & Brown, A. C. The role of biophysical properties of provisional matrix proteins in wound repair. *Matrix Biology* **60**–**61**, 124–140 (2017).
36. Lam, W. A. *et al.* Mechanics and contraction dynamics of single platelets and implications for clot stiffening. *Nat. Mater.* **10**, 61–66 (2011).
37. Wufsus, A. R. *et al.* Elastic behavior and platelet retraction in low- and high-density fibrin gels. *Biophys. J.* **108**, 173–83 (2015).
38. Winer, J. P., Oake, S. & Janmey, P. A. Non-Linear Elasticity of Extracellular Matrices Enables Contractile Cells to Communicate Local Position and Orientation. *PLoS One* **4**,

e6382 (2009).
39. Litvinov, R. I. & Weisel, J. W. Fibrin mechanical properties and their structural origins. *Matrix Biol.* **60**–**61**, 110–123 (2017).
40. Campbell, R. A., Aleman, M. M., Gray, L. D., Falvo, M. R. & Wolberg, A. S. Flow profoundly influences fibrin network structure: Implications for fibrin formation and clot stability in haemostasis. *Thrombosis and Haemostasis* **104**, 1281–1284 (2010).
41. Weisel, J. W. & Litvinov, R. I. Fibrin formation, structure and properties. *Subcell. Biochem.* **82**, 405–456 (2017).
42. Brown, A. C. *et al.* Ultrasoft microgels displaying emergent platelet-like behaviours. *Nat. Mater.* **13**, 1108–1114 (2014).
43. Welsch, N., Brown, A. C., Barker, T. H. & Lyon, L. A. Enhancing clot properties through fibrin-specific self-cross-linked PEG side-chain microgels. *Colloids Surfaces B Biointerfaces* **166**, 89–97 (2018).
44. Brown, A. C. & Barker, T. H. Fibrin-based biomaterials: Modulation of macroscopic properties through rational design at the molecular level. *Acta Biomater.* **10**, 1502–1514 (2014).
45. Stabenfeldt, S. E., Gourley, M., Krishnan, L., Hoying, J. B. & Barker, T. H. Engineering fibrin polymers through engagement of alternative polymerization mechanisms. *Biomaterials* **33**, 535–544 (2012).
46. Chan, L. W. *et al.* A synthetic fibrin cross-linking polymer for modulating clot properties and inducing hemostasis. *Sci. Transl. Med.* **7**, 277ra29 (2015).
47. Lamm, R. J. *et al.* Peptide valency plays an important role in the activity of a synthetic fibrin-crosslinking polymer. *Biomaterials* **132**, 96–104 (2017).

Chapter III: Phase Separation of Intrinsically Disordered Protein Polymers Mechanically Stiffens Fibrin Clots

Adapted from: **Urosev, I**., Lopez, J., Nash, M. A., Phase Separation of Intrinsically Disordered Protein Polymers Mechanically Stiffens Fibrin Clots. *Adv. Funct. Mater.* 2020, 30, 2005245.

Abstract

Fibrin (Fb) networks self-assemble through the coagulation cascade and serve as the structural foundation of blood clots. Following severe trauma or drug therapy, reduced integrity of Fb networks can lead to formation of clots with inadequate mechanical properties. A key feature of therapeutic interventions for hemostasis is therefore the ability to restore mechanical strength to clots formed under coagulopathic conditions. Here an intrinsically disordered protein based on an elastin-like polypeptide (ELP) sequence is described, that specifically binds Fb and modulates its mechanical properties. Hemostatic ELPs (hELPs)were designed containing N- and C-terminal peptide tags that were selectivity recognized by human transglutaminase factor XIIIa, and covalently linked into fibrin networks via the natural coagulation cascade. Phase separation of hELPs above their lower critical solution temperature (LCST) led to stiffening and rescue of clot biophysical properties under simulated conditions of dilutive coagulopathy. In addition to phase-dependent stiffening, the resulting hELP-Fb networks exhibited resistance to plasmin degradation, reduced pore sizes, and accelerated gelation rate following initiation of clotting. These results demonstrate the ability of protein-based phase separation to modulate the physical and biochemical properties of blood clots and suggest protein phase separation as a new mechanism for achieving hemostasis in clinical settings.

Introduction

Severe trauma is a major cause of death among individuals 45 years of age and younger, and is projected to account for as many as 8.4 million deaths per year in 2020. A plurality of these deaths are caused by failure to achieve hemostasis.[1–3] In cases of severe bleeding, clotting factors are rapidly depleted at the site of injury leading to a condition known as trauma-induced coagulopathy (TIC) in as many as 25% of trauma patients with an associated increase in mortality.[4,5] To date, there are few reports of intravenous hemostatic agents that can be infused systemically to treat inaccessible or uncompressible injury sites. Current standards of care involve transfusion of blood products such as frozen plasma or platelets, or the administration of clotting proteins, but these approaches are hampered by drawbacks such as high cost, short shelf-life, limited efficacy, and special storage requirements.[6,7]

Hemostasis occurs in two phases, the primary phase of which involves activation and aggregation of circulating platelets at the injury site, forming a platelet plug. In the secondary phase, fibrin (Fb) is polymerized, forming an insoluble protein hydrogel (i.e. clot) that provides structural support and hinders blood flow.[8] In this secondary phase, Fb networks form when activated thrombin cleaves fibrinopeptides from the precursor protein fibrinogen (Fg), revealing sequences known as knobs A and B. The knobs non-covalently bind to sites referred to as holes A and B on the distal ends of neighboring Fb/Fg, allowing Fb to self-associate in a half-staggered conformation and form protofibrils. These protofibrils then bundle together to form fibres and eventually an insoluble Fb network.[9,10] Fb networks are subsequently stabilized through covalent cross-links formed by a reaction between lysine and glutamine residues catalyzed by activated clotting-associated transglutaminase, FXIIIa.[11] Fb and FXIIIa are therefore both important players in hemostasis and represent valid molecular targets for hemostatic control systems.

Targeting Fb with synthetic systems is challenging because of the difficulty in obtaining specific high-affinity binders that discriminate between gelled Fb and circulating Fg. Since Fb clots and soluble Fg share sequence and structural homology, there are only a small number of conformational epitopes that can serve as a basis for molecular discrimination.[12] Nonetheless, phage display has been used successfully to isolate Fb-specific binders.[13,14] This has led to the development of Fb-targeting hemostats based on grafting Fb-binding peptides

or nanobodies onto synthetic polymers or particles that bind Fb and support clot formation *in vivo*.[15–17]

Here, we present an alternative novel mechanism for specifically targeting Fb and supporting clot formation using phase separation of elastin-like polypeptides (ELPs). ELPs are intrinsically disordered protein polymers derived from the hydrophobic domain of the human extracellular matrix protein tropoelastin. ELPs comprise repetitive VPGXG pentapeptides, where X can be any amino acid excluding proline.[18] ELPs are widely used as drug delivery vehicles, components of hydrogels for tissue repair, monodisperse mechano-linkers in single-molecule experiments, and as components in protein purification and biomarker detection.[19–25] A key advantage of ELP-based molecular systems over other natural and synthetic polymers is that they are produced by genetic engineering, and therefore precisely programmable at the DNA/amino acid level with no polydispersity.[21] ELPs are intrinsically disordered proteins and undergo stimuli-responsive phase separation into protein-rich coacervates at temperatures above their lower critical solution temperature (LCST). This process is driven by dehydration of the ELP[26–28], and is tunable based on the length and composition of the ELP sequence.[29]

Evidence is emerging that phase-separation is an important phenomenon in biology, commonly employed by cells to regulate RNA catalysis, modulate gene transcription, and control signaling.[30–32] In this context, ELPs are an ideal model system for studying and controlling molecular systems using phase separation. The phase-transition of ELPs can modulate properties of synthetic materials, for example, controlling the optical density and mechanical strength of hybrid PEG hydrogels.[33,34] Recently, ELP phase separation was used for mRNA sequestration and gene expression control in artificial protocells.[35] ELP phase separation has also been used to modulate properties of ELP-hybrid hydrogels.[36] For example, Wang *et al.* described hyaluronic acid-bound ELPs which formed a secondary network upon coacervation, thereby strengthening HA gels.[37]

Here, we designed and produced fibrin-binding hemostatic ELPs (hELPs) by introducing glutamine and lysine residues at the N and C terminal ends of an ELP. Glutamine residues were embedded within a contextual sequence motif that was efficiently recognized by the clotting factor FXIIIa.[38] This design enabled enzyme-mediated covalent integration of hELP polymers into Fb networks catalyzed by FXIIIa. When introduced into Fb clots *in vitro* at physiological temperature, hELP-rich coacervates imparted significant enhancement in clot

strength, resistance to perfusion, accelerated gelation following onset of clotting, and extended clot persistence in the presence of plasmin. HELPs lacking FXIIIa substrate tags or hELPS integrated into Fb clots below their transition temperature did not show comparable improvements in mechanical strength, indicating that both covalent integration and phase separation contribute to enhancing clot stiffness. These results demonstrate the ability of hELPs to enhance biophysical properties of blood clots through added cross-liking and phase separation. We foresee that these materials can provide a synthetic alternative or supplement to current standards of care that are based on blood product transfusion, and therefore may avoid issues that are associated with using naturally-derived interventions.

Materials & Methods

Unless otherwise stated, all chemicals were purchased from Sigma-Aldrich (Buchs, Switzerland). Plasmids with genes encoding for ELP($A_2V_8E_1$), ELP($A_2V_8E_1$)-Tgf11, ELP($A_2V_8E_1$)-GSKGS, ELP($A_2V_8E_1$)-Tgf11(Q65G), and ELP($A_2V_8E_1$)-GSGGS were synthesized by GeneArt (Thermo Scientific). Human fibrinogen (FIB 3, plasminogen, fibronectin and von Willebrand Factor depleted), thrombin, and FXIIIa were purchased from Enzyme Research Laboratories (Rheinfelden, Switzerland). Fluorescently tagged fibrinogen (Fg-488) was purchased from Thermo Scientific (Basel, Switzerland).

ELP expression & Purification

hELP and conELP proteins were designed and produced using standard molecular cloning techniques. Genes encoding the full length ELPs were produced starting from one of five 11-pentapeptide gene monomers: A2V8E1-Tgf11, A2V8E1, A2V8E1-GSKGS, A2V8E1-Tgf11(Q65G), or A2V8E1-GSGGS. These were iteratively digested and ligated together according to a previously described technique for the elongation of repetitive gene sequences, known as Recursive Directional Ligation.[39] Once a gene encoding an ELP of the desired length and composition was prepared, it was inserted into a pet28a expression vector, and the resulting plasmid was transformed into BL21 (DE3) *E. coli*. ELPs were expressed for 24 h at 37 ˚C in 1L of Terrific Broth (TB) without the addition of inducers, relying instead on the leakiness of the T7 promoter. Following expression, the cell pellet was centrifuged, re-suspended in 40 mL 20/150 mM HEPES/NaCl, and lysed by 3 cycles of ultrasonic disruption.

The lysate was centrifuged at 4 ˚C to remove cellular debris, and the ELPs were subsequently purified by Iterative Transition Cycling (ITC).[40] Briefly, 1 M NaCl was added to the supernatant remaining after centrifugation of the cell lysate. The sample was heated to 65 ˚C for 10 minutes, and centrifuged at 18 000 g at 40 ˚C for 15 min. The supernatant was discarded, and the resulting pellet was resuspended in 6 mL of cold HEPES buffer. The resuspended pellet was centrifuged again at 18 000 g at 4 ˚C for 15 min, and any contaminants that could not be resolubilized in cold buffer were discarded. Together these steps constituted one round of ITC, and the process was repeated two more times to yield the final ELP solutions, which were aliquoted and stored as-is at -20 ˚C prior to use. Typical yields for a single expression ranged from 50 – 100 mg / L of culture.

Characterization of ELP Cloud Points

The cloud points of hELPs and conELPs were measured at 30 µM concentration. ELPs were dissolved in 20/150 mM HEPES/NaCl buffer (w/ 20 mM $CaCl_2$) to the appropriate concentration, transferred to cuvettes, and placed into a UV-Vis spectrophotometer (Evolution 260 Bio, Thermo Scientific) at 15 ˚C. Samples were allowed to equilibrate to the starting temperature for 10 minutes, after which a temperature ramp was performed from 15 – 60 ˚C at a rate of 1 ˚C min^{-1}. Absorbance at 350 nm was measured every 0.25 min, and a blank reading from a cuvette containing only HEPES was subtracted from this value to yield the corrected absorbance value; this was then converted to transmittance and normalized to maximum and minimum absorbance values. The cloud point for each ELP was defined as the point where the normalized transmittance fell below 95%.

In vitro Crosslinking of ELPs by FXIIIa

The ability of hELPs or conELPs to be crosslinked by FXIII was assessed by SDS-PAGE. hELPs or conELPs were diluted to a concentration of 50 µM in HEPES buffer; 0.2 U mL^{-1} Thrombin, and 20 mM $CaCl_2$ were also added to each sample in order to replicate the standard clotting conditions used throughout this work. FXIIIa was added to experimental samples at a final concentration of 10 µg mL^{-1}, while control samples received an equal volume of HEPES buffer. All samples were then incubated at 37 ˚C for 1 h, and subsequently run on a non-reducing SDS-PAGE. Samples were stained using a Coomassie-based Instant Blue stain, and imaged using a ChemiDoc Mp imaging system (BioRad).

Rheological Measurements of ELP-containing Fb Clots

The mechanical properties of *in vitro* Fb clots containing 30, 20, 10, or 5 μM hELP, 30 μM conELP, or an equal volume of HEPES buffer were assessed using an Anton Paar MCR 302 Rheometer with a cone-plate geometry (d = 25 mm; 1˚ angle). To determine their oscillatory shear moduli, frequency sweep measurements where performed, whereby clotting solutions were prepared containing 1.5, 2.2, or 3.0 mg mL^{-1} fibrinogen (Fg), hELP, conELP, or HEPES buffer, 20 mM $CaCl_2$, and 0.2 U mL^{-1} Thrombin. Immediately upon the addition of Thrombin, 90 μL of the clot solution was transferred to the preheated Peltier plate of the rheometer at 22 or 37 ˚C, the measuring cone was lowered onto the sample, and the cone was spun at 60 rpm for 5 seconds to ensure proper mixing and sample distribution. Silicone oil (η = 100 cSt) was applied to the edges of the sample in order to prevent evaporation, and the clot was allowed to equilibrate for 1 h, after which time a frequency sweep was performed from 0.1 – 3 Hz (γ = 1%; previously determined to be within the Linear Viscoelastic Region (LVE) for this material).

To assess the effects of ELPs on the strain-stiffening behaviour of Fb clots, samples containing 2.2 mg mL^{-1} Fg, and 30 μM hELP, conELP, or HEPES buffer were formed as before at 37 ˚C between the cone and plate of the rheometer. Following equilibration for 1 h, an oscillatory strain sweep was performed from 0.1 – 100% strain (f = 1 Hz).

To follow the gelation kinetics of Fb clots formed in the presence of ELPs, clotting solutions were prepared as described above (with 2.2 mg mL^{-1} Fg, and 30 μM conELP, or 5, 10, 20, or 30 μM hELP, or HEPES), and then placed between the cone and plate of the rheometer at 37 ˚C, immediately following the addition of $CaCl_2$ and Thrombin. A small amplitude oscillatory shear stress was applied to the forming clot ((γ = 1%; f = 1 Hz) and the evolution of G’ and G’’ were measured for 1 h. The gel point for each clot was defined as the point where G’ exceeded G’’ and did not subsequently fall below G’’ for the remainder of the experiment.

Thromboelastography (TEG)

A TEG 5000 (Haemonetics, Signy, Switzerland) was used to conduct thromboelastographic measurements on clots. Clotting solutions were prepared with 1.5 or 3.0 mg mL^{-1} Fg, and 30 μM conELP, hELP, or a HEPES buffer control. These solutions were

warmed to 37 ˚C, $CaCl_2$ and thrombin were added to concentrations of 20 mM and 0.2 U mL^{-1}, respectively, and 360 µL of solution was then transferred to the cup of the TEG 5000. The pins of the TEG were quickly inserted into the clotting solution, with care being taken to ensure that the time from the addition of the final clotting components to the insertion of the pin was similar between samples. The cups of the TEG would then oscillate around the free-standing pin, which would become displaced to a greater degree as the clot began to solidify. The experiment was allowed to run until the max amplitude of the sample was established.

Turbidimetry measurements of gelation kinetics

The evolution of turbidity in gelling Fb clots was measured over a range of wavelengths in order to study gelation kinetics. In a typical experiment, clotting solutions consisting of 2.2 mg mL^{-1} Fg, 20 mM $CaCl_2$, 0.1 U mL^{-1} thrombin, and one of 30 µM hELP, 30 µM conELP, or HEPES, were prepared in cuvettes and immediately transferred to an Evolution 260 Bio UV-Vis spectrophotometer (Thermo Scientific) that had been preheated to 37 ˚C. Absorbance was then measured 350 nm, and this measurement was repeated every 15 s for the 1-hour time course of the experiment.

Perfusion Assay for Determining Fb Clot Pore Size

The pore sizes of Fb clots with or without ELPs were evaluated via a perfusion assay which had been adapted from a previous work by Carr and Hardin.[41] Clots were formed at the bottom of upright gravity filtration columns which had had their tips cut off and sealed by parafilm, in order to support the clotting solution during gelation. 1 mL of clotting solution was used in each experiment, consisting of 1.5 mg mL^{-1}, 20 mM $CaCl_2$, 0.1 U mL^{-1} Thrombin, and 30 µM hELP or conELP, or an equal volume of HEPES buffer. Clots were allowed to form for 1 h at 22 or 37 ˚C, after which time 13 mL of isotonic and isothermal HEPES buffer was dispensed on top of each clot, and the clots were allowed to equilibrate for 10 minutes. The flow rate was then determined gravimetrically, by measuring the mass of buffer passing through the clots every 10 minutes for 50 minutes. The pore radii (r_p) of clots with and without ELPs were then calculated from the volumetric flow rate according to Darcy's Law, and a model developed by Carr and Hardin for determining the pore sizes of Fb clots containing embedded erythrocytes:[41]

$$Da = \frac{V\eta h}{AtP} \quad \text{Eq. 3-1}$$

$$r_p = \frac{0.5093}{Da^{-1/2}} \quad \text{Eq. 3-2}$$

where *V* is the volumetric flow rate, η is the viscosity of water (0.9544 mPa s @ 22 ˚C, 0.6913 mPa s @ 37 ˚C), *h* is the length of the clot, *A* is the cross-sectional surface area, *t* is time, and *P* is the average hydrostatic pressure exerted by buffer above the clot over the course of the experiment.

Fluorescent labelling of hELPs

To study FXIIIa-mediated integration of hELPs into Fb clots, we labelled hELPs and conELPs preferentially at the N-termini of the proteins with the fluorescent dye Atto647-N-hydroxysuccinimide (Atto647-NHS). By performing the reaction at pH 8, we selectively targeted α-amino groups with lower pK_a, preserving lysine *ε*-amino groups in the K-block for FXIIIa-mediated cross-linking post labelling. Using the extinction coefficients for hELP/conELP (ε_{280} = 2.75 x 10^4 M^{-1} cm^{-1}) and Atto647 (ε_{647} = 1.5 x 10^5 M^{-1} cm^{-1}), we determined the average number of fluorescent dye molecules per ELP molecule to be ~ 0.95. We tested whether fluorescent-hELPs (f-hELPs) maintained the ability to be cross-linked by FXIIIa using SDS-PAGE. Disappearance of the single f-hELP band at ~69.5 kDa in samples containing FXIIIa indicated that sufficient active lysine residues remained following fluorescent labelling with Atto647-NHS to allow f-hELPs to be cross-linked by FXIIIa (**Appendix Figure A1**).

Confocal Imaging

Confocal microscopy was used to study the integration of hELPs into Fb networks. For imaging experiments, clots were formed in the channels of an Ibidi µ-slide VI 0.5 (Glass Bottom) from 40 µL clotting solutions consisting of 1.5 mg mL^{-1} fibrinogen (spiked with 1% fluorescent Fg-488), 0.2 U mL^{-1} thrombin, 20 mM $CaCl_2$, and one of 30 µM f-hELP, 30 µM f-conELP, or HEPES buffer. Clots were formed for 1 h at either 22 or 37 ˚C, and then transferred to the imaging chamber of a Nikon Ti2-A1 confocal microscope with a 60x objective, which had been preheated to the relevant temperature. 40 µL of buffer were added to each port of the slide in order to avoid loss of water from the clot over the course of the experiment. 5.06

μm, 5-slice z-stacks were then taken at three different positions in each clot using first 488 (Fb channel) and then subsequently 640 nm (ELP channel) lasers. Three different clots were imaged per treatment group.

Plasminolysis assay

For degradation experiments, clots were formed in μ-slide ibidi 8-well chambered coverslips from 100 μL of clotting solution consisting of 1.5 mg mL^{-1} fibrinogen (spiked with 1% Fg-488), 0.2 U mL^{-1} thrombin, 20 mM $CaCl_2$, and one of 30 μM hELP, 30 μM conELP, or HEPES buffer. Samples were allowed to gel for 1 h at 37 ˚C, after which half of each formed clot was cut out of the wells of the coverslip with a scalpel. The cover slips were then placed into the imaging chamber of the microscope (with a 40x objective) at 37 ˚C, and the edge of the Fb network was located using the 488 nm laser. A preheated solution of 10 μg mL^{-1} plasmin was then applied to the edge of the clot, and images were taken every 10 s until the clot had been completely removed from the microscope field-of-view. Images were taken at three different positions in each clot, and three different clots were made for each treatment group.

SEM imaging

Fibrin clots were prepared on 12 mm glass coverslips, from solutions with the following concentrations of components: 1.5 mg mL^{-1} Fg, 0.2 U mL^{-1} thrombin, 20 mM $CaCl_2$, and one of 30 μM hELP, 30 μM conELP, or HEPES buffer. All of the components were mixed together, less $CaCl_2$ and thrombin, the solution was preheated to 37 ˚C, then the final two components were added, and 130 μL of this solution was transferred to the surface of the coverslip. Clots were allowed to form for 1 h at 37 ˚C, after which they were transferred to a solution of 2.5 % glutaraldehyde (also at 37 ˚C), and fixed for 1 h. Samples were then washed 5 times in DI H_2O, for 5 minutes per wash, and then dehydrated in increasing percentages of ethanol (25, 50, 75, 100, 100; 10 minutes per treatment). Samples were subsequently dried by critical point drying, and then sputter-coated in platinum before being imaged in a Hitachi S-4800 SEM (Hitachi, Japan).

In vitro cell viability assay

The effects of ELP coacervates on the viability of human dermal fibroblasts (neonatal; HDFn) cells were investigated by means of a resazurin-based assay. HDFn cells were seeded into the wells of a 96-well tissue culture treated plate at a density of 20 000 cells/well and were incubated for 24 h at 37 ˚C, 5 % CO_2. Cells were then treated with stock solutions of conELP or hELP dissolved in DMEM, to final concentrations of 30, 50, or 80 μM ELP. Cells in control wells were treated with an equivalent volume of DMEM, and then the plate was incubated for an additional 24 h at 37 ˚C, 5 % CO_2. A stock solution of resazurin in 10 mM PBS was then applied to each experimental and control well, up to a final concentration of 10 μg mL^{-1}, the plate was incubated at 37 ˚C for 4 h, and then the fluorescence of each well was measured on a Safire II plate reader (λ_{exc} = 531 nm, λ_{emi} = 572 nm). The final cell viability for each treatment was determined by taking the average fluorescence intensity per treatment (minus a cell-free blank) and dividing it by the average fluorescence intensity of the ELP-free control.

Characterization of cell spreading in ELP-fibrin clots

Three-dimensional cell culture of human dermal fibroblasts (neonatal, HDFn) was used to assess the effect of ELPs on the migration of cells in fibrin clots, in a protocol that was adapted from the literature.[15,42] In a typical experiment, HDFn cells were grown to a confluence of 70 – 80% in a T75 flask with DMEM (10% FBS, 1% Pen/Strep). Cells were subsequently trypsinized, spun down, and re-suspended in DMEM to a concentration of 100 000 cells/mL. Cells were then seeded in the wells of a 96-well Nunclon Sphera microplate (Thermo Scientific) to a final concentration of 12 500 cells/mL in 200 μL of DMEM, and then the plate was spun at 250 g for 5 minutes. The plate was then incubated at 37 ˚C, 5% CO2 for 72 hours to allow spheroids to form. After 72 hours, fibrin clots with or without ELPs (at a range of fibrin and ELP concentrations) were formed from 100 μL of clotting solution (Fg, ELP, 20 mM CaCl2, 0.1 U mL^{-1} thrombin) on the surface of flat-bottomed 48-well plates (Starstedt). Clots were allowed to gel for 1 hour at 37 ˚C. After this time, 100 μL of media was removed from Nunclon plates, and replaced with 100 μL of 2x clotting solution, after which the entire 200 μL mixture along with the spheroid was transferred to the coated 48-well plates and allowed to gel for 1 hour at 37 ˚C. 500 μL of DMEM was added on top of the clots, and

spheroids were imaged at 10x magnification on a brightfield microscope. Plates were then incubated at 37 ˚C, 5% CO2 for up to 72 hours, and spheroids were imaged every 24 hours in order to monitor cell spreading. Media was replaced after 48 hours.

Results & Discussion

Design and characterization of hemostatic ELPs (hELPs)

We designed hELPs with an ABC triblock architecture (**Figure 3-1A**). The repetitive ELP component present in all three blocks comprised 11 VPGXG pentapeptides with alanine, valine, and glutamic acid

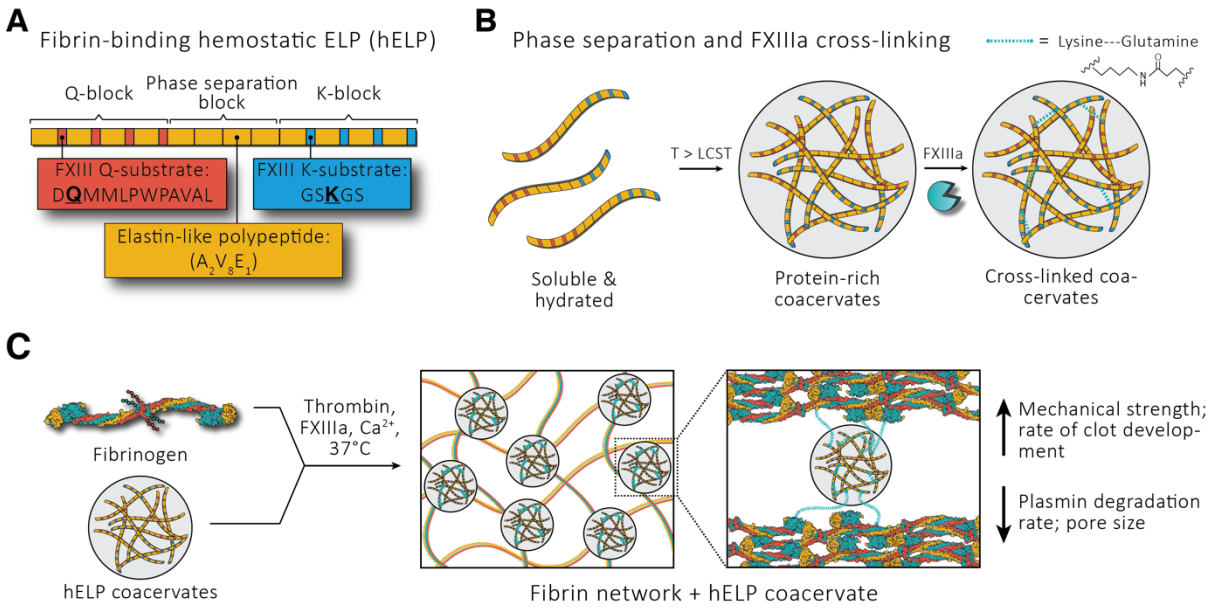

Figure 3-1. Schematic representation of hELP design, and integration into Fb clots. A) hELPs were designed as triblock copolymers containing a Q-block, a phase separation block, and a K-block. B) Above the LCST, hELPs phase separate to form coacervates, which can be covalently cross-linked by FXIIIa. C) Upon mixing with fibrinogen, thrombin and FXIII, hELP coacervates covalently integrate into Fb networks and improve mechanical strength in a phase-dependent manner, and also improve the rate of clot development following the initiation of clotting, reduce the plasmin degradation rate, and reduce the Fb network pore size. Depictions of hELPs are schematic only, and may not reflect molecular structure.

residues in guest positions at a ratio of 2:8:1 ($A_2V_8E_1$). Coacervation of ELPs above their LCST is accompanied by formation of ordered structures (e.g., β-spirals), and reduction in solvent accessible surface area.[29] The LCST of ELPs is influenced by a number of factors, including

chain length, concentration, guest residue composition, and external factors such as ionic strength and pH.[43] Based on prior literature, we designed hELPs to have an LCST slightly below physiological temperature so that coacervation was triggered when hELPs entered the physiological environment. In addition to the ELP component, the N-terminal hELP block, referred to as the Q-block, also contained 4 transglutaminase tags (**Figure 3-1, Appendix Table 3A-1**), each comprising a single glutamine residue embedded within a contextual sequence (DQMMLPWPAVAL). This contextual sequence was derived from prior work[38] which used phage display to identify a glutamine donor sequence that is recognized with high efficiency by FXIIIa. By embedding these glutamine donor sequences in the broader hELP sequence, we hypothesized that hELPs would selectively integrate into Fb networks at wound sites where FXIII is activated, while avoiding off-target interactions with soluble fibrinogen.[44,45] We furthermore mutated a lysine residue within the contextual sequence to alanine (K11A), in order to eliminate the possibility of cross-links forming between Q-blocks. The middle phase separation block consisted of 4 consecutive A2V8E1 units, totaling 48 pentapeptide repeats. This block physically separated the Q and K-blocks and extended the overall length of the hELP, thereby driving the LCST below physiological temperature. The K-block followed the phase separation block at the C-terminus of hELPs, and comprised 4 lysine-donor sequences (GSKGS), which served as the complementary partner to glutamine in the reaction catalyzed by FXIIIa. A control ELP (conELP) was also prepared with the same sequence as hELP, except that glutamine and lysine residues were mutated to glycine such that conELP was not cross-linked by FXIIIa.

We cloned, expressed and purified hELPs and conELPs by inverse transition cycling (ITC), and measured LCSTs using a cloud point assay.[46] Molecular weights of hELPs and conELPs were confirmed by mass spectrometry (**Figure 3-2**). At a working concentration of 30 μM, both hELP and conELP exhibited cloud points below 37 ˚C (32.7 and 34.1 ˚C respectively), indicating that both ELPs were aggregated at physiological temperature (Figure 2c). Next, we confirmed the functionality of the Q- and K-blocks by testing the ability of FXIIIa to cross-link hELP in the absence of Fg using SDS-PAGE (Figure 2d). A reduction in intensity of the band corresponding to single hELP polymers (~ 69.5 kDa), and the appearance of bands of higher molecular weights corresponding to hELP dimers and multimers confirmed that FXIIIa was capable of cross-linking hELPs. Meanwhile, samples of conELP incubated with FXIIIa were not cross-linked.

Integration of hELPs into Fb networks

We N-terminally labelled hELPs and conELPs with Atto647-N-hydroxysuccinimide (red channel) and confirmed they were still cross-linked by FXIIIa (**Appendix Figure 3A-1**). Fluorescent-hELPs (f-hELPs) or fluorescent-conELPs (f-conELPs) were then integrated into Fb clots spiked with 1 % AlexaFluor 488-labelled fibrinogen (Fg-488, green channel). We used two color confocal fluorescence microscopy to characterize hELP and Fb network morphology, degree of hELP and Fb colocalization, and the influence of hELP phase transition on clot architecture. At 22 ˚C, all three clots (HEPES-Fb, conELP-Fb and hELP-Fb) resulted in well-defined Fb networks when imaged in the green Fb channel (**Figure 3-3**). When imaged in the red hELP channel, f-hELP fluorescence similarly showed an ordered network with high degree of spatial colocalization between hELP and Fb signals. We observed little to no fluorescence intensity in the red channel when only HEPES buffer or f-conELP were added during formation of Fb networks.

To quantify hELP and Fb spatial colocalization, we used Coloc2 in ImageJ to calculate Pearson's correlation coefficients (PCC).[47] For f-hELP-Fb clots at 22 ˚C, a PCC between f-hELP and Fb channels of 0.69 $\pm$ 0.1 indicated high spatial correlation. For f-conELP-Fb clots, a PCC value of 0.05 ± 0.09 indicated no spatial correlation (**Figure 3-3B**). These results demonstrate that when hELP is mixed with Fb and FXIIIa below the LCST, it is specifically cross-link and localizes to Fb fibres.

At 37 ˚C, above the hELP LCST (**Figure 3-3C**), the structures observed in conELP-Fb and hELP-Fb clots were consistent with the expected phase separation. Punctate spots of high ELP density indicated the formation of ELP-rich coacervates at T > LCST. The density of ELP-rich coacervates was greater in f-hELP-Fb clots than in f-conELP-Fb clots due to conELPs lacking the Q and K residues required for covalent integration. F-hELP coacervates were not randomly distributed relative to the Fb network, exhibiting some colocalization with Fb fibrils. Image analysis of hELP-Fb clots at 37 ˚C yielded a PCC value of 0.163 ± 0.04. For f-conELP-Fb clots formed at 37 °C, we measured a PCC value of -0.04 ± 0.06, indicating no spatial correlation. The average diameter of hELP coacervates was determined from threshold images of three separate clots, and was found to be 0.73 $\pm$ 0.10 μm (**Appendix Figure A2**). The unimodal distribution of hELP coacervate sizes with a clear central peak suggests an energy balance that caps the growth of hELP coacervates inside Fb gels. Prior work on enzymatically cross-linked

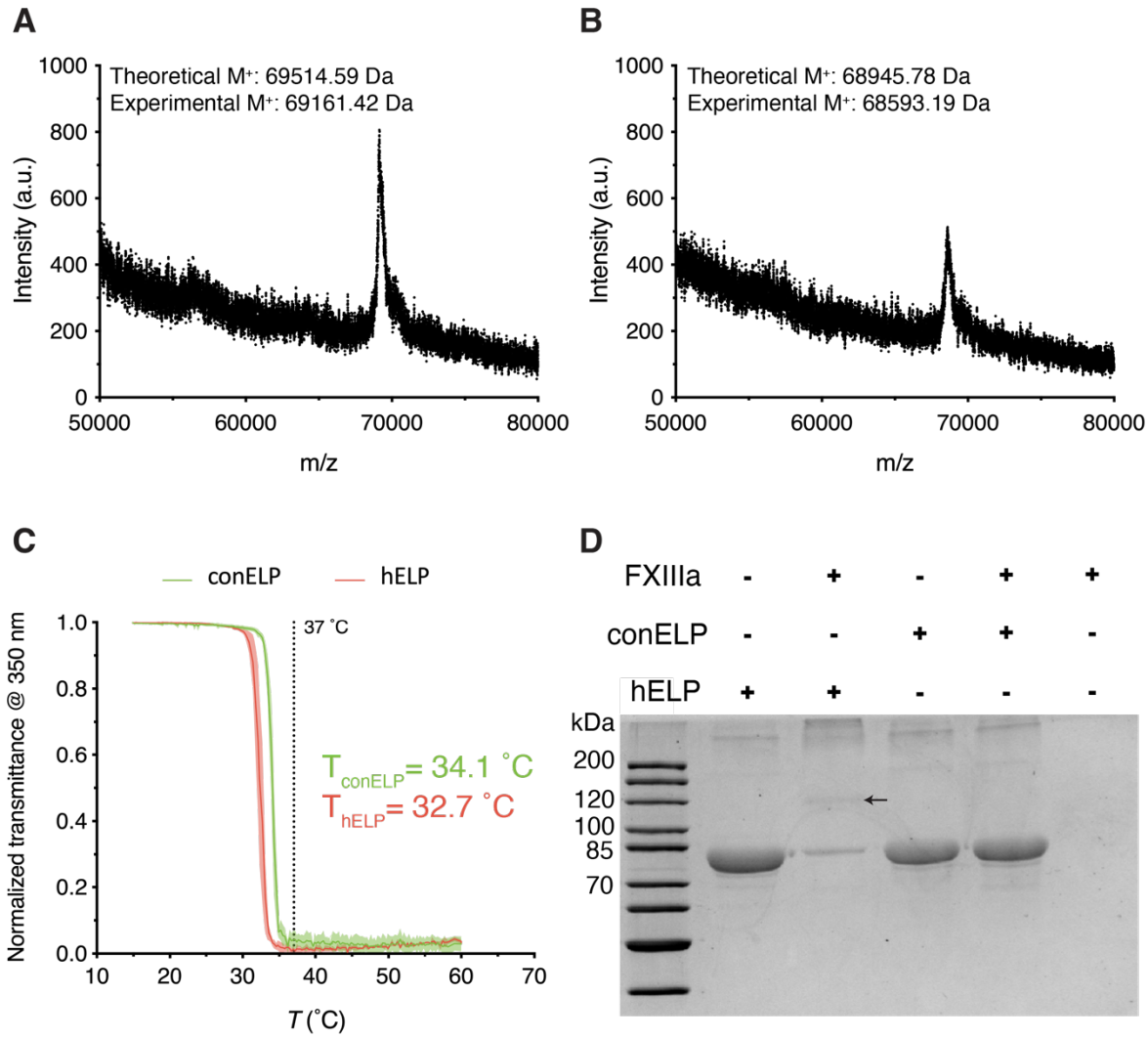

Figure 3-2. Characterization of ELPs. MALDI-TOF mass spectrometry measurements of A) hELP and B) conELP after purification by ITC. C) Cloud points were determined for 30 µM solutions of hELP or conELP in 20/150 mM HEPES/NaCl + 20 mM $CaCl_2$. Cloud points were defined as the temperature at which normalized transmittance fell below 0.5. Data shown are mean ± SD (shaded area) (n = 2). D) SDS-PAGE gel following incubation of 50 µM hELP or conELP with 10 µg mL^{-1} human FXIIIa for 1 hour at 37 ˚C. The arrow indicates the position corresponding to hELP dimers.

ELP hydrogels[48], or enzymatic integration of ELPs into collagen networks[49] has reported that enzyme-mediated cross-linking was not inhibited above the LCST. Our results are also consistent with these findings, and indicate that coacervation did not inhibit hELP association with Fb networks. In fact, multivalent hELP-rich coacervates with locally increased concentration Q- and K-blocks may enhance FXIIIa-mediated cross-linking.

SEM images of 1.5 mg mL^{-1} Fb clots formed at 37 ˚C in the presence of 30 µM ELP or HEPES buffer further highlight the structural effects hELPs have on Fb networks (**Figure 3-3D**).

ConELP-Fb clots and HEPES-Fb clots both showed porous networks of thick fibres with relatively low degrees of branching. The addition of hELPs led to the formation of denser Fb networks, with thinner and more highly branched fibres. Furthermore, round aggregates bearing similarity to the coacervates observed in confocal microscopy were observed along the length of many of the fibres. The size of the putative ELP coacervates in the SEM images is significantly smaller than that determined from confocal microscopy images. We attributed this size different to dehydration of the samples during SEM sample preparation.

FXIII is highly selective during the initial glutamine-binding step of the acyl transfer reaction, and less selective during the secondary step involving lysine recognition.[38] Typically FXIII cross-links Fb γ-chains into dimers, and α-chains into multimers. Cross-linking of γ-chains is known to occur more quickly, and involves γ406K on one chain linking to γ398/399Q of another chain.[45,50] Cross-linking of Fb α-chains by FXIII also occurs at multiple Q/K residue pairs.[45] Numerous Q and K-residues on Fb γ-chains and α-chains are therefore the likely sites for hELP coacervate cross-linking through the Q- and K-blocks.

The potential for hELPs to be cross-linked by other transglutaminases does exist, however, the glutamine donor sequence used in the Q-block has high specificity for human FXIII, and low reactivity with another ubiquitous transglutaminase, TGase 2.[38] Furthermore, FXIII is activated most effectively when bound to fibrin at wound sites, therefore the concentration of FXIIIa is highest at these sites, with minimal systemic concentration found in the blood. Following FXIII activation and fibrin cross-linking, both FXIII and FXIIIa are broken down by proteases released by polymorphonuclear granulocytes (PMNs), further limiting their presence in blood.[45] Based on these factors, we expect that hELP cross-linking will be localized to wound sites in vivo, and that the potential for off-target interactions of hELPs following intravenous administration is minimal.

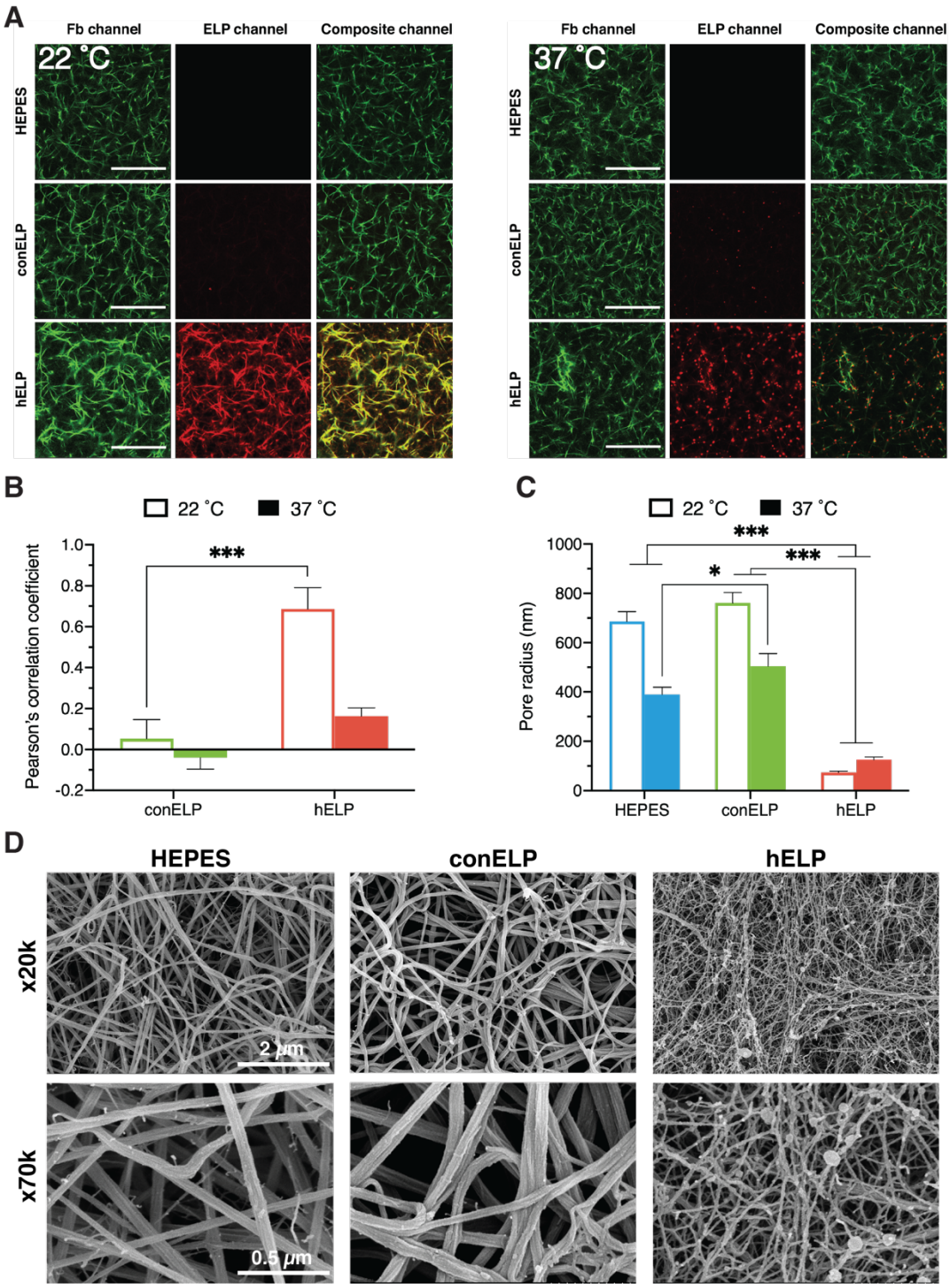

Figure 3-3. Characterizing structural morphology of hELP-Fb clots. A) Two color confocal fluorescence microscopy of 1.5 mg mL^{-1} Fb clots formed at 22 or 37 ˚C, with 30 µM f-conELP, 30 µM f-hELP or HEPES buffer as additives. Scale bars are 30 µm. B) Comparison of Pearson's correlation coefficients quantifying spatial colocalization of signals from the Fb (green) or ELP (red) channels in confocal fluorescence images. C) Pore sizing of 1.5 mg mL^{-1} Fb clots containing 30 µM hELP, 30 µM conELP, or HEPES buffer. D) SEM images of 1.5 mg mL^{-1} Fb clots formed at 37 ˚C, with HEPES, 30 µM conELP or 30 µM hELP as additives. Images were taken at 20000 and 70000x magnifications. Statistical significance in panels b and c was determined using one-way analysis of variance (ANOVA) with Tukey's Post Hoc test. *P <0.05, ***P < 0.001. All data in panels b and c are shown as mean ± SD (n = 3).

Quantification of pore sizes

Pore size is an important architectural feature that contributes to Fb clot stiffness and resistance to enzymatic degradation.[51] Covalent cross-linking of Fb fibrils by FXIIIa reduces pore size, while supplemental FXIIIa *in vitro* increases stiffness and resistance to fibrinolysis.[52,53] We investigated the effect of hELPs using a gravimetric perfusion assay where we measured liquid flow rates through hELP-Fb clots and then used Darcy's law and a model developed by Carr and Hardin to estimate pore size.[41,51]

At 22 ˚C, the flow rates through HEPES-Fb and conELP-Fb control clots were ~100x higher than the flow rates through hELP-Fb clots (**Appendix Figure A3**). These flow rates translated into average pore radii of 686.6 ± 39.3, 761.2 ± 41.8, and 73.6 ± 5.4 nm for HEPES-Fb, conELP-Fb, and hELP-Fb clots, respectively (**Figure 3-3C**). The ~10-fold smaller pore radius observed for hELP-Fb clots represented a significantly larger pore size reduction than previously reported for clots treated with either supplementary FXIII (a 2.1x reduction),[52] or synthetic fibrin-binding polymers (a 1.5x reduction).[51] SEM analysis of HEPES-Fb, conELP-Fb, and hELP-Fb under vacuum was also qualitatively consistent with pore size reduction **(Figure 3-3D).**

At 37 ˚C, pore radii in both HEPES-Fb and conELP-Fb control clots were smaller than at 22 ˚C (390.3 ± 28.9 nm and 504.3 ± 51.3 nm, respectively), which we attributed to a temperature-dependence of FXIIIa activity.[45] In hELP-Fb clots however, the pore radius at 37 ˚C was 124.8 ± 11.5 nm, slightly larger but not significantly different from the radius at 22 ˚C (**Figure 3-3C**). An increase in temperature from 22°C to 37°C therefore did not lead to a significant change in apparent pore size as measured by gravimetric perfusion for hELP-Fb clots, as was observed in the controls. This could indicate that hELP-Fb clots are already maximally cross-linked at 22 °C.

Gelation Kinetics

We investigated the effect of hELPs on gelation kinetics of 2.2 mg mL^{-1} Fb clots using low-strain oscillatory shear rheology under physiological conditions, focusing in particular on the shear storage (*G'*) and loss (*G''*) moduli. HEPES-Fb and conELP-Fb clots, an initial lag phase was followed by a period of rapid gelation, and a secondary phase of slower asymptotic growth of *G'* **(Table 3-1; Figure 3-4**). The gelation time for conELP-Fb and HEPES-Fb clots

(defined as the point where *G'* > *G''*) occurred at 390 and 330 s, respectively, while the gel point for hELP-Fb clots (with 30 µM hELP) occurred significantly later at 540 s. In order to determine if steric hinderance of Fb clot formation was occurring due to high concentrations of hELP, we also performed the experiment on clots containing 20, 10, and 5 µM hELP, and found that the gel point occurred earlier than controls in Fb clots with 10 µM hELP. Following onset of gelation, *G'* of hELP-Fb clots increased more rapidly than in HEPES-Fb or conELP-Fb clot at all hELP concentrations, however this effect was most pronounced with the addition of 20 and 30 µM hELP. In clinical hemostasis, Fg concentrations below ~2.3 mg mL^{-1} are associated with increased mortality.[51] By defining the maximum *G'* achieved by HEPES-Fb clots over 3600 s in this experiment as the critical threshold (specifically, 127.6 ± 18.1 Pa), we could quantify the time required for hELP-Fb clots to reach a stiffness significantly greater than that of clots formed at this critical Fg concentration. Clots formed with 30 µM hELP exceeded this threshold after 1860 s, clots formed with 20 µM hELP did so after 1470 s, and clots formed with 10 µM hELP did so after 2160 s. ConELP-Fb clots, and clots formed with 5 µM hELP never significantly exceeded this threshold. The presence of hELP coacervates therefore had an inhibitory effect on time until initiation of clotting, but a positive effect on the subsequent rate of clot development.

We further investigated the effect of hELPs on gelation kinetics using a turbidity assay in a UV-Vis spectrophotometer (**Figure 3-5A**). Prior work has shown that the gelation of Fb clots correlates with an increase in the turbidity of the clot.[51,54,55] In our experiment, absorbance values of gelling Fb clots were measured at 350 nm over a period of 1 h at 37 ˚C. Several distinct gelation profiles emerged across the different groups. HEPES-Fb clots showed a brief initial lag phase of gelation, followed by a gradual increase in absorbance over a period of approximately 6 minutes, after which absorbance reached a plateau at 0.75 ± 0.12 AUs. ConELP-Fb clots had a similar initial lag phase, but this was followed by a more rapid increase in absorbance lasting approximately 45 s, after which a plateau was reached at 0.38 ± 0.07, which was significantly lower than the one seen in HEPES-Fb clots. The absorbance profile of hELP-Fb clots showed a lag phase and growth phase that were similar in length to the ones observed in conELP-Fb clots, however, hELP-Fb clots reached a significantly higher plateau absorbance of approx. 0.9 ± 0.02.

Table 3-1. Gelation kinetics parameters from rheological measurements of 2.2 mg mL^{-1} Fb clots forming at 37 ˚C

Sample	Gel point [s]	Time until $G' > G'_{2.2}$[a] [s]	Max $\partial G'/\partial t$ [Pa s^{-1}]
HEPES	330	N/A	0.08
30 µM conELP	390	N/A	0.13
5 µM hELP	480	N/A	0.14
10 µM hELP	300	2160	0.21
20 µM hELP	690	1470	0.28
30 µM hELP	540	1860	0.27

[a)]The time until G' of sample exceeds the maximum G' of the HEPES control

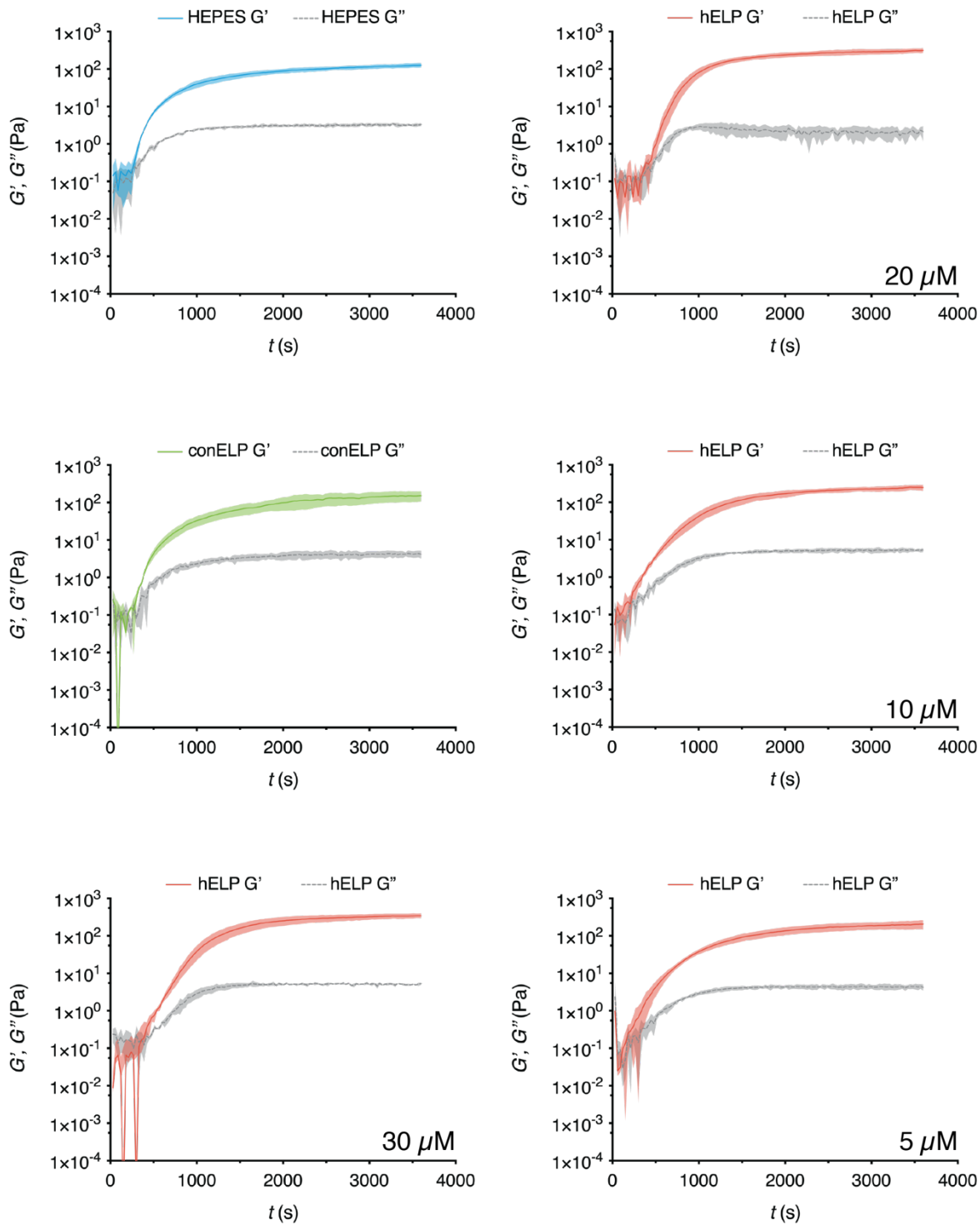

Figure 3-4. Rheological measurements of clot gelation kinetics. Evolving storage (G') and loss moduli (G'') of gelling 2.2 mg mL^{-1} Fb clots with 0.1 U mL^{-1} thrombin and 20 mM $CaCl_2$; containing HEPES, 30 μM conELP, or 30 – 5 μM hELP as measured over 1 h gelation time at 37 ˚C. Clots were subjected to a constant oscillatory shear stress (γ = 0.1 %; f = 1 Hz). Shaded areas show one standard deviation from the mean (n = 3).

Influence of hELPs in thromboelastography

Thromboelastography (TEG) is a clinical technique for measuring the clotting capacity of blood, which is based on the displacement of a free-moving pin, submerged in a clotting blood sample within a rotating cup.[56] Here, we evaluated three TEG parameters, namely reaction time (R), which measures the time to initiation of clot formation (i.e. the time until pin displacement reaches 2 mm), α-angle which measures the rate of clot development after the R point has been reached, and maximum amplitude (MA) which measures clot stiffness in terms of the maximum displacement achieved by the pin over the course of the experiment. Here too, a similar picture emerged of two-phases of hELP-Fb clot formation as was observed in the turbidimetric and rheological experiments described above. The initiation of clotting required more time in hELP-Fb clots than in conELP-Fb or HEPES-Fb clots, at both low and high Fb concentrations (**Figure 3-5B**). However, following the onset of clotting, HELP-Fb clots containing 1.5 mg mL^{-1} Fb had a significantly higher α-angle (41.43 ± 2.15˚) than HEPES-Fb or conELP-Fb controls, (27.83 ± 1.95°, 25.93 ± 3.26° respectively) (**Figure 3-5C**). When the Fb concentration was increased to 3.0 mg mL^{-1}, the increase in α-angle for hELP-Fb clots relative to controls was more modest. In this case, hELP-Fb clots had an α-angle of 58.2 ± 1.6˚ while α-angles for HEPES-Fb and conELP-Fb clots were 47.9 ± 2.31˚ and 47.07 ± 4.04˚, respectively. In previous studies, FXIII was found to be critical to the secondary phase of clot stiffening during gelation, and as hELPs are integrated into Fb clots by FXIII, it may be the case that their presence increases the rate of this secondary phase.[57] Therefore, while the initial onset of clotting takes longer in the presence of hELPs (as indicated by the increased R value), the subsequent rate of clot development is also increased; ultimately, the efficacy of hELPs as hemostats will depend on the interplay of these two factors *in vivo*.

The effect of hELPs on MA values was similar to the one observed with the α-angle. For hELP-Fb clots containing 30 μM hELP and 1.5 mg mL^{-1} Fb, MA rose 62 % and 59 % relative to HEPES and conELP-containing clots, respectively. For hELP-Fb clots formed with 3.0 mg mL^{-1} Fb, MA was 16 % higher than HEPES-Fb clots, and 24.5 % higher than conELP-Fb clots (**Figure 3-5D**). Taken together, these TEG results were consistent with shear rheology, and indicated that hELPs had a more pronounced positive effect on clot properties for clots with lower, sub-critical threshold concentrations of fibrin.

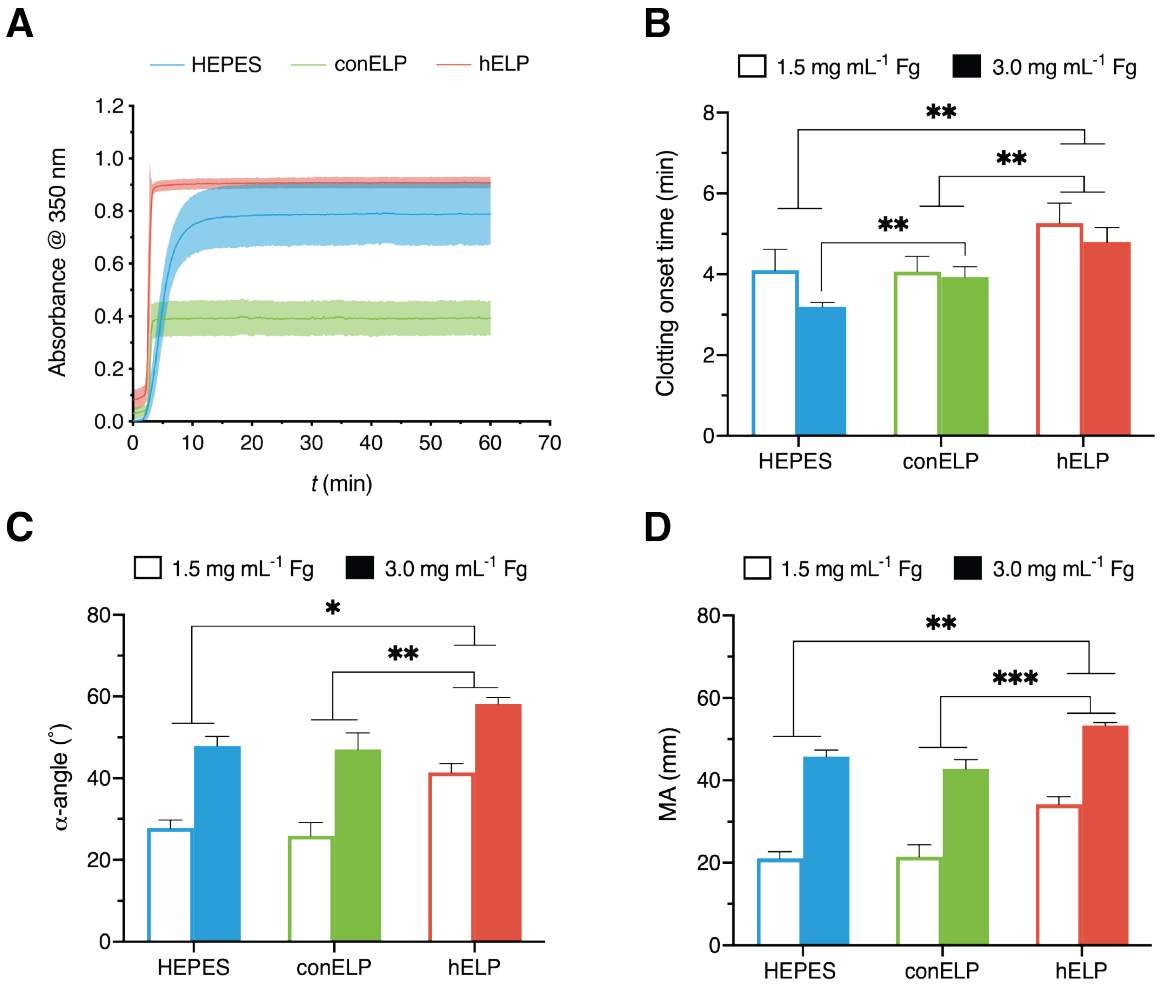

Figure 3-5. Gelation kinetics and TEG measurements of Fb clots in the presence of hELP or conELP. A) Absorbance of gelling 2.2 mg mL^{-1} Fb clots containing 30 µM hELP, conELP, or HEPES buffer at 37 ˚C at 350 nm. Measurements were taken at 15 second intervals over a period of 1 hour. B) Clotting onset time (R), C) α-angle and, D) maximum amplitude (MA) of Fb clots containing 30 µM hELP, conELP, or HEPES buffer as measured by thromboelastography at 37 ˚C. Data in panels b, c, and d are shown as mean ± SD (n = 3) *P < 0.05, **P < 0.01, ***P < 0.001; one-way ANOVA with Tukey's post hoc test.

Effect of hELP coacervates on Fb clot mechanics

We used oscillatory shear rheology to measure the effect of hELPs on clot stiffness (*G'*) with Fb concentrations above and below the critical Fb concentration threshold of 2.2 mg mL^{-1}. At 22 ˚C, no significant differences in *G'* were observed at any Fb concentration for HEPES-Fb, conELP-Fb or hELP-Fb clots (**Figure 3-6A**). At 37 ˚C, however, we found a significant increase in *G'* across all Fb concentrations for hELP-Fb clots. HELP-Fb clots with the lowest Fb concentration (1.5 mg mL^{-1}) exhibited *G'* of 201.3 ± 16.4 Pa, which was significantly higher than those of conELP-Fb (71.0 ± 11.6 Pa) or HEPES-Fb (45.0 ± 12.8 Pa) clots. The *G'* of hELP-Fb clots formed with 1.5 mg mL^{-1} Fb was equivalent to the *G'* of control clots formed at a

physiological Fb concentration of 2.2 mg mL^{-1}. This indicated that at T > LCST, hELP coacervates restored clot stiffness to physiological values under simulated conditions of TIC and depleted Fg.[58]

The phase-transition-dependence of the stiffening effect of hELPs in Fb clots can be explained in several ways. Firstly, the high local concentration of hELP molecules in the coacervate may promote the formation of more intermolecular hELP-hELP cross-links, establishing a secondary network. *In* vivo, a similar effect is observed in the phase-separation driven formation of biomolecular condensates, wherein local concentration enhancement of substrates and enzymes can accelerate chemical reactions. This has been shown to increase rates of reaction in actin polymerization[59] and RNA catalysis, for example.[31] Secondly, aggregation of hELPs above their LCST may drive the formation of a secondary network of cross-links between Fb molecules, independent of the formation of inter-hELP cross-links. The formation of secondary networks in hydrogels by thermal assembly of ELPs was also reported by Wang *et al.*, who showed that the aggregation of hydrazide-modified ELPs cross-linked into Hyaluronic Acid hydrogels resulted in a mechanical stiffening of those materials.[37] Finally, the phase separation of hELPs bound to Fb may exert mechanical forces on Fb fibres, creating a strain-stiffening effect even in the absence of external tension, recapitulating the active cell-driven contractile strain-stiffening that occurs in fibrin networks having imbedded fibroblasts and platelets.[60] Strain-stiffening is a well-known property of Fb networks and ELP coacervation is known to stiffen ELP hydrogels and exert mechanical forces.[61–63] There is evidence that the mechanical force of molecular aggregation is applied in other contexts *in vivo*: Shin *et al.* recently showed that the phase-separation of intrinsically disordered proteins associated with chromatin functions to physically pull-together distal genomic elements, while mechanically excluding others, in a mechanism that controls DNA transcription.[64] However, given that the stiffening effect is observed for hELPs that are pre-heated/aggregated prior to Fb polymerization, active contraction/stiffening of the network by hELP coacervates may not be a major contributor to the stiffening of hELP-Fb clots.

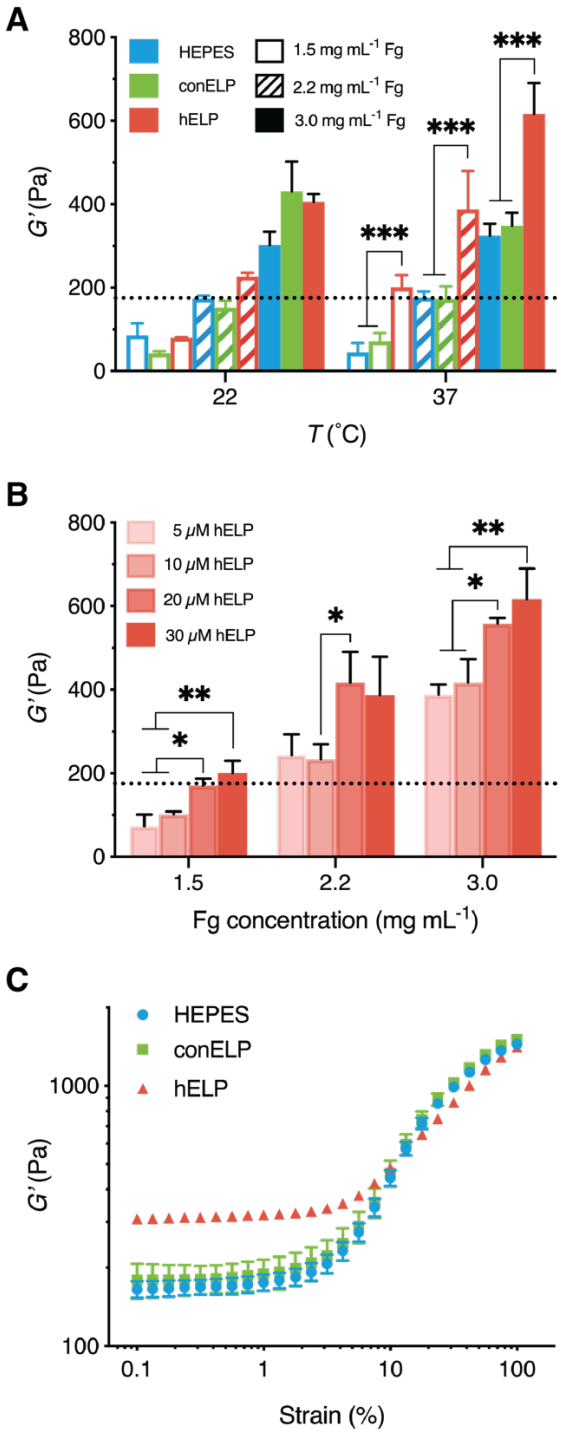

Figure 3-6. In vitro characterization of mechanical properties of hELP-Fb clots. a) Average shear storage moduli of Fb clots containing either 30 μM hELP, conELP, or an equivalent volume of HEPES buffer. Gels were allowed to form for 1 hour between the cone and plate of the rheometer at either 22 ˚C or 37 ˚C, after which a frequency sweep was performed from 0.1 – 3 Hz at 1% strain. The dotted line indicates the critical physiological threshold stiffness corresponding to the average shear storage modulus of the 2.2 mg mL^{-1} Fb HEPES control clot. b) Average shear storage moduli of 1.5 – 3.0 mg mL^{-1} Fb clots formed at 37 ˚C with 5 – 30 μM hELP as an additive. The dotted line indicates the shear storage modulus of a 2.2 mg mL^{-1} Fb HEPES control clot. c) Strain sweeps from 0.1 – 100% (f = 1 Hz) of 2.2 mg mL^{-1} Fb gels containing 30 μM hELP, conELP, or HEPES buffer at 37 ˚C. Data in all panels are shown as mean ± SD (n = 3)) *P < 0.05, **P < 0.01, ***P < 0.001; one-way ANOVA with Tukey's post hoc test.

Additionally, we investigated how different concentrations of hELP influence the mechanical stiffening of hELP-Fb clots. Frequency sweeps were performed at 37 ˚C as described above, with clots consisting of 1.5 – 3.0 mg mL^{-1} Fg, and 5, 10, 20, or 30 μM hELP (**Figure 3-6B**). When the concentration of Fg was below the critical threshold, only hELP at concentrations of 20 and 30 μM were sufficient to raise the mechanical strength of clots from subcritical to threshold levels. At Fg concentrations of 2.2 mg mL^{-1}, all concentrations of hELP were able to raise the strength of clots above that of the HEPES control (*G'* = 175.0 ± 15.5 Pa), however, the increase in stiffness was much larger for clots with 20 or 30 μM hELP (*G'* = 416.9 ± 73.8, and 387.2 ± 92.1 Pa, respectively), than for clots with 5 or 10 μM hELP (*G'* = 243.2 ± 50.4, and 233.4 ± 35.4 Pa, respectively). A similar pattern was observed at the highest concentration of Fg tested, where clots with 20 or 30 μM hELP had shear storage moduli of 557.8 ± 13.9 and 616.9 ± 73.1, respectively, and clots formed with 5 or 10 μM hELP had shear storage moduli of 388.2 ± 23.9 and 417.2 ± 56.1, respectively.

Influence of hELPs on strain-stiffening of Fb clots

Strain-stiffening in Fb clots has been attributed to the multi-scale structural organization of Fb networks, from single monomers, to protofibrils, to protofibril bundles, and fibres. According to this theory, as Fb networks are strained, force is first entropically dissipated by minimizing thermal fluctuations of flexible inter-fibril cross-links, and subsequently through the stretching of fibrils themselves. Eventually, at higher tension the secondary, tertiary, and quaternary structural elements of folded regions within Fb domains are denatured, giving rise to strain stiffening behavior that is uncommon in synthetic cross-linked polymer networks.[65,66]

To determine what effect hELPs have on Fb strain-stiffening, we performed oscillatory rheology using strain ramps from 0.1 – 100% (**Figure 3-6C**). At low strains (0.1 – 1 %), hELP-Fb clots containing 30 μM hELP and 2.2 mg mL^{-1} Fb exhibited an increase in *G'* as compared to conELP-Fb or HEPES-Fb clots, consistent with observations in the low amplitude frequency sweep experiments (Figure 5a). At medium (1 –10%) and high strains (10 – 100%), all clots showed strain-stiffening behavior, however, the onset strain of the stiffening was higher for hELP-Fb (~ 10%) than for conELP-Fb or HEPES-Fb clots (~2-3%). The rate of strain stiffening was higher in HEPES-Fb and conELP-Fb clots than for hELP-Fb clots, as indicated by the maxima of the first derivative for each curve (38.1, 38.8, and 23.1 Pa, respectively). At 100 %

strain, *G'* for all clots was roughly equal (~1400 – 1500 Pa). Comparing *G'* between 0.1 and 100 % strain, hELP-Fb clots stiffened 4.6-fold, while conELP-Fb and HEPES-Fb clots stiffened 8.8 and 8.4-fold, respectively. Considering these results in the context of Fb hierarchical structure, it seems likely that by cross-linking protofibrils, hELPs minimize thermal fluctuations of unstructured regions of the network in the low strain range.[65] Once the clot is sufficiently stretched, the elastic response is dominated by stretching of individual fibres, and therefore the addition of additional cross-links in the form of hELP coacervates no longer plays a role. Previous studies have shown that supplemental FXIII increases the elastic modulus of Fb clots at low strains within the linear viscoelastic region for fibrin, but not in the non-linear portion of the stress-strain curve, similar to what we observed here with addition of hELPs.[57]

Effect of hELP coacervates on plasminolysis

In the body, clots are enzymatically degraded by the protease plasmin, which is generated from plasminogen upon activation by tissue-plasminogen activator (tPa).[52] The proteolytic activity of plasmin is regulated spatio-temporally by binding of tPa and plasminogen to exposed cryptic binding sites on Fb clots.[67] It has previously been shown that cross-linking by FXIIIa has an inhibitory effect on fibrinolysis *in vivo*.[52] Since hELP coacervates are covalently integrated into Fb clots by FXIIIa, we hypothesized that hELPs could extend the lifetime of Fb clots in the presence of plasmin. To evaluate this, we performed time-lapse confocal microscopy.

Fluorescent Fb clots (formed with 1.5 mg mL^{-1} Fg) containing 30 µM hELP, conELP, or an equivalent volume of HEPES were formed in a chambered coverslip, and a solution of plasmin at physiological concentration (10 µg mL^{-1}) was applied to the clot front.[51] Images were taken at regular time intervals and analyzed in order to assess the proportion of clot lysed over time. Results indicated large differences in plasminolysis rates between hELP and control clots. Typically, HEPES control clots were completely degraded from the microscope field of view 4 minutes after the application of plasmin, whereas roughly 20 % of conELP-Fb and 85 % of hELP-Fb clot remained (**Figure 3-7**). The lysis rate in hELP-Fb clots was roughly three times slower than that found in conELP-Fb clots, and roughly five times slower than that found in HEPES-Fb clots. HELPs do not contain sequences recognized by plasmin[68], therefore the additional non-degradable component in the gel inhibited fibrinolysis.

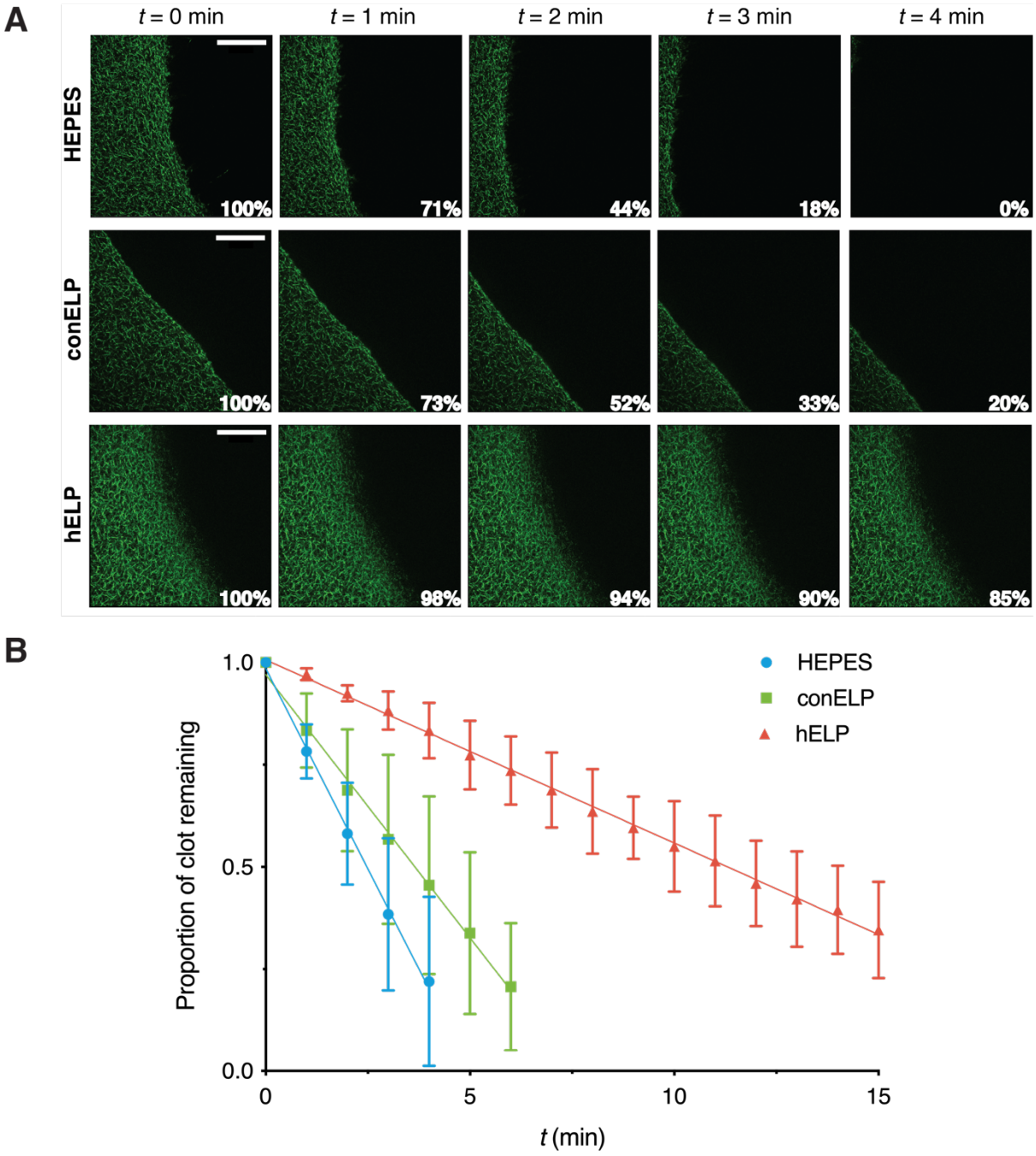

Figure 3-7. Degradation of Fb clots by a 10 μg mL^{-1} plasmin solution. a) Time-lapse Confocal images of 1.5 mg mL-1 Fb clots containing 30 μM hELP, conELP, or HEPES buffer, following exposure of the clot front to 10 μg mL^{-1} plasmin at 37 ˚C. Scale bars are 60 μm. b) Quantification of the proportion of clot lysed over time for 1.5 mg mL-1 Fb clots containing 30 μM hELP, conELP, or HEPES buffer, as determined from confocal images of multiple clots (n = 3).

Cytotoxicity of hELPs

ELPs are generally accepted as biocompatible and non-toxic, however, as with many recombinantly produced proteins from *E. Coli* there is the potential for the retention of bacterial endotoxins (i.e. lipopolysaccharides, LPS) in the purified protein product, which can lead to inflammatory and immune responses in the body.[18,69] Here, we applied an *in vitro* resazurin-based cytoxicity assay on neonatal human dermal fibroblasts (HDFn) to measure cytotoxicty of hELPs. For this experiment, ELPs were subjected to additional dialysis and lypholization steps following ITC purification to remove low molecular weight and non-aggregated LPS. No significant reduction in cell viability was observed following 24 h exposure of HDFn cells to hELP and conELP at the standard working concentration of 30 µM, as compared to untreated control cells (**Figure 3-8**). There was a significant reduction in HDFn viability observed when cells were exposed to 50 µM conELP, while exposure to 80 µM ELP led to a significant reduction in cell viability for both hELP and conELP treatments. However, even at the highest tested concentration of 80 µM, cell viability did not fall below 80 % of the control. hELP and conELP therefore have minimal cytotoxic effects under these conditions.

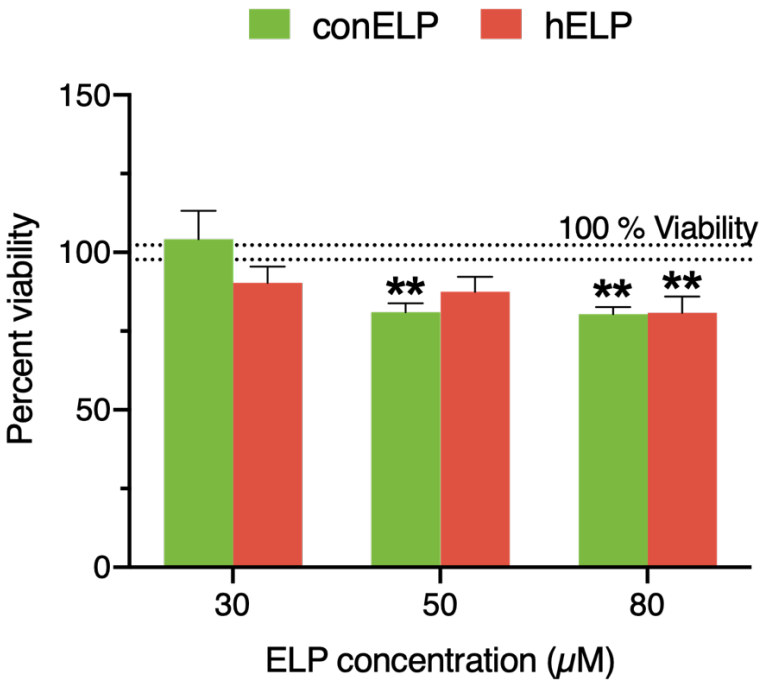

Figure 3-8. Cell viability of human dermal fibroblasts (neonatal; HDFn) following 24 h exposure to various concentrations of purified hELP and conELP under physiological conditions, as compared to a control containing only media. The area between the dotted lines is equivalent to the viability of cells in control wells ± SD. Data are shown as mean ± SD (n = 4) **P < 0.01; one-way ANOVA with Tukey's post hoc test.

Cell spreading in fibrin-hELP clots

Infiltration of fibroblasts and other cells into clots following the cessation of bleeding is an important factor in wound healing.[70] It is typically understood that stem cells and other cell types move towards stiffer regions of a substrate, and studies of stem cells cultured on hydrogel surfaces with stiffness gradients have supported the idea of durotaxis.[71,72] Similar findings have been observed for fibroblasts grown in fibrin clots that have been stiffened by artificial platelets.[15] However, the migration of cells into fibrin clots is a complex process, and some evidence exists to suggest that softer clots promote the speed of fibroblast infiltration, if not necessarily accumulation of fibroblasts in particular regions of the clot.[73] Here, we sought to determine what effect hELPs had on human dermal fibroblast migration in clots formed from varying concentrations of Fg and hELP, when those cells were culture in three dimensions *in vitro*. HDFn cells were grown as spheroids in low-adherence microplates, and then transferred into a gelling clot solution; their spreading was then measured as a function of their outgrowth from their original position within each fibrin clot. The first assay was done in a solution consisting of 1.5 mg mL^{-1} Fg and 30 μM ELP, or an equivalent volume of HEPES. Cells in HEPES clots spread almost 16-fold on average after 72 hours, while cells in hELP clots spread approx. 6-fold, and those in conELP clots spread 2-fold (**Figure 3-9**). In order to determine if there was an optimal Fg and hELP concentration for HDFn spreading, a subsequent assay was conducted in clots formed from an array of Fg (1.5, 2.2, and 3.0 mg mL^{-1}) and hELP (10, 20, and 30 μM) concentrations. Under all conditions cells spread to the greatest degree in clots formed without hELP, and then hELP addition inhibited cell spreading to a similar degree regardless of concentration (**Figure 3-10**). Interestingly, in controls without hELP, cell spreading was greatest at the lowest Fg concentration, and therefore both increasing Fg and hELP concentration had an inhibitory effect on cell spreading.

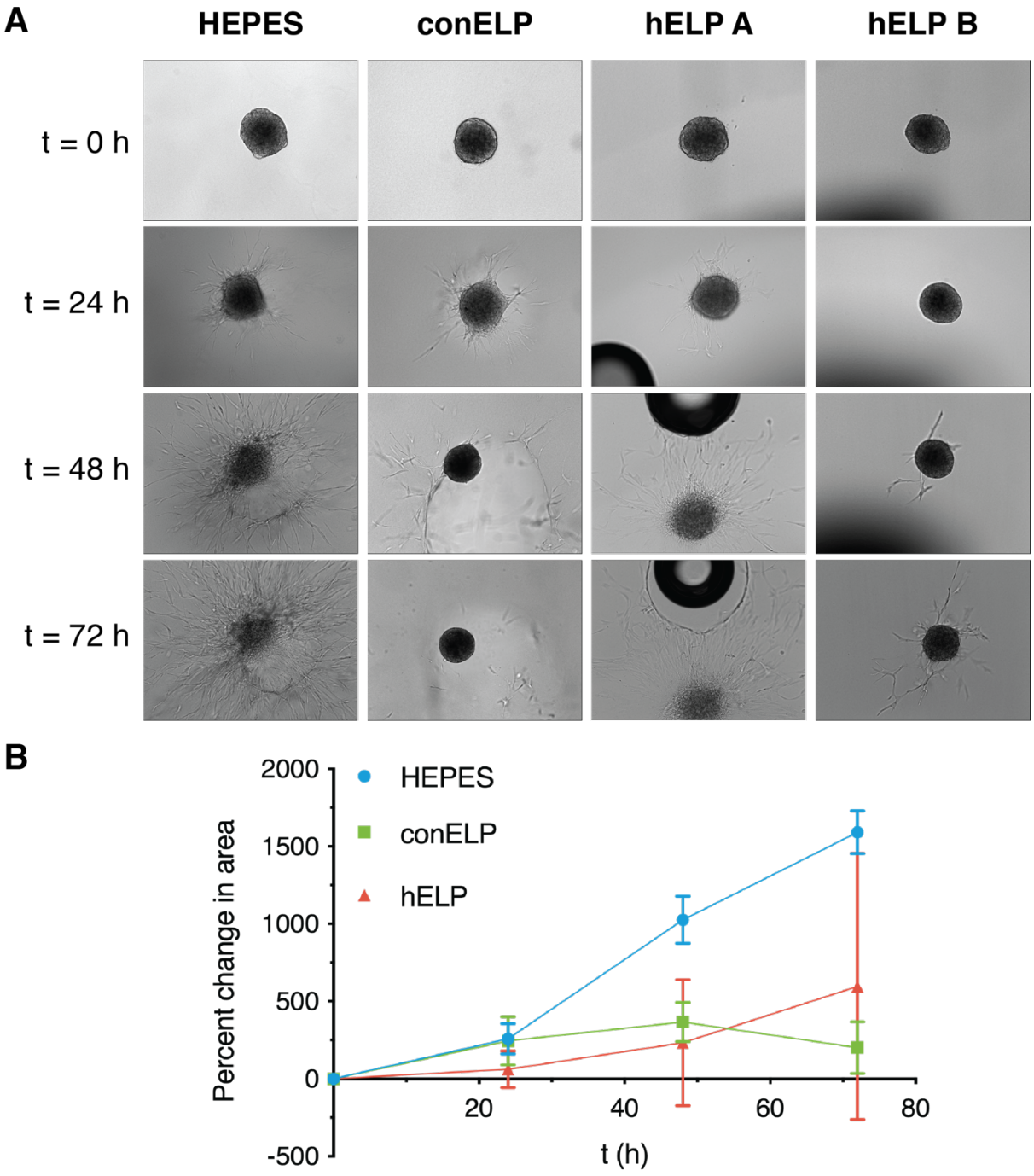

Figure 3-9. Spreading of HDFn cells cultured in fibrin clots containing 30 μM ELP or HEPES in 3D. Cells were embedded as spheroids into gelling fibrin clots, and then their migration away from the initial spheroid was followed by brightfield microscopy over 72 hours. A) Representative images of spheroids in HEPES, conELP, and two different hELP clots over the course of the experiment. B) The percent change in area of the outer limit of cell migration as compared to the initial area of each spheroid at t = 0 (n = 3).

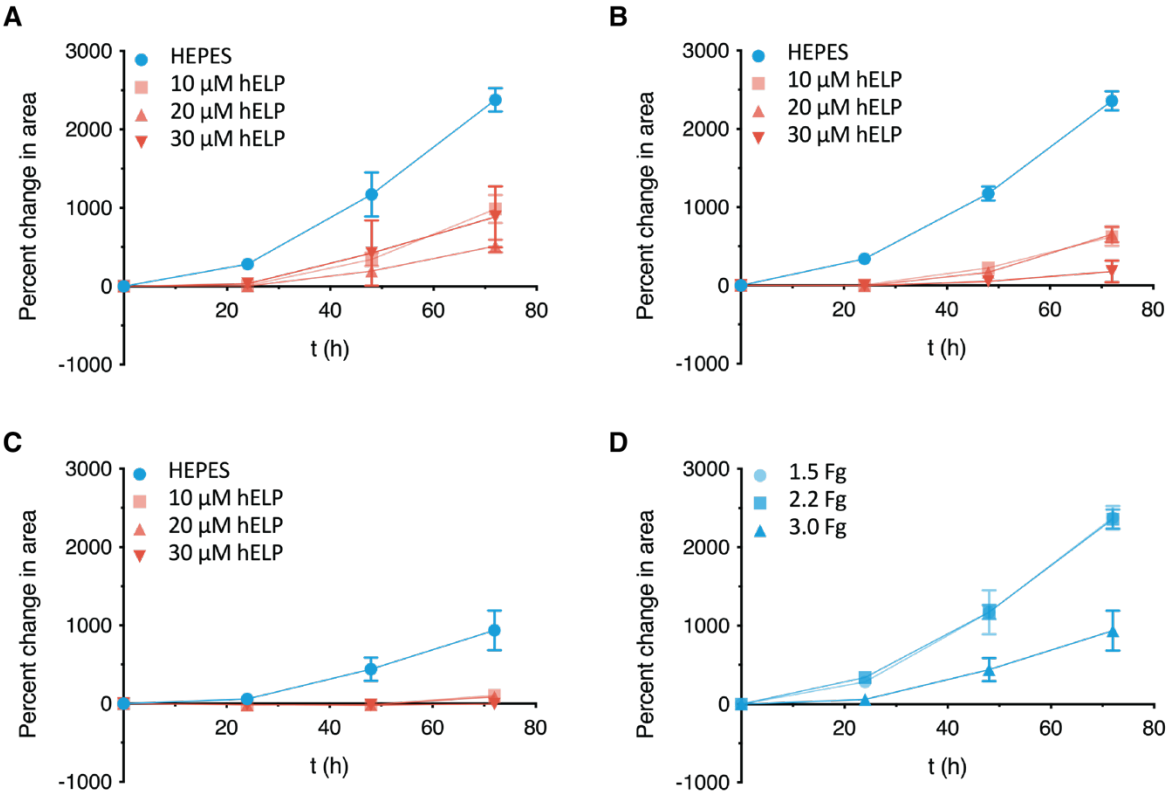

Figure 3-10. Spreading of HDFn cells cultured in 3D in fibrin clots consisting of 20 mM $CaCl_2$, 0.2 U mL^{-1} thrombin, varying concentrations of hELP, and A) 1.5, B) 2.2, and C) 3.0 mg mL^{-1} Fg. D) A comparison of HDFn spreading in fibrin clots formed with 1.5 – 3.0 mg mL^{-1} Fg.

Conclusion

We report a novel mechanism for strengthening fibrin clots based on FXIIIa-mediated cross-linking and coacervation of ELPs. Our new design for hemostatic elastin-like polypeptides (hELPs) containing N- and C-terminal repetitive Q and K-block sequences allowed them to be covalently integrated into fibrin clots via the natural clotting cascade. This approach does not require addition of cross-linking agents or bio-orthogonal functional groups, and occurs through the action of the human clotting associated transglutaminase FXIIIa. At physiological temperatures above the LCST, hELP coacervates improved the mechanical strength of fibrin clots formed under both normal and simulated coagulopathic conditions. Stiffening was not observed for fibrin networks formed in the presence of a control ELP (conELP) having non-reactive mutated FXIIIa-recognition sequences or for hELP-Fb networks formed at temperatures below LCST. This indicated that both covalent integration and phase-transition of hELPs were necessary to impart clot stiffening.

HELPs were found to reduce the flow rate of buffer through fibrin clots, thereby improving the sealing properties of these materials. The addition of hELPs to Fb networks increased kinetic gelation rate following the initiation of clotting, and increased their resistance to plasmin degradation. Furthermore, hELPs were found to be non-cytotoxic, although they did inhibit the spreading of fibroblasts through fibrin clots. We foresee this mechanism of clot stiffening based on coacervation to be applicable in clinical settings for bleeding control, as well as in the treatment of other diseases involving components of the extra-cellular matrix or in the context of tissue engineering, wherein material stiffness plays an important role.

Acknowledgements

I would like to thank Eva Bieler of the University of Basel Nanoimaging Institute for her assistance with acquiring SEM images. This work was supported by the University of Basel, ETH Zurich, the Swiss Nanoscience Institute, and the European Research Council (ERC Starting Grant MMA, 715207).

References

1. Curry, N. *et al.* The acute management of trauma hemorrhage: a systematic review of randomized controlled trials. *Crit. Care* **15**, R92 (2011).
2. Cothren, C. C., Moore, E. E., Hedegaard, H. B. & Meng, K. Epidemiology of Urban Trauma Deaths: A Comprehensive Reassessment 10 Years Later. *World J. Surg.* **31**, 1507–1511 (2007).
3. Murray, C. J. & Lopez, A. D. Alternative projections of mortality and disability by cause 1990–2020: Global Burden of Disease Study. *Lancet* **349**, 1498–1504 (1997).
4. Brohi, K., Singh, J., Heron, M. & Coats, T. Acute Traumatic Coagulopathy. *J. Trauma Inj. Infect. Crit. Care* **54**, 1127–1130 (2003).
5. Davenport, R. *et al.* Functional definition and characterization of acute traumatic coagulopathy. *Crit. Care Med.* **39**, 2652–2658 (2011).
6. Spahn, D. R. *et al.* Management of bleeding and coagulopathy following major trauma: an updated European guideline. *Crit. Care* **17**, R76 (2013).

7. Brokloff, J. Blood transfusion: An independent risk factor for post injury multiple organ failure. *J. Oral Maxillofac. Surg.* **55**, 1361 (1997).
8. Chan, L. W., White, N. J. & Pun, S. H. Synthetic Strategies for Engineering Intravenous Hemostats. *Bioconjug. Chem.* **26**, 1224–1236 (2015).
9. Chernysh, I. N., Nagaswami, C., Purohit, P. K. & Weisel, J. W. Fibrin clots are equilibrium polymers that can be remodeled without proteolytic digestion. *Sci. Rep.* **2**, 879 (2012).
10. Grannis, G. F. Plasma Fibrinogen: Determination, Normal Values, Physiopathologic Shifts, and Fluctuations. *Clin. Chem.* **16**, (1970).
11. Inbal, A. & Dardik, R. Role of Coagulation Factor XIII (FXIII) in Angiogenesis and Tissue Repair. *Pathophysiol. Haemost. Thromb.* **35**, 162–165 (2006).
12. Kattula, S., Byrnes, J. R. & Wolberg, A. S. Fibrinogen and Fibrin in Hemostasis and Thrombosis. *Arterioscler. Thromb. Vasc. Biol.* **37**, (2017).
13. Putelli, A., Kiefer, J. D., Zadory, M., Matasci, M. & Neri, D. A fibrin-specific monoclonal antibody from a designed phage display library inhibits clot formation and localizes to tumors in vivo. *J. Mol. Biol.* **426**, 3606–3618 (2014).
14. Yan, J. P., Ko, J. H. & Qi, Y. P. Generation and characterization of a novel single-chain antibody fragment specific against human fibrin clots from phage display antibody library. *Thromb. Res.* **114**, 205–211 (2004).
15. Nandi, S. *et al.* Platelet-like particles dynamically stiffen fibrin matrices and improve wound healing outcomes. *Biomater. Sci.* (2019). doi:10.1039/C8BM01201F
16. Brown, A. C. *et al.* Ultrasoft microgels displaying emergent platelet-like behaviours. *Nat. Mater.* **13**, 1108–1114 (2014).
17. Chan, L. W. *et al.* A synthetic fibrin cross-linking polymer for modulating clot properties and inducing hemostasis. *Sci. Transl. Med.* **7**, (2015).
18. MacEwan, S. R. & Chilkoti, A. Elastin-like polypeptides: Biomedical applications of tunable biopolymers. *Biopolymers* **94**, 60–77 (2010).
19. Trabbic-Carlson, K., Liu, L., Kim, B. & Chilkoti, A. Expression and purification of recombinant proteins from Escherichia coli: Comparison of an elastin-like polypeptide fusion with an oligohistidine fusion. *Protein Sci.* **13**, 3274–3284 (2004).
20. McHale, M. K., Setton, L. A. & Chilkoti, A. Synthesis and in vitro evaluation of enzymatically cross-linked elastin-like polypeptide gels for cartilaginous tissue repair.

Tissue Eng. **11**, 1768–1779 (2005).

21. MacEwan, S. R. & Chilkoti, A. Applications of elastin-like polypeptides in drug delivery. *J. Control. Release* **190**, 314–330 (2014).
22. Ta, D. T., Vanella, R. & Nash, M. A. Bioorthogonal Elastin-like Polypeptide Scaffolds for Immunoassay Enhancement. *ACS Appl. Mater. Interfaces* **10**, 30147–30154 (2018).
23. Ta, D. T., Vanella, R. & Nash, M. A. Magnetic Separation of Elastin-like Polypeptide Receptors for Enrichment of Cellular and Molecular Targets. *Nano Lett.* **17**, 7932–7939 (2017).
24. Ott, W. *et al.* Elastin-like Polypeptide Linkers for Single-Molecule Force Spectroscopy. *ACS Nano* **11**, 6346–6354 (2017).
25. Ott, W., Nicolaus, T., Gaub, H. E. & Nash, M. A. Sequence-Independent Cloning and Post-Translational Modification of Repetitive Protein Polymers through Sortase and Sfp-Mediated Enzymatic Ligation. *Biomacromolecules* **17**, 1330–1338 (2016).
26. Quiroz, F. G. & Chilkoti, A. Sequence heuristics to encode phase behaviour in intrinsically disordered protein polymers. *Nat. Mater.* **14**, 1164–1171 (2015).
27. Valiaev, A., Lim, D. W., Oas, T. G., Chilkoti, A. & Zauscher, S. Force-induced prolyl cis-trans isomerization in elastin-like polypeptides. *J. Am. Chem. Soc.* **129**, 6491–6497 (2007).
28. Valiaev, A. *et al.* Hydration and conformational mechanics of single, end-tethered elastin-like polypeptides. *J. Am. Chem. Soc.* **130**, 10939–10946 (2008).
29. Li, N. K., Quiroz, F. G., Hall, C. K., Chilkoti, A. & Yingling, Y. G. Molecular Description of the LCST Behavior of an Elastin-Like Polypeptide. *Biomacromolecules* **15**, 3522–3530 (2014).
30. Banani, S. F., Lee, H. O., Hyman, A. A. & Rosen, M. K. Biomolecular condensates: Organizers of cellular biochemistry. *Nature Reviews Molecular Cell Biology* **18**, 285–298 (2017).
31. Strulson, C. A., Molden, R. C., Keating, C. D. & Bevilacqua, P. C. RNA catalysis through compartmentalization. *Nat. Chem.* **4**, 941–946 (2012).
32. Shin, Y. *et al.* Liquid Nuclear Condensates Mechanically Sense and Restructure the Genome. *Cell* **175**, 1481-1491.e13 (2018).
33. Meco, E. & Lampe, K. J. Impact of Elastin-like Protein Temperature Transition on PEG-ELP Hybrid Hydrogel Properties. *Biomacromolecules* **20**, 1914–1925 (2019).

34. Wang, H., Cai, L., Paul, A., Enejder, A. & Heilshorn, S. C. Hybrid Elastin-like Polypeptide–Polyethylene Glycol (ELP-PEG) Hydrogels with Improved Transparency and Independent Control of Matrix Mechanics and Cell Ligand Density. *Biomacromolecules* **15**, 3421–3428 (2014).
35. Simon, J. R., Eghtesadi, S. A., Dzuricky, M., You, L. & Chilkoti, A. Engineered Ribonucleoprotein Granules Inhibit Translation in Protocells. *Mol. Cell* **75**, 66-75.e5 (2019).
36. Duan, T. & Li, H. In situ Phase Transition of Elastin-like Polypeptide Chains Regulates Thermo-Responsive Properties of Elastomeric Protein-Based Hydrogels. *Biomacromolecules* acs.biomac.0c00206 (2020). doi:10.1021/acs.biomac.0c00206
37. Wang, H. *et al.* Covalently Adaptable Elastin-Like Protein-Hyaluronic Acid (ELP-HA) Hybrid Hydrogels with Secondary Thermoresponsive Crosslinking for Injectable Stem Cell Delivery. *Adv. Funct. Mater.* **27**, 1605609 (2017).
38. Sugimura, Y. *et al.* Screening for the Preferred Substrate Sequence of Transglutaminase Using a Phage-displayed Peptide Library. *J. Biol. Chem.* **281**, 17699–17706 (2006).
39. Meyer, D. E. & Chilkoti, A. Genetically encoded synthesis of protein-based polymers with precisely specified molecular weight and sequence by recursive directional ligation: examples from the elastin-like polypeptide system. *Biomacromolecules* **3**, 357–367 (2002).
40. Hassouneh, W., Christensen, T. & Chilkoti, A. Elastin-like Polypeptides as a Purification Tag for Recombinant Proteins. *Curr. Protoc. Protein Sci.* **CHAPTER**, Unit (2010).
41. Carr, M. E. & Hardin, C. L. Fibrin has larger pores when formed in the presence of erythrocytes. *Am. J. Physiol.* **253**, H1069-73 (1987).
42. Nandi, S. & Brown, A. C. Characterizing Cell Migration Within Three-dimensional In Vitro Wound Environments. *J. Vis. Exp.* e56099 (2017). doi:10.3791/56099
43. McDaniel, J. R., Radford, D. C. & Chilkoti, A. A Unified Model for De Novo Design of Elastin-like Polypeptides with Tunable Inverse Transition Temperatures. *Biomacromolecules* **14**, 2866–2872 (2013).
44. Bagoly, Z., Koncz, Z., Hársfalvi, J. & Muszbek, L. Factor XIII, clot structure, thrombosis. *Thrombosis Research* **129**, 382–387 (2012).

45. Muszbek, L., Bereczky, Z., Bagoly, Z., Komáromi, I. & Katona, É. Factor XIII: A Coagulation Factor With Multiple Plasmatic and Cellular Functions. *Physiol. Rev.* **91**, 931–972 (2011).
46. Boutris, C., Chatzi, E. G. & Kiparissides, C. Characterization of the LCST behaviour of aqueous poly(N-isopropylacrylamide) solutions by thermal and cloud point techniques. *Polymer (Guildf).* **38**, 2567–2570 (1997).
47. Adler, J. & Parmryd, I. Quantifying colocalization by correlation: The pearson correlation coefficient is superior to the Mander's overlap coefficient. *Cytom. Part A* **77**, 733–742 (2010).
48. McHale, M. K., Setton, L. A. & Chilkoti, A. Synthesis and *in Vitro* Evaluation of Enzymatically Cross-Linked Elastin-Like Polypeptide Gels for Cartilaginous Tissue Repair. *Tissue Eng.* **11**, 1768–1779 (2005).
49. Garcia, Y. *et al.* In vitro characterization of a collagen scaffold enzymatically cross-linked with a tailored elastin-like polymer. *Tissue Eng. - Part A* **15**, 887–899 (2009).
50. Mosesson, M. W. Fibrinogen and fibrin structure and functions. in *Journal of Thrombosis and Haemostasis* **3**, 1894–1904 (John Wiley & Sons, Ltd, 2005).
51. Chan, L. W. *et al.* A synthetic fibrin cross-linking polymer for modulating clot properties and inducing hemostasis. *Sci. Transl. Med.* **7**, 277ra29 (2015).
52. Hethershaw, E. L. *et al.* The effect of blood coagulation factor XIII on fibrin clot structure and fibrinolysis. *J. Thromb. Haemost.* **12**, 197–205 (2014).
53. Theusinger, O. M., Baulig, W., Asmis, L. M., Seifert, B. & Spahn, D. R. In vitro factor XIII supplementation increases clot firmness in rotation thromboelastometry (ROTEM®). *Thromb. Haemost.* **104**, 385–391 (2010).
54. Wolberg, A. S. Thrombin generation and fibrin clot structure. *Blood Rev.* **21**, 131–142 (2007).
55. Mihalko, E. & Brown, A. C. Clot Structure and Implications for Bleeding and Thrombosis. *Semin. Thromb. Hemost.* (2019). doi:10.1055/s-0039-1696944
56. Whiting, D. & DiNardo, J. A. TEG and ROTEM: Technology and clinical applications. *Am. J. Hematol.* **89**, 228–232 (2014).
57. Kurniawan, N. A., Grimbergen, J., Koopman, J. & Koenderink, G. H. Factor XIII stiffens fibrin clots by causing fiber compaction. *J. Thromb. Haemost.* **12**, 1687–1696 (2014).
58. FRITH, D. *et al.* Definition and drivers of acute traumatic coagulopathy: clinical and

experimental investigations. *J. Thromb. Haemost.* **8**, 1919–1925 (2010).

59. Li, P. *et al.* Phase transitions in the assembly of multivalent signalling proteins. *Nature* **483**, 336–340 (2012).
60. Jansen, K. A., Bacabac, R. G., Piechocka, I. K. & Koenderink, G. H. Cells actively stiffen fibrin networks by generating contractile stress. *Biophys. J.* **105**, 2240–2251 (2013).
61. Urry, D. W., Haynes, B., Zhang, H., Harris, R. D. & Prasad, K. U. Mechanochemical coupling in synthetic polypeptides by modulation of an inverse temperature transition. *Proc. Natl. Acad. Sci. U. S. A.* **85**, 3407–3411 (1988).
62. Urry, D. W., Haynes, B. & Harris, R. D. Temperature dependence of length of elastin and its polypentapeptide. *Biochem. Biophys. Res. Commun.* **141**, 749–755 (1986).
63. Trabbic-Carlson, K., Setton, L. A. & Chilkoti, A. Swelling and mechanical behaviors of chemically cross-linked hydrogels of elastin-like polypeptides. *Biomacromolecules* **4**, 572–580 (2003).
64. Shin, Y. *et al.* Liquid Nuclear Condensates Mechanically Sense and Restructure the Genome. *Cell* **175**, 1481-1491.e13 (2018).
65. Piechocka, I. K., Bacabac, R. G., Potters, M., MacKintosh, F. C. & Koenderink, G. H. Structural Hierarchy Governs Fibrin Gel Mechanics. *Biophys. J.* **98**, 2281–2289 (2010).
66. Piechocka, I. K. *et al.* Multi-scale strain-stiffening of semiflexible bundle networks. *Soft Matter* **12**, 2145–2156 (2016).
67. Medved, L. & Nieuwenhuizen, W. Molecular mechanisms of initiation of fibrinolysis by fibrin. *Thromb. Haemost.* **89**, 409–19 (2003).
68. Cesarman-Maus, G. & Hajjar, K. A. Molecular mechanisms of fibrinolysis. *Br. J. Haematol.* **129**, 307–321 (2005).
69. Bryant, C. E., Spring, D. R., Gangloff, M. & Gay, N. J. The molecular basis of the host response to lipopolysaccharide. *Nature Reviews Microbiology* **8**, 8–14 (2010).
70. Tremel, A. *et al.* Cell migration and proliferation during monolayer formation and wound healing. *Chem. Eng. Sci.* **64**, 247–253 (2009).
71. Hadjipanayi, E., Mudera, V. & Brown, R. A. Guiding cell migration in 3D: A collagen matrix with graded directional stiffness. *Cell Motil. Cytoskeleton* **66**, 121–128 (2009).
72. Tse, J. R. & Engler, A. J. Stiffness gradients mimicking in vivo tissue variation regulate mesenchymal stem cell fate. *PLoS One* **6**, 15978 (2011).

73. Leon-Valdivieso, C. Y. *et al.* Fibroblast migration correlates with matrix softness. Astudy in knob-hole engineered fibrin. *APL Bioeng.* **2**, 036102 (2018).

Appendix

Table 3A-1. hELP and conELP protein sequence

ELP	Sequence
hELP: ELP($A_2V_8E_1$-Tgf11)$_4$-($A_2V_8E_1$)$_4$-($A_2V_8E_1$-GSKGS)$_4$	MGHGVGVPGVGVPGAGVPGVGVPGVGVPGVGVPGVGVPGVGVPGVGVPG VGVPGEGVPGAGSGDQMMLPWPAVALSGVPGVGVPGVGVPGAGVPGVGV PGVGVPGVGVPGVGVPGVGVPGVGVPGVGVPGEGVPGAGSGDQMMLPWP AVALSGVPGVGVPGVGVPGAGVPGVGVPGVGVPGVGVPGVGVPGVGVPGV GVPGVGVPGEGVPGAGSGDQMMLPWPAVALSGVPGVGVPGVGVPGAGVP GVGVPGVGVPGVGVPGVGVPGVGVPGVGVPGVGVPGEGVPGAGSGDQM MLPWPAVALSGVPGVGVPGVGVPGAGVPGVGVPGVGVPGVGVPGVGVPGV GVPGVGVPGVGVPGEGVPGAGVPGVGVPGVGVPGAGVPGVGVPGVGVPGV GVPGVGVPGVGVPGVGVPGVGVPGEGVPGAGVPGVGVPGVGVPGVGVPGV GVPGVGVPGVGVPGVGVPGVGVPGVGVPGVGVPGEGVPGAGVPGVGVPGV GVPGAGVPGVGVPGVGVPGVGVPGVGVPGVGVPGVGVPGVGVPGEGVPGA GVPGVGVPGVGVPGAGVPGVGVPGVGVPGVGVPGVGVPGVGVPGVGVPG VGVPGEGVPGAGSGGSKGSSGVPGVGVPGVGVPGAGVPGVGVPGVGVPGV GVPGVGVPGVGVPGVGVPGVGVPGEGVPGAGSGGSKGSSGVPGVGVPGVG VPGAGVPGVGVPGVGVPGVGVPGVGVPGVGVPGVGVPGVGVPGVGVPGEGVPGAG SGGSKGSSGVPGVGVPGVGVPGAGVPGVGVPGVGVPGVGVPGVGVPGVGV PGVGVPGVGVPGEGVPGAGSGGSKGSSGVPGWLDSLEFIA
conELP: ELP($A_2V_8E_1$-Tgf11(Q65G))$_4$-($A_2V_8E_1$)$_4$-($A_2V_8E_1$-GSGGS)$_4$	MGHGVGVPGVGVPGAGVPGVGVPGVGVPGVGVPGVGVPGVGVPGVGVPG VGVPGEGVPGAGSGDGMMLPWPAVALSGVPGVGVPGVGVPGAGVPGVGV PGVGVPGVGVPGVGVPGVGVPGVGVPGVGVPGEGVPGAGSGDGMMLPWP AVALSGVPGVGVPGVGVPGAGVPGVGVPGVGVPGVGVPGVGVPGVGVPGV GVPGVGVPGEGVPGAGSGDGMMLPWPAVALSGVPGVGVPGVGVPGAGVP GVGVPGVGVPGVGVPGVGVPGVGVPGVGVPGVGVPGEGVPGAGSGDGMM LPWPAVALSGVPGVGVPGVGVPGAGVPGVGVPGVGVPGVGVPGVGVPGVG VPGVGVPGVGVPGEGVPGAGVPGVGVPGVGVPGAGVPGVGVPGVGVPGVG VPGVGVPGVGVPGVGVPGVGVPGEGVPGAGVPGVGVPGVGVPGAGVPGVG VPGVGVPGVGVPGVGVPGVGVPGVGVPGVGVPGVGVPGEGVPGAGVPGVGVPGVG VPGAGVPGVGVPGVGVPGVGVPGVGVPGVGVPGVGVPGVGVPGEGVPGAG VPGVGVPGVGVPGAGVPGVGVPGVGVPGVGVPGVGVPGVGVPGVGVPGV GVPGEGVPGAGSGGSGGSSGVPGVGVPGVGVPGAGVPGVGVPGVGVPGVG VPGVGVPGVGVPGVGVPGVGVPGEGVPGAGSGGSGGSSGVPGVGVPGVGV PGAGVPGVGVPGVGVPGVGVPGVGVPGVGVPGVGVPGVGVPGVGVPGEGVPGAGS GGSGGSSGVPGVGVPGVGVPGAGVPGVGVPGVGVPGVGVPGVGVPGVGVP GVGVPGVGVPGEGVPGAGSGGSGGSSGVPGWLDSLEFIA

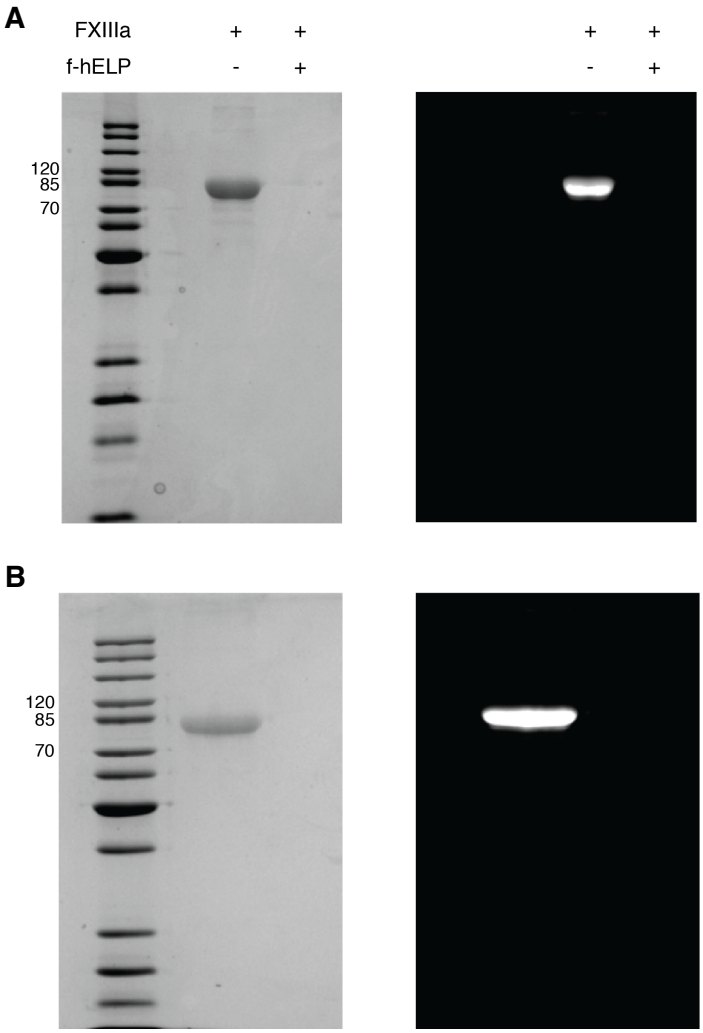

Figure 3A-1. Functionalization of ELPs with fluorescent Atto-647-NHS. a) SDS-PAGE gel of 12.5 µM f-hELP following incubation with 10 µg mL^{-1} FXIIIa for 1 h at 37 ˚C. Commassie blue stained gel (L) and the same gel under fluorescent illumination (λ_{exc} = 655 nm, λ_{abs}= 695 nm) (R). b) SDS-PAGE gel of 12.5 µM f-conELP following commassie blue staining (L) and the same gel under fluorescent illumination (λ_{exc} = 655 nm, λ_{abs}= 695 nm) (R).

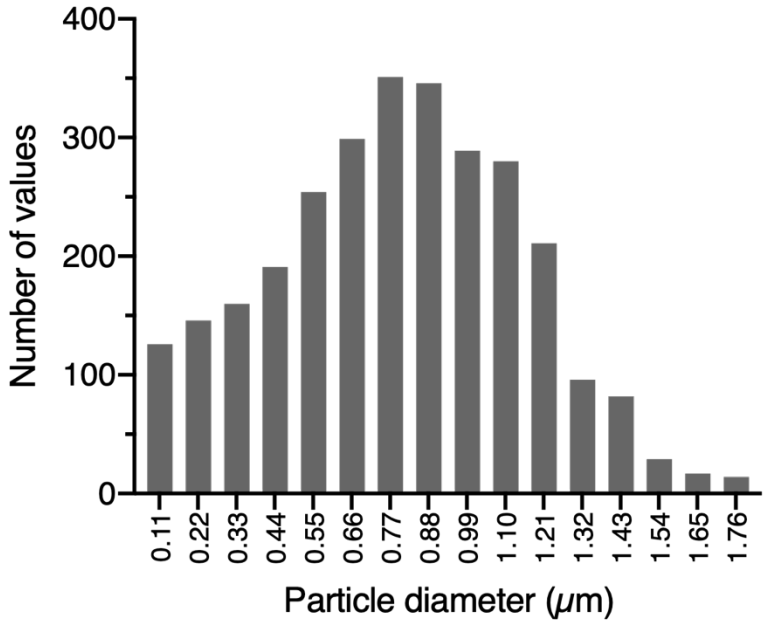

Figure 3A-2. hELP coacervate size distribution in 1.5 mg mL^{-1} Fb clots formed at 37 ˚C. Particle sizes were determined from confocal images of three different clots containing 30 µM hELP, at 60x magnification.

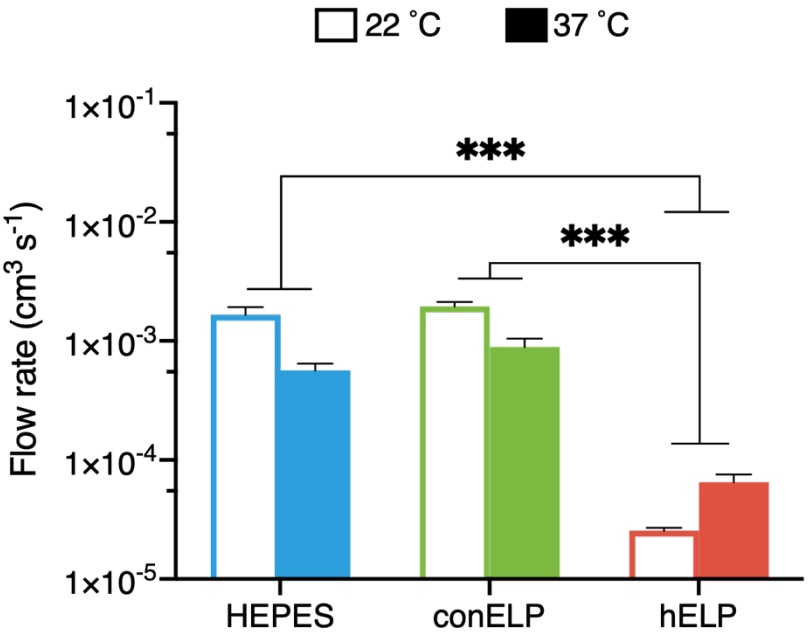

Figure 3A-3. Differences in the volumetric flow rate of isotonic HEPES buffer through Fb clots containing HEPES buffer, 30 µM conELP, or 30 µM hELP at 22 or 37 ˚C. Clots were formed with 1.5 mg mL^{-1} Fg, 20 mM $CaCl_2$, and 0.2 U mL^{-1} thrombin. Statistical significance was determined by means of a one-way analysis of variance (ANOVA) with Tukey's Post Hoc test. ***P < 0.001.

Chapter IV: Alternative hELP designs and application of hELPs in a rat acute bleeding model

Abstract

The ultimate clinical potential of an intravenous hemostatic agent hinges upon its ability to effectively promote the cessation of bleeding following systemic administration. Assessment of potential hemostats in *in vivo* animal models, is therefore a critical step along the pathway to their clinical application. Here, we apply hELP in a rat acute bleeding model, in order to determine the effect of hELPs on the survivability of animals with femoral artery injuries. The hELPs that were administered intravenously include hELP(4Tg-4K) (described in the previous chapter), and hELP(4Tg-4Tg) which is an updated version of the hELP design with glutamine-containing sequences that can be recognized by FXIII at both N and C termini. hELP(4Tg-4Tg) was found to outperform hELP(4Tg-4K) in the degree to which it improved clot mechanical properties *in vitro*, and this was reflected in improved survivability of animals treated with hELP(4Tg-4Tg) as compared to hELP(4Tg-4K), or controls, in the rat bleeding model. Furthermore, rats treated with hELP(4Tg-4Tg) were better able to maintain baseline mean arterial pressures (MAP), and had fewer re-bleeding events following the achievement of hemostasis. Together, these results point to the large parameter space that can be manipulated in order to improve the hemostatic efficacy of hELPs, and provide a rationale for the application of hELPs in further *in vivo* studies.

Introduction

hELPs are the first elastin-like polypeptides to be designed for use as intravenous hemostats.[1,2] They are particularly unique in this sphere, insomuch as their coacervation is required for their exerting a positive effect on the mechanical strength of fibrin clots *in vitro*.[3] In studies of other fibrin-binding polymeric hemostats, an increase in clot mechanical strength

was found to correlate with efficacy in animal models of bleeding, and so it may be the case that hELP coacervation is necessary for their effectively promoting hemostasis *in vivo*.[4] As the T_t of ELPs can be tuned by modifying their hydrophobicity, length, and charge, there are many design parameters which can be modulated in order to improve the degree to which ELPs are coacervated under physiological conditions. Furthermore, ELP sequences are controlled at the genetic level, which allows for simple and precise adjustments of characteristics such as valency, or the identity of binding domains.

The valency, structure, and composition of intravenous hemostats based on synthetic polymers can be tuned to some degree.[5–8] However, they are necessarily limited in this capacity by currently available polymer synthesis techniques (such as reversible addition fragmentation chain transfer) that can only approach monodispersity, and which include monomers in approximately stoichiometric ratios. This means that precision control of functional monomer position is not possible, and that batch-to-batch variation is inevitable.[9] The structure of hELPs on the other hand, is determined by their genetic sequence, which means that they can be tuned at the single residue level, and that they are perfectly monodisperse. Here, we took advantage of that precise control to produce a modified version of our previously reported hELP design; one which includes glutamine-containing transglutaminase (Tg) tags at both N and C termini (hELP(4Tg-4Tg)), as opposed to the original Tg tags at the N terminus, and lysine residues at the C terminus (hELP(4Tg-4K)). We believed that this design may promote more specific binding of hELPs to fibrin catalyzed by FXIII, and therefore improve their hemostatic efficacy. This hypothesis was investigated using *in vitro* assays, and a rat acute bleeding model. We found that hELP(4Tg-4Tg) improved the mechanical strength of clots formed at high fibrinogen concentrations to a greater degree than hELP(4Tg-4K), and that hELP(4Tg-4Tg) outperformed hELP(4Tg-4K) as well as controls in the rat bleeding model. These results provide a rationale for the continued application of hELPs *in vivo*, and point to the large parameter space that can be manipulated in order to potentially improve the hemostatic properties of these materials.

Materials & Methods

Nomenclature

hELP(4Tg-4K) is the same ABC triblock protein described in the previous chapter, having the full sequence $(A2V8E1\text{-}Tg)_4$-$(A2V8E1)_4$-$(A2V8E1\text{-}GSKGS)_4$, where Tg is the 12-residue sequence DQMMLPWPAVAL. hELP(4Tg-4Tg) is an ABA triblock protein with the full sequence $(A2V8E1\text{-}Tg)_4$-$(A2V8E1)_4$-$(A2V8E1\text{-}Tg)_4$ (**Appendix Table 4A-1**).

In vitro characterization of the effects of hELPs on fibrin clots

Thromboelastography (TEG) used to characterize the effect of the newly designed hELP(4Tg-4Tg) on fibrin clot properties *in vitro* according to the method outlined in the previous chapter. Briefly, clot components consisting of 1.5 or 3.0 mg mL^{-1} fibrinogen, 20 mM $CaCl_2$, 0.2 U mL^{-1} Thrombin, and 30 µM hELP(4Tg-4Tg) in 20/150 mM HEPES/NaCl buffer at pH 7.4 were mixed in the cup of the TEG at 37 ˚C, after which the pin of the TEG was inserted into the center of the clotting solution. Clots were monitored for a period of one hour, and three replicates were completed per treatment.

Rheology was also used to assess the effects of hELP(4Tg-4Tg) on the mechanical stiffness of fibrin clots as previously described. Briefly, 90 µL of the clotting solution described above were placed on the Peltier plate of the rheometer at 37 ˚C. A measuring cone (d = 25 mm, angle = 1˚) was lowered onto the sample, and the head was spun at 60 RPM for 5 seconds in order to ensure proper sample mixing. The clot was allowed to form for 1 hour, and sample evaporation was prevented during this time by low viscosity silicone oil (100 cSt) distributed around the sample edge. After one hour, an oscillatory frequency sweep was performed at 1% strain (within the linear viscoelastic region for this material), from 0.1 – 3 Hz.

Study Design

The efficacy of hELPs as hemostatic agents was evaluated using a rat in vivo model of bleeding. Design of the study and production of ELPs was carried out at the University of Basel, while live animal experiments were conducted by Charles River Laboratories (Mattawan, MI, USA). Twenty male CD rats (Charles River Laboratories, Raleigh, North Carolina) were divided into 4 study groups: hELP(4Tg-4K), hELP(4Tg-4Tg), conELPs (control ELPs; as described in the previous chapter, these are ELPs where glutamine and lysine

residues have been mutated to glycine, and so they cannot be covalently integrated into fibrin by FXIII), and 0.9% saline as a volume control. On the day of surgery, rats were anesthetized using isoflurane, placed on warming beds, and had two catheters inserted: one in the carotid artery, and another in the jugular vein. Once baseline levels of CO_2, O_2, and lactate were established, clamps were placed proximal and distal ends of the left femoral artery, after which a 3 mm incision was made in that artery. A controlled catheter bleed was subsequently conducted to lower each animal's mean arterial pressure (MAP) to 40 – 60 mm Hg, after which point the clamps on the femoral artery were removed, and the rats were given a bolus injection (up to 2 mL min^{-1}) at a volume of 5 mL kg^{-1}. The targeted final concentration of ELP in the blood was 30 µM, assuming a blood volume of 64 mL kg^{-1} for each rat (this translated to a dose of approx. 140 mg of ELP / kg of body weight). Following clamp removal, animals were allowed to bleed freely for 15 minutes, while blood loss volumes were measured using pre-weighed gauze. After the 15-minute free-bleed period, a blood sample was taken for measurement of blood gases, as well as prothrombin time. Saline was then administered to animals as needed, in order to raise MAP above 60 mm Hg (at a rate of 3 mL/kg/min, and up to a total volume of 60 mL kg^{-1}). Blood loss volume and MAP were continuously monitored until MAP fell below 20 mm Hg, or until the end point of the experiment (t = 75 m), at which time animals were euthanized (**Figure 4-1**). This study design was approved by the Institutional Animal Care and Use Committee at Charles River Laboratories.

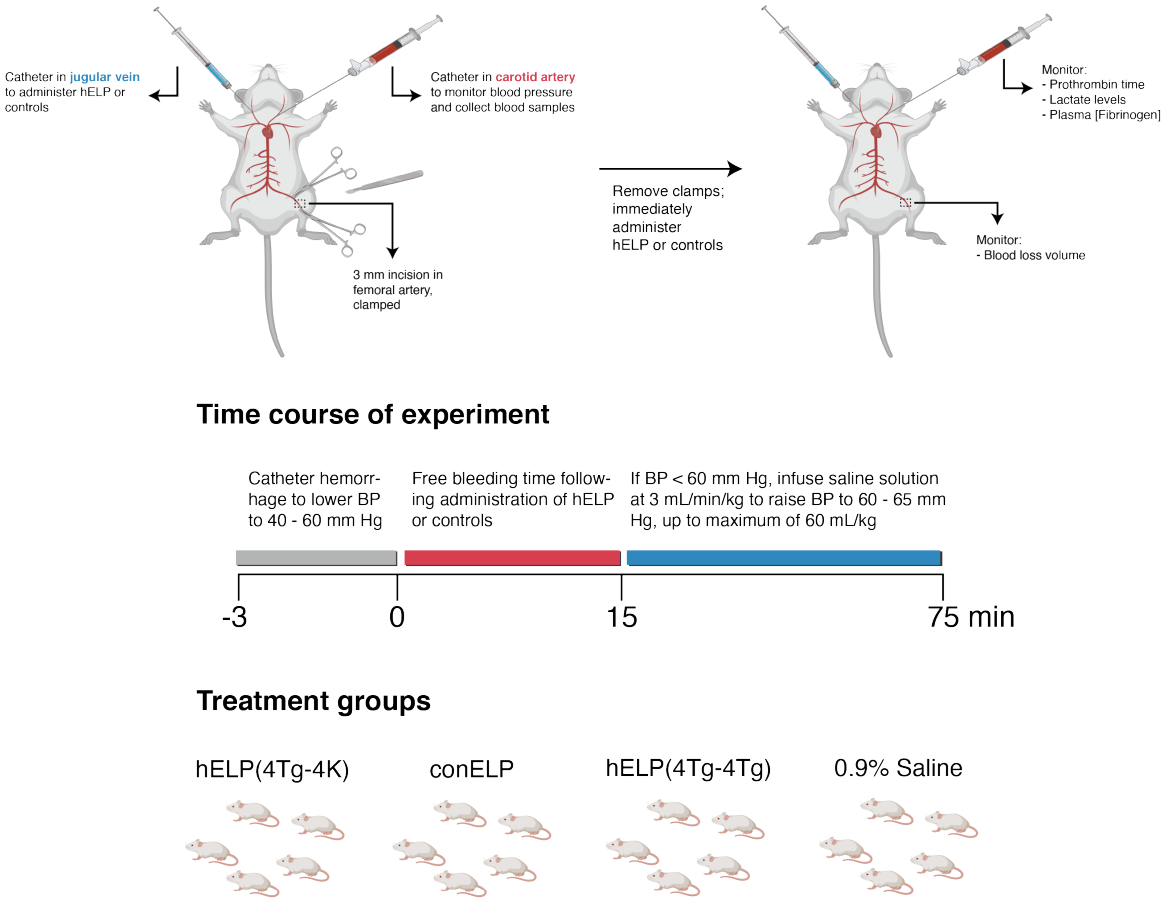

Figure 4-2. Schematic outline of a rat in vivo bleeding model*, showing the experimental setup, the time course of the experiment, and the treatment/control groups being tested, each containing 5 animals.*

Results & Discussion

Expression of hELPs and characterization of their phase transition temperatures under physiological conditions

The hELP(4Tg-4Tg) design was chosen in order to assess whether the presence of lysine residues in the original hELP(4Tg-4K) was necessary or beneficial to their hemostatic efficacy. hELPs were expressed in E. Coli, and purified to high yields by inverse transition cycling (**Figure 4-2**). As previously noted, one of the more useful and unique properties of ELPs is their ability to phase separate when heated above their lower critical solution temperature (LCST).[10] We have previously established that coacervation is necessary for the mechanical stiffening effect observed when hELPs are covalently bound to fibrin.[3] Here, the LCST of hELP(4Tg-4Tg) was compared to that of hELP(4Tg-4K) in physiological buffer: 10 mM PBS + 3mM $CaCl_2$ at pH = 7.4. $CaCl_2$ was added at a concentration equivalent to the average

serum calcium concentration in rats; in humans the upper limit of normal calcium concentration in the blood is slightly less, at 2.5 mM.[11,12] Under these conditions, hELP(4Tg-4Tg) had a T_t = 31 ˚C, and hELP(4Tg-4K) had a T_t = 34.6 ˚C at a concentration of 30 µM (**Figure 4-2**). The LCST of ELPs depends upon two intrinsic factors, namely, hydrophobicity and length.[13] As hELP(4Tg-4Tg) and hELP(4Tg-4K) have roughly the same contour length and molecular weight (73.3 and 69.5 kDa, respectively), it is likely that increased hydrophobicity due to the presence of hydrophobic leucine and methionine residues in Tg tags plays a role in the reduced T_t of hELP(4Tg-4Tg). Furthermore, Tg tags contain aromatic tryptophan residues which can participate in pi-pi stacking interactions; similar interactions between aromatic residues are believed to play an important role in promoting phase transition of other intrinsically disordered proteins/proteins with intrinsically disordered regions.[14]

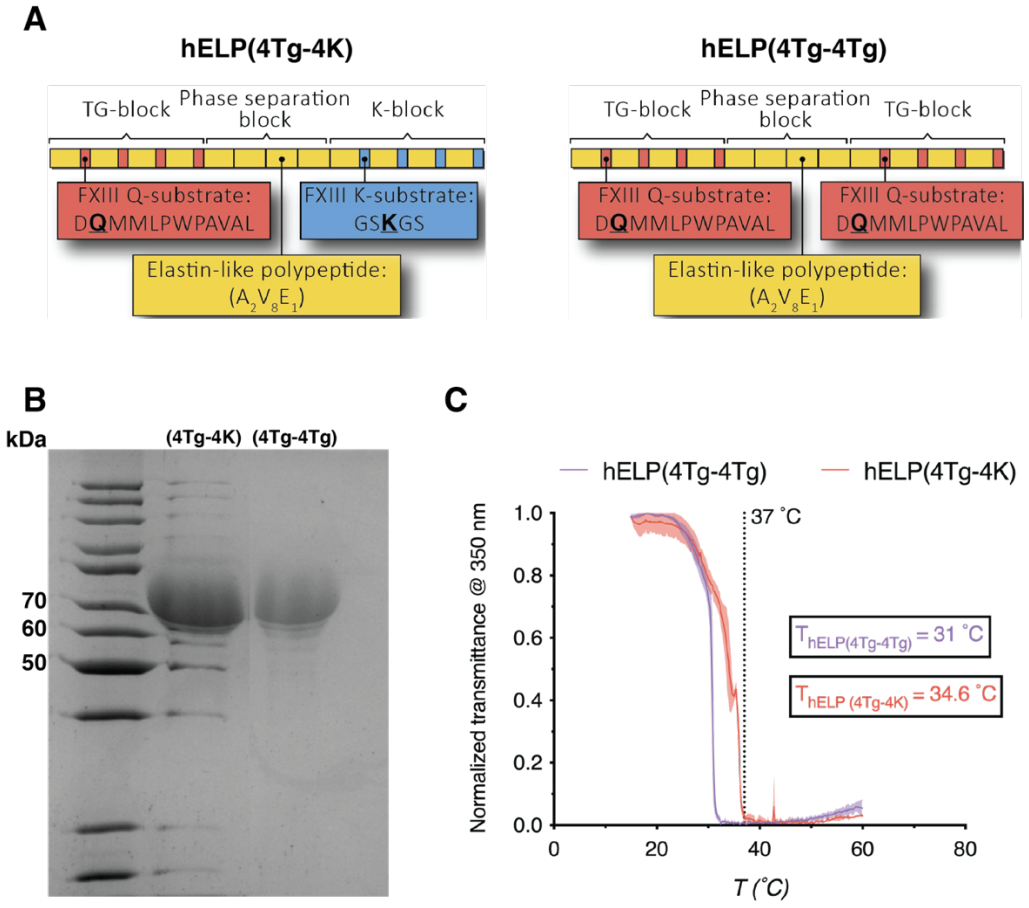

Figure 4-3. Design of hELPs and their characterization in vitro. A) Schematic of hELP(4Tg-4K) and hELP(4Tg-4Tg) sequences. B) High yield and purity following expression of hELPs in E. Coli, and purification via inverse transition cycling. C) Phase transition of hELPs under physiological conditions (10 mM PBS + 3mM $CaCl_2$ at pH = 7.4); the shaded areas indicate one SD from the mean (n = 3). T_t was defined as the temperature at which normalized transmittance fell below 0.5.

Effects of hELPs on fibrin clots *in vitro*

The previous chapter established that the binding of hELP(4Tg-4K) coacervates to fibrin networks resulted in improvements in the mechanical and functional properties of those clots, as measured by *in vitro* tests such as rheology and TEG. Here, those tests were used as a benchmark in order to compare the effect of the new hELP(4Tg-4Tg) design to that of the previous hELP design. TEG measurements provide a clinically relevant measurement of clot properties, including clotting onset time (the R value), rate of clot development (α-angle), and maximum clot strength (max amplitude, MA).[15] There were no significant differences between clotting onset times in clots treated with 30 μM hELP(4Tg-4K) or hELP(4Tg-4K), at either low (1.5 mg mL^{-1}) or high (3.0 mg mL^{-1}) fibrinogen (Fg) concentrations (**Figure 4-3**). The same was true in regards to the MA achieved by those clots. The α-angle however, was lower in hELP(4Tg-4Tg) clots at both fibrinogen concentrations tested than in hELP(4Tg-4K)-containing clots, indicating that the rate of clot formation was slower in the former treatment case. This was confirmed by the measured K value (i.e. the time required for pin displacement to go from 2 to 20 mm), which was significantly different between hELP(4Tg-4Tg) and hELP(4Tg-4K) clots formed with 1.5 mg mL^{-1} Fg (11.3 ± 2.0 and 4.3 ± 0.3 m respectively), but not between clots formed with 3.0 mg mL^{-1} Fg (5.2 ± 0.7 and 2.4 ± 0.2 m respectively) (**Appendix Figure 4A-1**).

Rheological measurements indicate that both hELPs tested increase the mechanical stiffness of fibrin clots formed at sub-critical Fg concentrations (1.5 mg mL^{-1}) up to a storage modulus of 201.3 ± 16.4 Pa with hELP(4Tg-4K), and 241.1 ± 26.6 Pa with hELP(4Tg-4Tg) (**Figure 4-3D**). Both hELPs increased the stiffness of these clots above the critical threshold modulus, which is the stiffness of a clot formed with 2.2 mg mL^{-1} Fg. When a patient's blood Fg concentration falls below this threshold, mortality is markedly increased.[16] In clots formed at the upper bound of physiological Fg concentration (3.0 mg mL^{-1}), the difference in the effect of hELP(4Tg-4K) and hELP(4Tg-4Tg) is much more significant, with the moduli of these clots being 616.9 ± 42.2 Pa and 1619.4 ± 68.2 Pa, respectively. This result seems to indicate that covalent cross-linking between hELPs themselves is not necessary for their fibrin clot stiffening effect, as such cross-linking cannot occur between hELP(4Tg-4Tg) chains, which lack the lysine partner necessary for the γ-glutamyl-ϵ-lysyl reaction catalyzed by FXIII.[17] Potential explanations for the increased stiffness of hELP(4Tg-4Tg)-containing clots at higher Fg

concentrations center on the valency and T_t of this hELP. Firstly, transglutaminases are known to be much more selective in regards to the glutamine residue that they bind in the first step of catalysis, as compared to the lysine that is involved in a later step. Given that there are a greater number of glutamine-containing sequences with high affinity for FXIIIa in hELP(4Tg-4Tg),it is possible that more cross-links can be formed between it and fibrin lysine residues, as compared to lysine residues from hELP(4Tg-4K) and fibrin glutamine residues.[17–19] This hypothesis is supported by the observation that the greatest increase in clot storage modulus is seen at higher Fg concentrations – where there would be a greater number of potential hELP-fibrin binding sites – despite the fact that both low and high concentration fibrin clots were treated with the same concentration of hELP (30 µM). Secondly, hELP(4Tg-4Tg) has a lower T_t than hELP(4Tg-4K), which reflects stronger hydrophobic interactions between hELP(4Tg-4Tg) chains at physiological temperatures, interactions that could stiffen fibrin networks when hELP(4Tg-4Tg) coacervates are bound to them.[20,21]

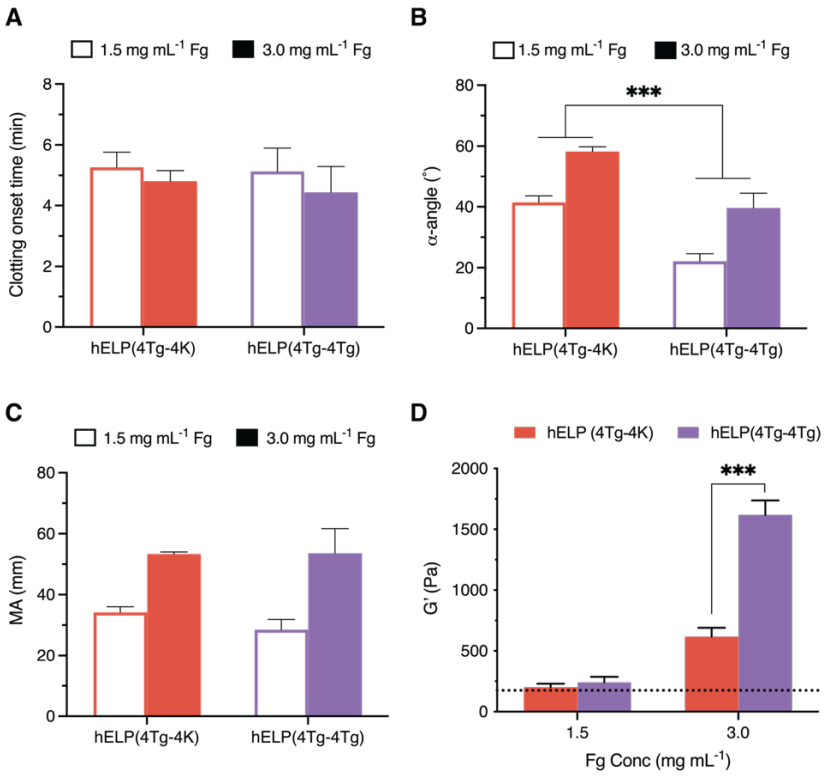

Figure 4-4. TEG and rheological characterization of the effect of hELPs on fibrin clot properties in vitro. A) Clotting onset time, B) α-angle, and C) max amplitude of clots formed with 30 µM hELP, as determined by TEG. Data are presented as mean ± SD (n = 3). ***P < 0.001 in one-way ANOVA with Tukey's post hoc test. D) Average shear storage moduli (G') of clots formed with 30 µM hELP as determined by oscillatory shear strain rheology (0.1 to 3 Hz at 1% strain). The dotted line indicates the G' of control clots formed at the critical Fg threshold concentration (2.2 mg mL^{-1}). Data are shown as mean ± SD (n = 3). ***P < 0.001 in a multiple t-tests comparison.

Assessment of hELP efficacy in a rat model of acute bleeding

The *in vivo* rat study was based on a femoral artery bleeding model that is commonly used to assess the efficacy of potential hemostats.[4,6,22] In order to test hELP efficacy in a clinically relevant manner, a few key points were attended to in the design of the study. Firstly, the MAP of rats was lowered via a controlled catheter bleed to 40 – 60 mm Hg prior to the initiation of the experiment, both to normalize baseline conditions among treatment groups, and to simulate conditions of trauma induced coagulopathy (TIC; mean adult rat blood pressure is usually around 100 mm Hg).[23] Secondly, hELPs or controls were only administered via intravenous injection through the jugular vein *after* the initiation of bleeding through a femoral artery injury, as this reflects an important potential use case for hELPs: intravenous administration to injured persons in the field or in hospital. Thirdly, the injury consisted of a 3 mm incision in the femoral artery, as a larger wound would provide a greater test of the hemostatic efficacy of hELPs, and as this is consist with other test of hemostats that have been reported in the literature.[4]

The first phase of the experiment involved fifteen minutes of free bleeding time following femoral artery injury and the administration of hELPs or controls (**Figure 4-4**). All five of the rats treated with hELP(4Tg-4Tg) survived this period, while one rat expired at the 14-minute mark in each of the hELP(4Tg-4K), and 0.9% saline treatment groups. Two animals expired prior to the 15-minute mark in the conELP treatment group (**Figure 4-5**). Following the free bleeding period, fluid resuscitation was used as necessary to raise the MAP of animals above the 60 mm Hg threshold. This procedure reflects the clinical practice of fluid resuscitation in patients with low blood pressure due to hemmorage, and also allows for the assessment of the clot reinforcing properties of hELPs, as clots with substandard mechanical properties will be less able to remain intact following an increase in MAP. 60% of the animals treated with hELP(4Tg-4Tg) survived the one-hour fluid resuscitation period, while the proportion of survivors was 40% in the 0.9% saline group, and 20% in each of the hELP(4Tg-4K) and conELP groups. There were no significant differences in the survival curves of each treatment group (P = 0.2407 from log-rank Mantel Cox test), however, 80% of animals treated with hELP(4Tg-4Tg) survived up to 65 minutes indicating a positive trend in survivability. It should also be noted that rats in the saline control group were on average heavier than those in other treatment groups as they were dosed on the final day of the study (**Appendix Figure**

4A-2). This could also have affected survival times. The high death rate in the hELP(4Tg-4K) group could be attributed to the significant number of re-bleeding events (4) that were observed following the onset of fluid resuscitation, as compared to one in each of the hELP(4Tg-4Tg) and 0.9% saline groups, and none in the conELP group (**Figure 4-6**). A caveat should be made here to say that the number of re-bleeding events should take into account survivability and MAP of each animal throughout the experiment; therefore, it is likely that no re-bleeding events were observed in the conELP group due to low survivability during the free-bleed period, and due to the low MAP of animals even after fluid resuscitation, rather than any improvement in the mechanical properties of clots by conELP. The high re-bleeding rate in animals treated with hELP(4Tg-4K) is surprising, given that this hELP was found to improve the mechanical properties of clots *in vitro* (Figure 3D; see also, previous chapter). A possible explanation for this, is that the T_t of this hELP (34.6 ˚C in physiologically buffer) was at times above the body temperature of some animals over the course of the experiment (this varied from 33.4 – 37.8 ˚C). In such cases, hELP(4Tg-4K) would not form a coacervate at its circulating concentration, which was shown to be important for clot stiffening (see previous chapter). Furthermore, while the presence of lysine in this hELP would allow it to be covalently bound to itself and to fibrin, lysine also constitutes a critical binding site for proteins that are involved in plasminolysis; binding of these proteins (such as tissue plasminogen activator, and plasminogen) leads to an increase in their rate of activation, and so it may also be the case that the presence of more lysine residues on hELP(4Tg-4K) molecules attached to fibrin networks lead to an increase in plasminolysis rate.[24]

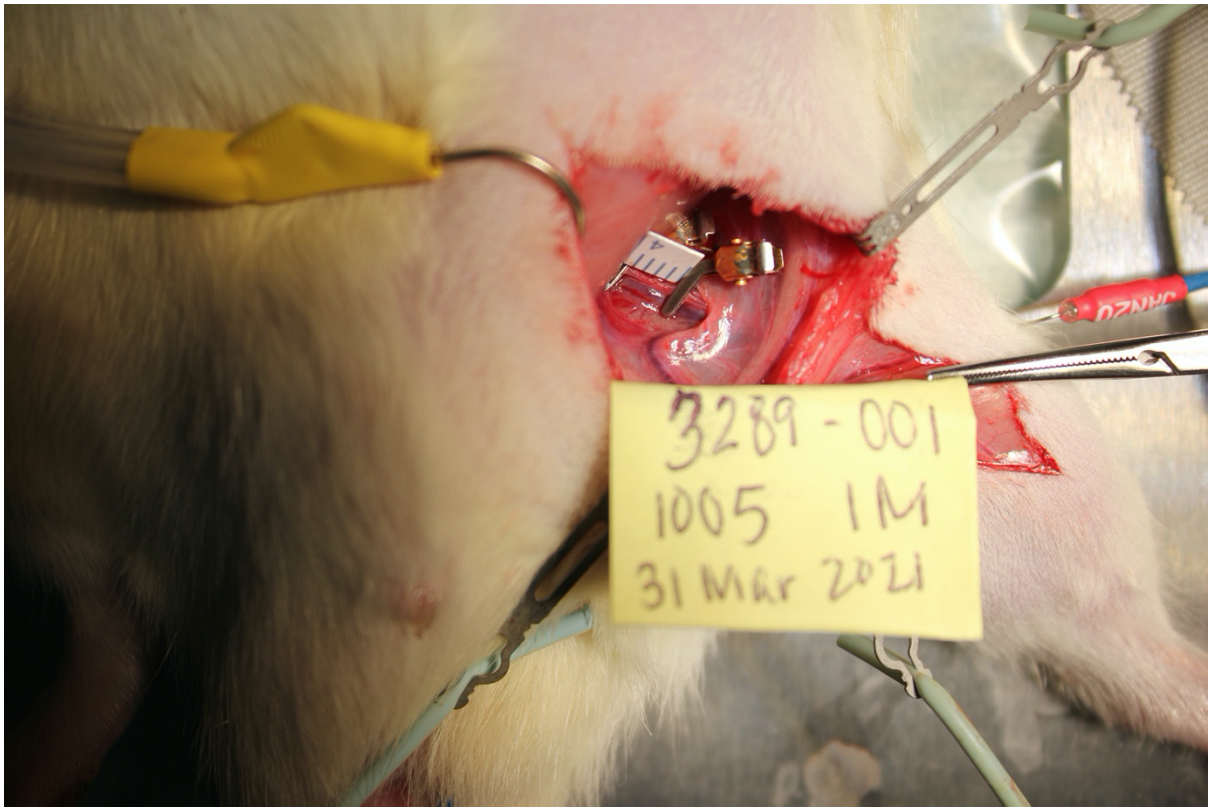

Figure 4-5. Image of the surgical setup for the rat acute bleeding model, showing the clamped femoral artery prior to a 3 mm incision being made.

Measurements of cumulative bleeding volumes as a function of body weight showed that following treatment with hELP(4Tg-4Tg), animals could lose as much as 30 mL kg^{-1} and still survive the experiment (**Figure 4-6**). In all treatment groups, animals that lost roughly 40 mL kg^{-1} of blood – approx. two thirds of their total blood volume – did not survive the experiment. All animals that survived the length of the experiment achieved hemostasis within 5 minutes, and then did not subsequently experience any re-bleeding events. Animals that were treated with hELP(4Tg-4Tg) lost 9% less blood per kg of body weight than animals that were treated with conELP, and 19% less blood than animals that were treated with hELP(4Tg-4K).

MAP is an important indicator of the health of trauma patients, and patients whose MAP drops below a critical threshold are more likely to die of hemorrhagic shock.[25] The healthy baseline MAP of rats varies according to their age, gender, and weight, but it is in the range of approx. 100 mm Hg.[26] Here, animals were put in a state of hypotension prior to the initiation of the experiment by having their MAP lowered to 40 – 60 mm Hg, in order to better reflect the expected status of patients who might suffer some degree of uncontrolled bleeding in the field prior to their arriving at hospital. Following the 15-minute free bleed

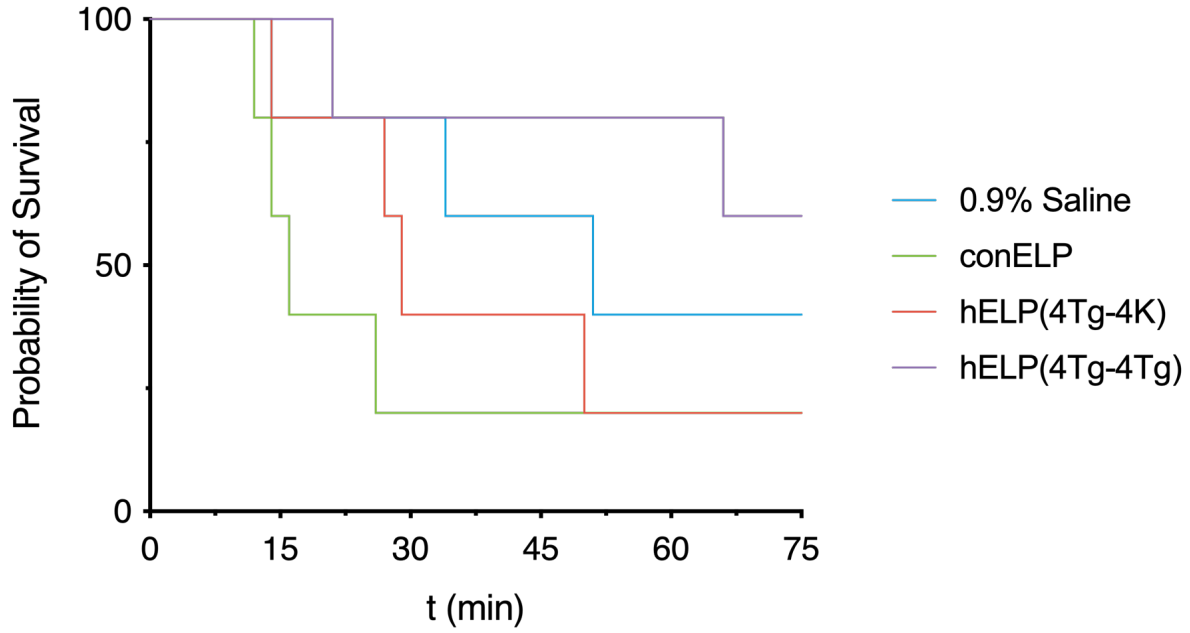

Figure 4-6. Survival curves of rats in a femoral artery injury bleeding model, following intravenous administration of approx. 140 mg kg^{-1} of ELP or an equivalent volume of 0.9% saline (n = 5). The first 15 minutes of the experiment (following release of clamps surrounding the femoral artery injury) constituted the free bleed period, after which time fluid resuscitation was undertaken in order to maintain MAP above 60 mm Hg when possible. Animals were euthanized when MAP fell below 20 mm Hg. There were no significant differences in survival between groups (P = 0.2407 from log-rank Mantel Cox test).

period, animals were given fluid infusions in order to raise their MAP above the 60 mm Hg threshold. All three of the hELP(4Tg-4Tg) treated animals that survived the experiment had MAPs above 60 mm Hg, and one of these was restored to a healthy baseline MAP of 109 mm Hg (**Figure 4-7**). In contrast, only one of the two animals that survived with the saline treatment had an MAP above 60 mm Hg at t = 75 min; the other survivor had an MAP of 23 mm Hg that was trending downwards toward the 20 mm Hg survival threshold. None of the animals that survived in the hELP(4Tg-4K) or conELP treatment groups had an MAP above 60 mm Hg at the end of the experiment. The administration of hELP(4Tg-4Tg) therefore had a positive effect on the ability of animals to maintain a high MAP, possibly owing to the formation of more mechanically robust clots that could remain intact after the onset of fluid resuscitation. Another predictor of mortality in hemorraghic patients is blood lactate concentration. Lactate is a product of anaerobic respiration, and an increase in its concentration in blood is indicative of poor tissue perfusion and hemorrhagic shock.[27] In the rat model used here, baseline blood lactate concentrations of < 1.2 mM were established

prior to the start of bleeding, and then measured again after the 15-minute free bleed period. There were no significant differences

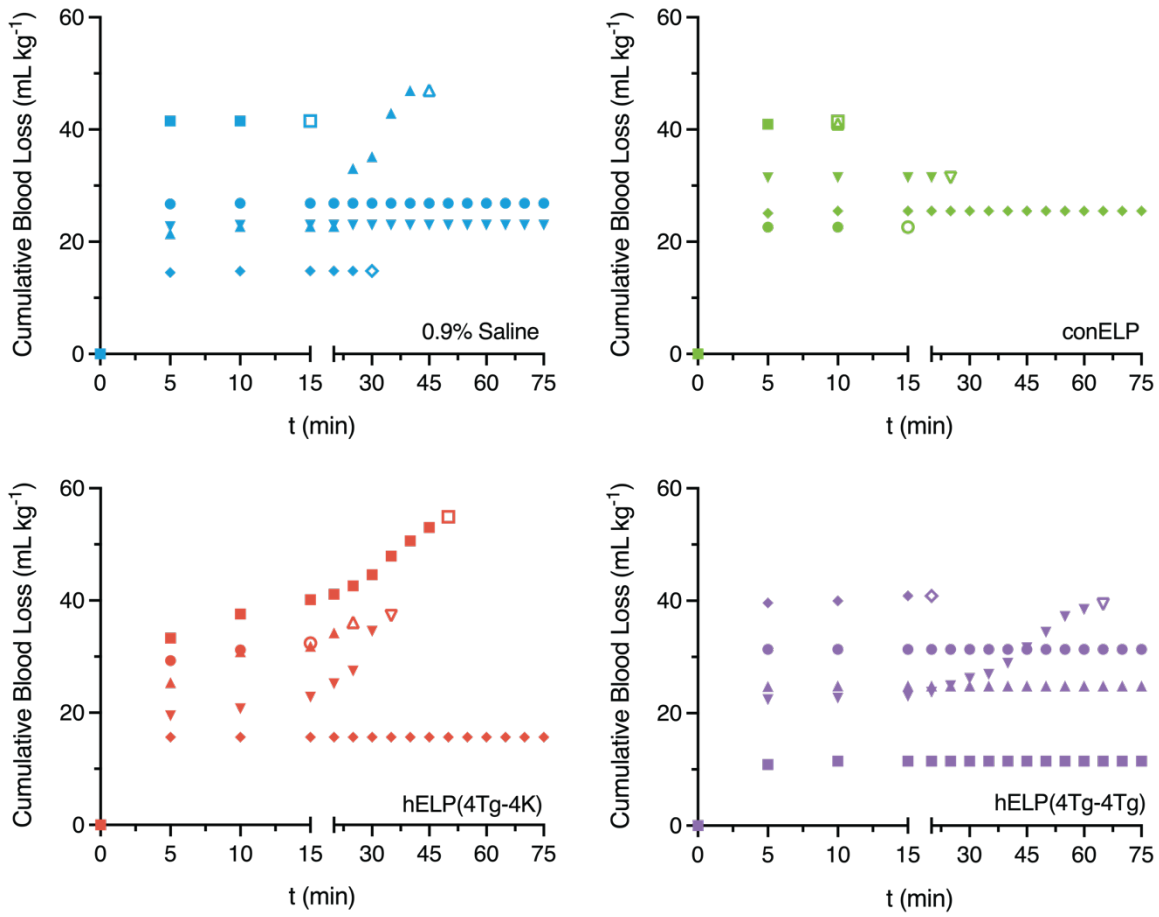

Figure 4-7. Cumulative bleeding volumes as a function of body weight in a rat bleeding model, following treatment with 30 µM ELP, or an equivalent volume of saline. Hollow symbols indicate the final measured blood loss volume prior to expiry of an animal. Re-bleeding events following the initiation of fluid infusion can be seen after the 15-minute time point.

between the blood lactate concentrations of animals in any of the treatment groups, and they all experienced an average 7.5 – 10-fold increase in lactate over the free-bleeding period (**Figure 8**). Oxygen saturation in the blood was also measured at the 0 and 15-minute time points. All of the animals treated with hELP(4Tg-4Tg) had O_2 saturation levels of 100% after the 15-minute free bleed period, whereas one animal in each of the other treatment groups had an oxygen saturation below the ideal baseline of 95% (**Figure 8**).

High infusion volumes in trauma patients are associated with increased incidences of coagulopathy due to hemodilution.[28] In this experiment, animals could receive infusions up to a maximum volume of 60 mL / kg of body weight. There were no significant differences in the proportion of the maximum allowable infusion volume given to animals in the saline or

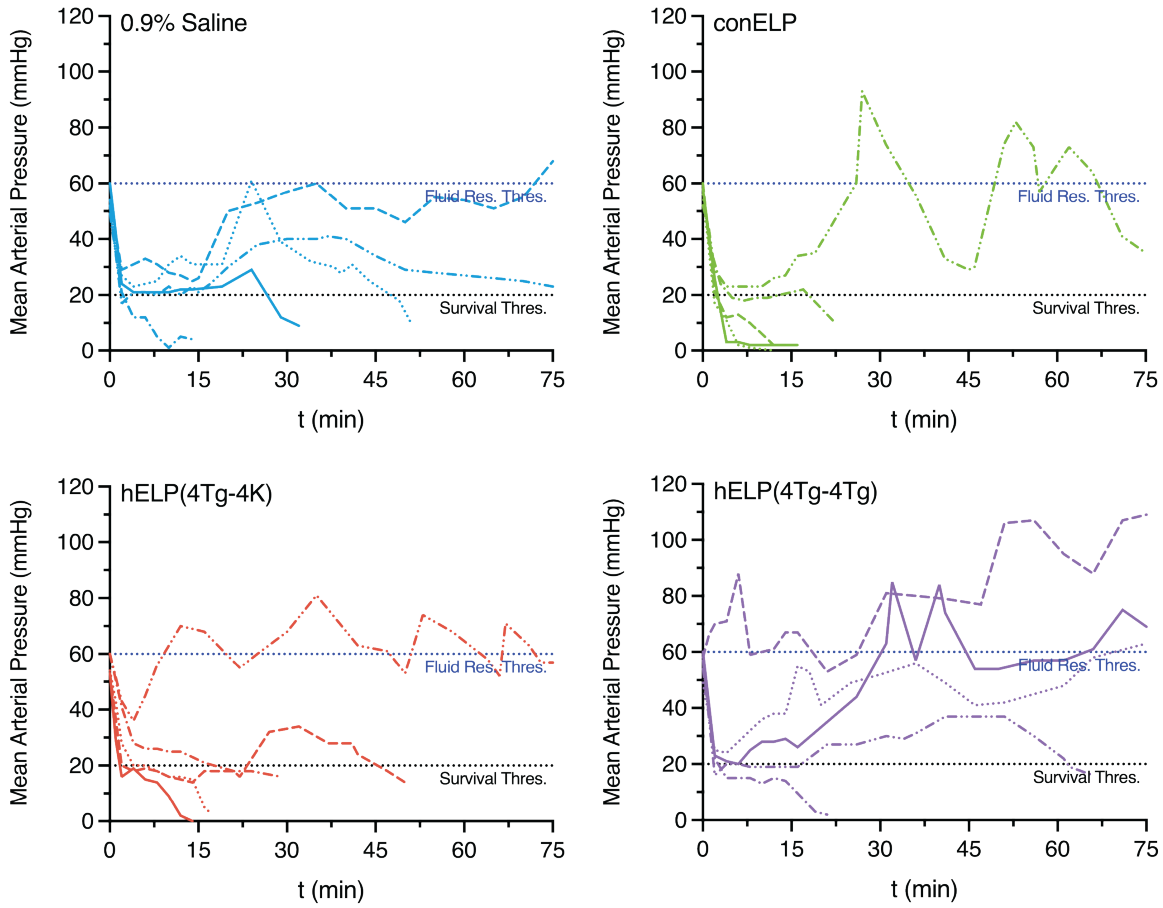

Figure 4-8. Mean arterial pressures (MAPs) of rats in an acute bleeding model, following administration of 30 µM ELP, or a volume control. After an initial 15-minute free-bleed period, fluid resuscitation was undertaken at a rate of 3 mL/kg/min (up to a maximum of 60 mL/kg), in order to raise the MAP of animals above a 60 mm Hg threshold. Animals whose MAP fell below 20 mm Hg prior to 75-minutes were euthanized.

hELP(4Tg-4Tg) treatment group, although one animal that was given hELP(4Tg-4Tg) did not require any fluid resuscitation at all (**Figure 4-8D**). As only one animal from each other treatment group survived the length of the experiment, these were not considered in the analysis.

The results of the rat acute bleeding model suggest that hELP(4Tg-4Tg) had a positive effect on survivability and reduced effects of hemorraghic shock, such as low MAP and low O_2 saturation. Furthermore, hELP(4Tg-4Tg) significantly outperformed hELP(4Tg-4K) in the prevention of re-bleeding events during fluid resuscitation. This reflects the improved ability of hELP(4Tg-4Tg) to mechanically stiffen fibrin clots *in vitro*, and suggests that rheology may be a suitable screening tool for assessing the efficacy of hELPs prior to their application in animal models. Future *in vivo* investigations of hELPs should focus on their biodistribution, in

order to ensure that off-target thrombi are not being formed, and on the relationship between hELP properties (e.g. T_t, length, valency, etc.) and their hemostatic efficacy.

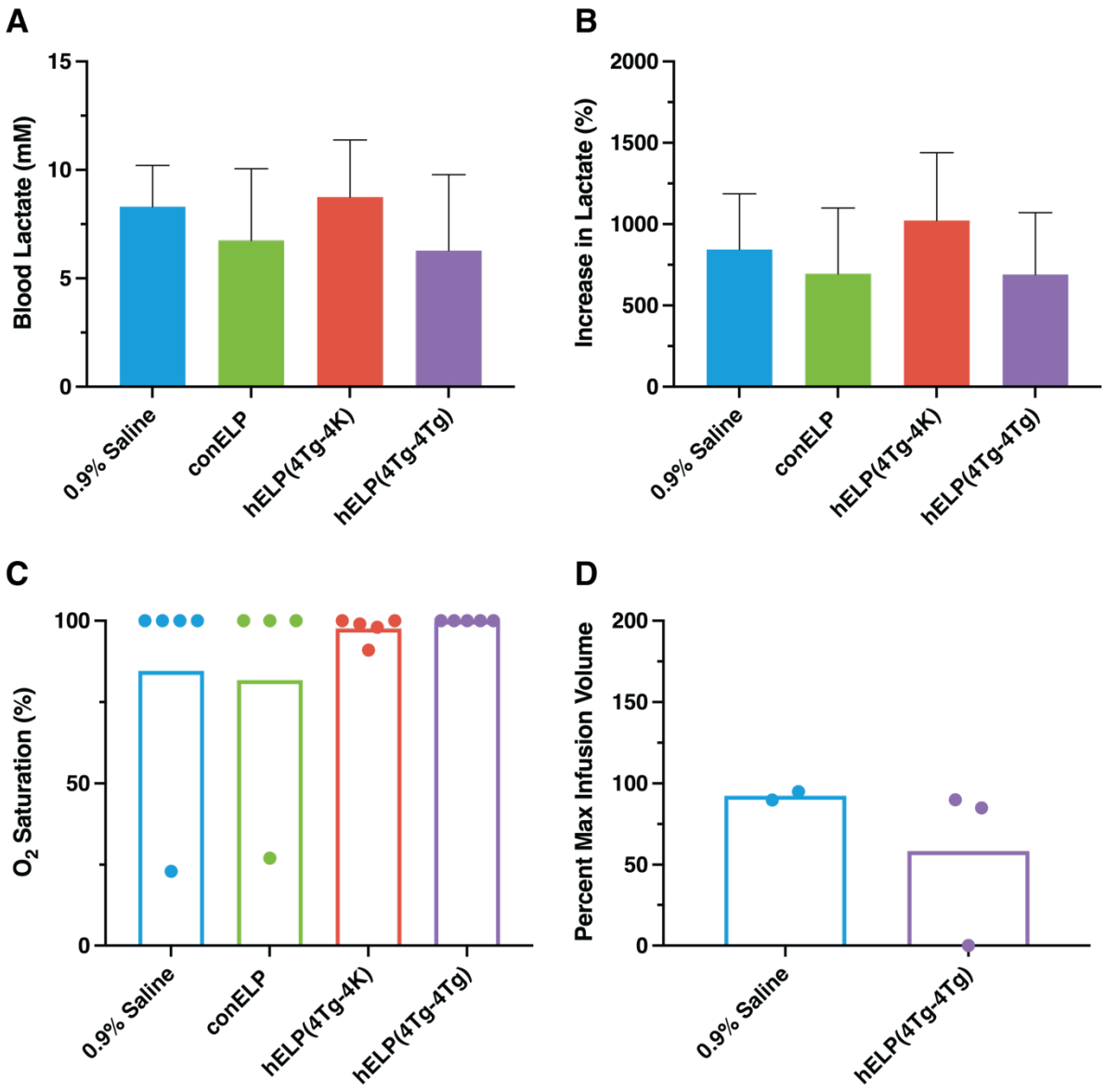

Figure 4-9. Markers of cardiovascular health in rats following femoral artery injury and treatment with 30 µM hELP or a volume control. A) Blood lactate concentration after the initial 15-minute free bleeding period. B) Increase in blood lactate from baseline after the 15-minute free bleed period. C) O_2 saturation in blood after the 15-minute free bleed period. Bars show mean O_2 saturation and symbols represent the O_2 saturation for each individual animal. D) Proportion of the max allowable infusion volume (60 mL/kg) that each animal received. Only animals surviving the full length of the experiment (t = 75 minutes) were considered in the experiment. Bars represent the mean percent max infusion volume, and symbols represent the percent max infusion volume for each animal.

Conclusion

Hemostatic elastin-like polypeptides (hELPs) were shown to improve the biophysical properties of clots *in vitro*. Here, the efficacy of a novel hELP design (hELP(4Tg-4Tg)) having only functional glutamine residues for covalent clot integration through the action of Factor XIII was compared with the previously reported hELP(4Tg-4K) design which contained both functional glutamine and lysine residues. hELP(4Tg-4Tg) was found to outperform hELP(4Tg-4K) in its ability to mechanically stiffen fibrin clots, especially those formed at higher physiological fibrin concentration. In order to see if this *in vitro* result translated to *in vivo* hemostatic efficacy, hELPs were applied in a rat model of acute femoral artery bleeding. hELP(4Tg-4Tg) was found to produce a positive trend in survivability as compared to hELP(4Tg-4K) or controls. In particular, rats treated with hELP(4Tg-4Tg) were better able to withstand fluid resuscitation and to maintain MAPs above baseline. The improved functionality of hELP(4Tg-4Tg) *in vivo* as compared to hELP(4Tg-4K) can be explained by the greater number of glutamine-containing Tg sequences in the former case, allowing for a greater number of cross-links to be formed between hELP(4Tg-4Tg) and fibrin lysine residues. Another explanation has to do with the fact that the T_t of hELP(4Tg-4Tg) is lower than hELP(4Tg-4K), and so hELP(4Tg-4Tg) is more likely to form stable coacervates at physiological temperature. This further highlights coacervation of hELPs as a critical factor in their ability to positively modulate clot properties. Ultimately, these results suggest that there is a large parameter space to be explored in terms of the relationship between hELP properties and their function. Our results set the groundwork for further studies on hELPs using *in vivo* animal models.

Acknowledgements

I would like to acknowledge Andreas Agrafiotis for his assistance in collecting hELP(4Tg-4Tg) *in vitro* data.

References

1. Chan, L. W., White, N. J. & Pun, S. H. Synthetic Strategies for Engineering Intravenous Hemostats. *Bioconjug. Chem.* **26**, 1224–1236 (2015).

2. Varanko, A. K., Su, J. C. & Chilkoti, A. Elastin-Like Polypeptides for Biomedical Applications. *Annu. Rev. Biomed. Eng.* **22**, 343–369 (2020).
3. Urosev, I., Lopez Morales, J. & Nash, M. A. Phase Separation of Intrinsically Disordered Protein Polymers Mechanically Stiffens Fibrin Clots. *Adv. Funct. Mater.* 2005245 (2020). doi:10.1002/adfm.202005245
4. Chan, L. W. *et al.* A synthetic fibrin cross-linking polymer for modulating clot properties and inducing hemostasis. *Sci. Transl. Med.* **7**, 277ra29 (2015).
5. Hickman, D. A., Pawlowski, C. L., Sekhon, U. D. S., Marks, J. & Gupta, A. Sen. Biomaterials and Advanced Technologies for Hemostatic Management of Bleeding. *Adv. Mater.* **30**, 1700859 (2018).
6. Bertram, J. P. *et al.* Intravenous Hemostat: Nanotechnology to Halt Bleeding. *Sci. Transl. Med.* **1**, (2009).
7. Lamm, R. J. *et al.* Peptide valency plays an important role in the activity of a synthetic fibrin-crosslinking polymer. *Biomaterials* **132**, 96–104 (2017).
8. Lamm, R. J. *et al.* Optimizing the Polymer Chemistry and Synthesis Method of PolySTAT, an Injectable Hemostat. *ACS Biomater. Sci. Eng.* **6**, 7011–7020 (2020).
9. Miura, Y. Controlled polymerization for the development of bioconjugate polymers and material. *Journal of Materials Chemistry B* **8**, 2010–2019 (2020).
10. Li, N. K., Quiroz, F. G., Hall, C. K., Chilkoti, A. & Yingling, Y. G. Molecular Description of the LCST Behavior of an Elastin-Like Polypeptide. *Biomacromolecules* **15**, 3522–3530 (2014).
11. Watchorn, E. The normal serum-calcium and magnesium of the rat: their relation to sex and age. *Biochem. J.* **27**, 1875–1878 (1933).
12. Normal Calcium Levels: What is a high calcium level? Normal and High Calcium Level Symptoms, Treatment, Diagnosis - UCLA. Available at: https://www.uclahealth.org/endocrine-center/normal-calcium-levels. (Accessed: 27th April 2021)
13. McDaniel, J. R., Radford, D. C. & Chilkoti, A. A Unified Model for De Novo Design of Elastin-like Polypeptides with Tunable Inverse Transition Temperatures. *Biomacromolecules* **14**, 2866–2872 (2013).
14. Dignon, G. L., Best, R. B. & Mittal, J. Biomolecular Phase Separation: From Molecular Driving Forces to Macroscopic Properties. *Annu. Rev. Phys. Chem.* **71**, 53–75 (2020).

15. Reikvam, H. *et al.* Thrombelastography. *Transfus. Apher. Sci.* **40**, 119–123 (2009).
16. Fries, D. & Martini, W. Z. Role of fibrinogen in trauma-induced coagulopathy. *Br. J. Anaesth.* **105**, 116–121 (2010).
17. Muszbek, L., Bereczky, Z., Bagoly, Z., Komáromi, I. & Katona, É. Factor XIII: A Coagulation Factor With Multiple Plasmatic and Cellular Functions. *Physiol. Rev.* **91**, 931–972 (2011).
18. Sugimura, Y. *et al.* Screening for the Preferred Substrate Sequence of Transglutaminase Using a Phage-displayed Peptide Library. *J. Biol. Chem.* **281**, 17699–17706 (2006).
19. Muszbek, L., Yee, V. C. & Hevessy, Z. Blood coagulation factor XIII: Structure and function. *Thrombosis Research* **94**, 271–305 (1999).
20. Urry, D. W. *et al.* Temperature of Polypeptide Inverse Temperature Transition Depends on Mean Residue Hydrophobicity. *J. Am. Chem. Soc.* **113**, 4346–4348 (1991).
21. Wang, H. *et al.* Covalently Adaptable Elastin-Like Protein-Hyaluronic Acid (ELP-HA) Hybrid Hydrogels with Secondary Thermoresponsive Crosslinking for Injectable Stem Cell Delivery. *Adv. Funct. Mater.* **27**, 1605609 (2017).
22. Brown, A. C. *et al.* Ultrasoft microgels displaying emergent platelet-like behaviours. *Nat. Mater.* **13**, 1108–1114 (2014).
23. John, A. E. & White, N. J. Platelets and Fibrinogen: Emerging Complexity in Trauma-Induced Coagulopathy. *Semin. Thromb. Hemost.* **46**, 125–133 (2020).
24. Chapin, J. C. & Hajjar, K. A. Fibrinolysis and the control of blood coagulation. *Blood Rev.* **29**, 17–24 (2015).
25. Asensio, J. A. *et al.* Reliable variables in the exsanguinated patient which indicate damage control and predict outcome. in *American Journal of Surgery* **182**, 743–751 (Elsevier, 2001).
26. Wang, Y. *et al.* Correction: Comparison of Invasive Blood Pressure Measurements from the Caudal Ventral Artery and the Femoral Artery in Male Adult SD and Wistar Rats. *PLoS One* **8**, (2013).
27. Odom, S. R. *et al.* Lactate clearance as a predictor of mortality in trauma patients. *J. Trauma Acute Care Surg.* **74**, 999–1004 (2013).
28. Chatrath, V., Khetarpal, R. & Ahuja, J. Fluid management in patients with trauma: Restrictive versus liberal approach. *Journal of Anaesthesiology Clinical Pharmacology*

31, 308–316 (2015).

Appendix

Table 4A-1. hELP(4Tg-4Tg) sequence

ELP	Sequence
hELP: ELP($A_2V_8E_1$-Tgf11)$_4$-($A_2V_8E_1$)$_4$-($A_2V_8E_1$-Tgf11)$_4$	MGHGVGVPGVGVPGAGVPGVGVPGVGVPGVGVPGVGVPGVGVPGVGVPG VGVPGEGVPGAGSGDQMMLPWPAVALSGVPGVGVPGVGVPGAGVPGVGV PGVGVPGVGVPGVGVPGVGVPGVGVPGVGVPGEGVPGAGSGDQMMLPWP AVALSGVPGVGVPGVGVPGAGVPGVGVPGVGVPGVGVPGVGVPGVGVPGV GVPGVGVPGEGVPGAGSGDQMMLPWPAVALSGVPGVGVPGVGVPGAGVP GVGVPGVGVPGVGVPGVGVPGVGVPGVGVPGVGVPGEGVPGAGSGDQM MLPWPAVALSGVPGVGVPGVGVPGAGVPGVGVPGVGVPGVGVPGVGVPGV GVPGVGVPGVGVPGEGVPGAGVPGVGVPGVGVPGAGVPGVGVPGVGVPGV GVPGVGVPGVGVPGVGVPGVGVPGEGVPGAGVPGVGVPGVGVPGAGVPGV GVPGVGVPGVGVPGVGVPGVGVPGVGVPGVGVPGEGVPGAGVPGVGVPGV GVPGAGVPGVGVPGVGVPGVGVPGVGVPGVGVPGVGVPGVGVPGEGVPGA GVPGVGVPGVGVPGAGVPGVGVPGVGVPGVGVPGVGVPGVGVPGVGVPG VGVPGEGVPGAGSGDQMMLPWPAVALSGVPGVGVPGVGVPGAGVPGVGV PGVGVPGVGVPGVGVPGVGVPGVGVPGVGVPGEGVPGAGSGDQMMLPWP AVALSGVPGVGVPGVGVPGAGVPGVGVPGVGVPGVGVPGVGVPGVGVPGV GVPGVGVPGEGVPGAGSGDQMMLPWPAVALSGVPGVGVPGVGVPGAGVP GVGVPGVGVPGVGVPGVGVPGVGVPGVGVPGVGVPGEGVPGAGSGDQM MLPWPAVALSGVPGWLDSLEFIA

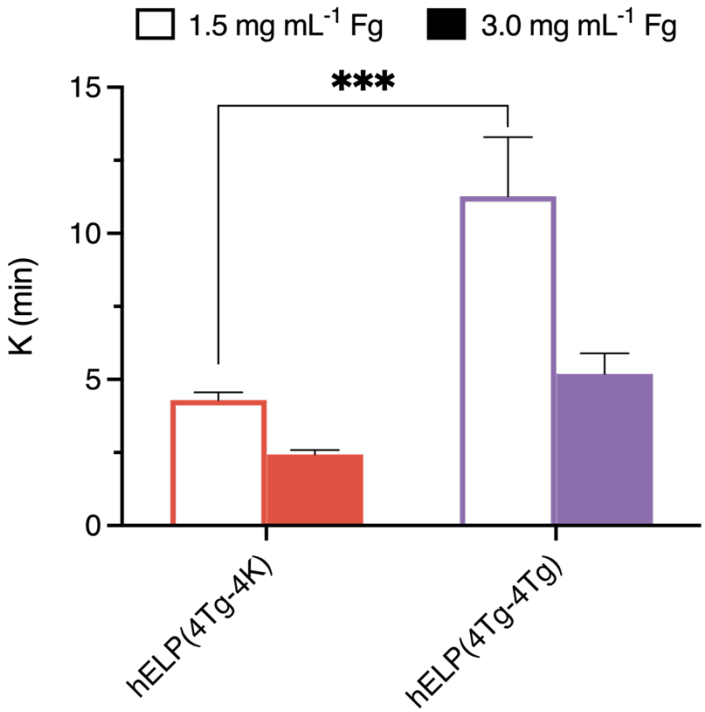

Figure 4A-1. K values from thromboelastography of fibrin clots with 30 µM hELP(4Tg-4K) or hELP(4Tg-4Tg). K is a measure of the time from 2 to 20 mm pin displacement and reflects the rate of clot formation

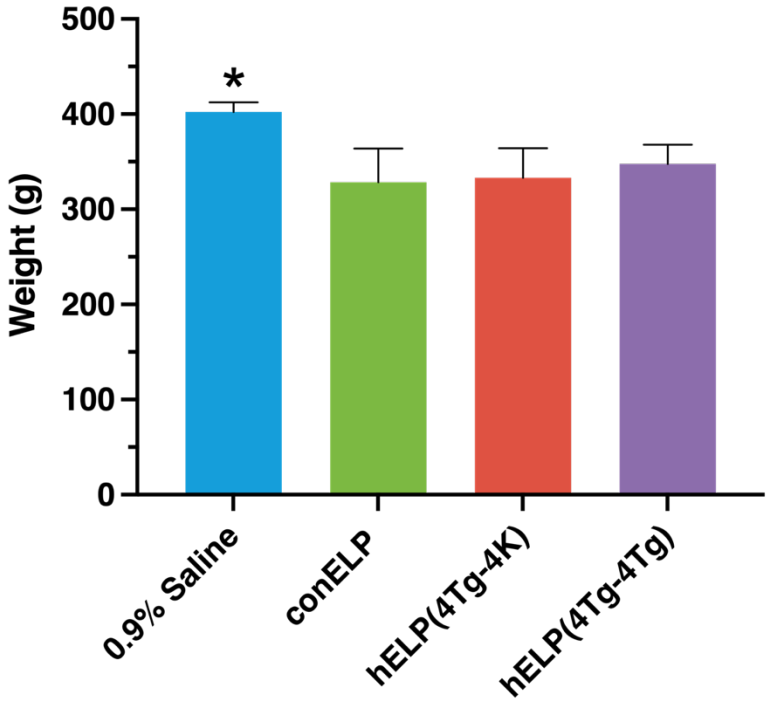

Figure 4A-2. Average body weights of rats in each treatment group of an acute bleeding model (n = 5).

Chapter V: Conclusions & Outlook

In the last decade, liquid-liquid phase separation (LLPS) of proteins has been established as a fundamental principle in the organization of cellular biochemistry, much like the lipid membrane or the transmembrane pore.[1] LLPS is now implicated in diverse processes such as signal transduction, RNA processing, repair of DNA damage, and ribosome biogenesis, among many others, and aberrations in this process are believed to play a significant role in the development of a variety of pathologies.[2,3] Clearly, phase separation is no longer simply the purview of synthetic polymers. And while there has been an explosion in the number of papers describing fundamental biological aspects of this phenomenon in recent years, there has also been a growing interest in investigating protein phase separation both as a therapeutic tool and a therapeutic target.[4] The aim of the work described in this thesis, was the application of a particular class of phase separating, intrinsically disordered proteins – elastin-like polypeptides (ELPs) – as hemostatic agents for the treatment of uncontrolled bleeding. ELPs represent some of the earliest known and most well studied intrinsically disordered proteins, and since their derivation from the hydrophobic regions of human tropoelastin more than 30 years ago, they have been used for a number of biomedical applications.[5] These applications include physically or chemically cross-linked hydrogels for tissue engineering, nanoparticles for drug delivery, or as space-filling gels to repair cartilage defects, among many others.[6] Where the current work differs from these previous technologies, is that it sought to use the phase separation of hemostatic elastin-like polypeptides (hELPs) not only for the self-assembly of therapeutics with various higher order structures, but also to directly improve the biophysical properties of a biological hydrogel – namely, blood clots – through the formation of a secondary network of physically cross-linked ELPs. Such a system has heretofore only been described *in vitro,* with ECM components that had been modified to include biorthogonal functional groups.[7] Successful application of hELPs in this capacity, in addition to yielding a potential intravenous hemostat, also suggests phase separation of proteins as a viable intervention for improving the biophysical properties of ECM that has developed substandard mechanical properties, due to injury or disease.

The design goals for hELPs that were set-out at the beginning of this work included phase separation under physiological conditions of temperature and ionic strength, selective integration into fibrin clots only at the site of injury, and improvement of the biophysical and hemostatic properties of clots upon integration. Chapter III describes the *in vitro* analysis of the first functional hELP, hELP(4Tg-4K), for its ability to meet these criteria. Specificity of binding was achieved by embedding glutamine residues in contextual sequences ("Tg" sequences) that were recognized with high specificity by the clotting associated transglutaminase, Factor XIII, which is activated following injury to the vasculature, and which is rapidly degraded in the bloodstream following clotting.[8] Lysine residues were added at the C-terminal end of this hELP, in order to allow for cross-linking of hELPs to fibrin glutamine residues, and to provide the potential for the stabilization of hELP coacervates through homologous covalent cross-linking. SDS-PAGE studies of hELP(4Tg-4K) showed that the glutamine and lysine residues of this protein could be cross-linked in the presence of FXIIIa, and that this was not the case for a control ELP (conELP) lacking those residues. hELP(4Tg-4K) was found to have a transition temperature below physiological temperature, and would therefore form coacervates at 37 ˚C. Integration of hELPs into fibrin clots was confirmed through confocal microscopy and SEM, which showed that hELP coacervates were distributed along fibrin fibres, while conELP coacervates were not similarly co-localized. This lent further support to the conclusion that covalent cross-linking of hELPs to fibrin networks by FXIIIa was necessary for the integration of hELPs into clots. Rheological studies showed that hELP(4Tg-4K) coacervates could rescue the mechanical properties of clots formed under dilutive conditions of simulated coagulopathy, as well as improve the mechanical properties of clots formed with normal physiological fibrinogen concentrations. Critically, this effect was only observed above the phase transition temperature of hELPs, indicating that aggregation of hELPs was necessary for their ability to improve clot mechanical properties. Integration of hELPs into clots also increased the rate at which they formed following the initiation of clotting, decreased the rate of clot plasmolysis, and decreased clot pore sizes, therefore decreasing their permeability to fluid flow. Furthermore, hELPs were found to be non-cytotoxic, although migration of human fibroblasts was inhibited in fibrin-hELP clots. Together, these results indicate that hELPs were able to improve the biophysical and functional properties of clots *in vitro*, and that the phase separation of proteins that are

covalently bound to fibrin is a potentially effective mechanism for the design of an intravenous hemostat.

The aim of the work presented in chapter IV was to validate hELPs as hemostats in an *in vivo* rat model of acute bleeding, and to investigate alternative hELP designs for potentially improved hemostatic efficacy. The new design described in this chapter, hELP(4Tg-4Tg), differed from the hELP(4Tg-4K) design described in the previous chapter, in that glutamine-containing Tg tags were included at both ends of the protein, replacing C-terminal lysine residues. The rationale for this updated design was based on the fact that FXIIIa is less selective for the lysine partner in the acyl transfer reaction that it catalyzes, and so it was hypothesized that removing lysine residues would increase the specificity of hELP integration into fibrin.[9] Furthermore, lysine residues on fibrin provide binding sites for plasminolysis-associated proteins and thereby increase the rate of fibrin degradation following clotting, and it was therefore a concern that hELP(4Tg-4K) might lead to an increase in plasminolysis *in vivo*.[10] Thromboelastography studies indicated that hELP(4Tg-4Tg) was able to improve clot mechanical properties to a similar degree as hELP(4Tg-4K), although the former hELP did not increase the rate of clot formation to the same extent as the latter. Rheological investigations showed that at higher fibrinogen concentrations, hELP(4Tg-4Tg) improved the mechanical stiffness of clots more than twice as much as hELP(4Tg-4K). This *in vitro* improvement seemed to translate to an improved efficacy in the rat model of acute femoral artery bleeding. The greatest number of survivors over the time course of the experiment were in the group treated with hELP(4Tg-4Tg), although there were no statistically significant differences in survival between treatment groups and controls as determined by a log-rank Mantel Cox test ($P = 0.2407$). However, all animals treated with hELP(4Tg-4Tg) did survive the initial 15-minute free bleed period of the experiment, which was not the case in any other group. Furthermore, all animals surviving in the hELP(4Tg-4Tg) treatment group finished the experiment with mean arterial pressures above baseline, which was also not the case for any other group. Animals treated with hELP(4Tg-4Tg) experienced fewer re-bleeding events than those treated with hELP(4Tg-4K) during fluid resuscitation. The results of the *in vivo* study described in chapter IV indicate that hELP(4Tg-4Tg) did indeed outperform hELP(4Tg-4K), suggesting that *in vitro* rheological analysis of hELP-fibrin clots may be a valid screening method for optimizing hELP designs. Furthermore, although significant differences in survival were not observed between treatment and control groups over the course of the experiment, positive results in survival

prior to 15 minutes, maintenance of mean arterial pressure, and the stability of clots during fluid resuscitation following treatment with hELP(4Tg-4Tg), provide a rationale for the further application and optimization of hELPs using animal models.

Outlook

The future development of hELP technology should proceed along parallel paths. The first path should focus on the development of hELPs for commercialization and clinical application. This work has demonstrated that hELPs can function as hemostats, that potentially address the challenges of safety and specificity that have led to a dearth of hemostatic agents that can be administered intravenously.[11] HELPs are particularly attractive for this application because they address some of the shortfalls that are associated with the current standard of care for uncontrolled bleeding from non-compressible injuries – transfusion of blood products – and with other intravenous hemostats that have been described in the literature. Firstly, they can be expressed easily in E. Coli, and purified using bulk processing methods that can easily be scaled up from a laboratory to an industrial scale; as such, it should be possible to produce them at relatively low cost compared to other biological therapeutics (which must often be expressed using eukaryotic systems), or other intravenous hemostats such as polySTAT (which require the production of costly synthetic peptides).[12–14] Secondly, hELPs (like other ELPs) are biocompatible and should be easily degradable by proteinases, reducing the potential for their harmful accumulation *in vivo*.[15] And lastly, hELPs should be stable when lyophilized and stored under ambient conditions for extended periods of time, allowing them to be applied in the field, or in clinics without sophisticated long-term storage facilities.[16] Many of these features also make hELPs attractive for use in topical fibrin-based hemostats, such as fibrin glues or fibrin-coated bandages, as they could supplement the mechanical stability of those materials and thereby reduce the amount of fibrin/fibrinogen required to make those therapies effective.[17]

The second path of hELP development should explore the large parameter space available in the design of hELPs, with the aim of optimizing the hemostatic efficacy of this technology. Tunable characteristics of hELPs include their length, valency (i.e. number of Tg sequences), and hydrophobicity; given the novelty of this type of hemostatic technology, the relationship between these characteristics and hELP functionality is not yet completely

understood. However, results from chapter IV do suggest that increased hydrophobicity may translate to improved efficacy, as hELP(4Tg-4Tg) has a lower transition temperature than hELP(4Tg-4K). Additionally, the architecture of hELP self-assembly can also be modulated. In their current iteration hELPs likely form bulk coacervates above their transition temperatures, but by changing the hELP backbone to include blocks with guest residues of different hydrophobicities, it should be possible to induce hELPs to form more ordered structures, such as micelles.[18,19]

Outside of their development as hemostatic agents, fibrin-hELP clots can also be applied as a scaffold material for tissue engineering or void filling applications. Fibrin gels are currently used for applications such as drug delivery, cartilaginous tissue repair, or the *in vitro* growth of muscle cells.[20–22] HELPs can be used to improve the mechanical stability of these materials without increasing the amount of fibrinogen that they require, or to otherwise modulate their properties. Additionally, hELPs could be functionalized post-expression to introduce orthogonal functional groups into fibrin networks, or to deliver molecules such as growth factors, significantly expanding the chemical diversity of fibrin gels.

From a broader perspective, hELPs represent a proof-of-concept for the use of phase separation of intrinsically disordered proteins in the treatment of ECM and tissue disorders arising from substandard mechanical properties. By simply replacing Tg tags with peptide sequences that target other ECM components, or by specifically delivering this material through, for example, direct injection into tissues, it may be possible to greatly expand the possible applications of this technology.

References

1. Banani, S. F., Lee, H. O., Hyman, A. A. & Rosen, M. K. Biomolecular condensates: Organizers of cellular biochemistry. *Nature Reviews Molecular Cell Biology* **18**, 285–298 (2017).
2. Alberti, S. Phase separation in biology. *Current Biology* **27**, R1097–R1102 (2017).
3. Shin, Y. & Brangwynne, C. P. Liquid phase condensation in cell physiology and disease. *Science* **357**, (2017).
4. Patel, A. *et al.* A Liquid-to-Solid Phase Transition of the ALS Protein FUS Accelerated by Disease Mutation. *Cell* **162**, 1066–1077 (2015).

5. Urry, D. W., Haynes, B. & Harris, R. D. Temperature dependence of length of elastin and its polypentapeptide. *Biochem. Biophys. Res. Commun.* **141**, 749–755 (1986).
6. Varanko, A. K., Su, J. C. & Chilkoti, A. Elastin-Like Polypeptides for Biomedical Applications. *Annu. Rev. Biomed. Eng.* **22**, 343–369 (2020).
7. Wang, H. *et al.* Covalently Adaptable Elastin-Like Protein-Hyaluronic Acid (ELP-HA) Hybrid Hydrogels with Secondary Thermoresponsive Crosslinking for Injectable Stem Cell Delivery. *Adv. Funct. Mater.* **27**, 1605609 (2017).
8. Muszbek, L., Bereczky, Z., Bagoly, Z., Komáromi, I. & Katona, É. Factor XIII: A Coagulation Factor With Multiple Plasmatic and Cellular Functions. *Physiol. Rev.* **91**, 931–972 (2011).
9. Sugimura, Y. *et al.* Screening for the Preferred Substrate Sequence of Transglutaminase Using a Phage-displayed Peptide Library. *J. Biol. Chem.* **281**, 17699–17706 (2006).
10. Cesarman-Maus, G. & Hajjar, K. A. Molecular mechanisms of fibrinolysis. *Br. J. Haematol.* **129**, 307–321 (2005).
11. Chan, L. W., White, N. J. & Pun, S. H. Synthetic Strategies for Engineering Intravenous Hemostats. *Bioconjug. Chem.* **26**, 1224–1236 (2015).
12. Almo, S. C. & Love, J. D. Better and faster: Improvements and optimization for mammalian recombinant protein production. *Current Opinion in Structural Biology* **26**, 39–43 (2014).
13. Chen, R. Bacterial expression systems for recombinant protein production: E. coli and beyond. *Biotechnol. Adv.* **30**, 1102–1107 (2012).
14. Lamm, R. J. *et al.* Optimizing the Polymer Chemistry and Synthesis Method of PolySTAT, an Injectable Hemostat. *ACS Biomater. Sci. Eng.* **6**, 7011–7020 (2020).
15. Liu, W. E. *et al.* Tumor accumulation, degradation and pharmacokinetics of elastin-like polypeptides in nude mice. *J. Control. Release* **116**, 170–178 (2006).
16. Zhang, Y. N. *et al.* A Highly Elastic and Rapidly Crosslinkable Elastin-Like Polypeptide-Based Hydrogel for Biomedical Applications. *Adv. Funct. Mater.* **25**, 4814–4826 (2015).
17. Tompeck, A. J. *et al.* A comprehensive review of topical hemostatic agents: The good, the bad, and the novel. *Journal of Trauma and Acute Care Surgery* **88**, E1–E21 (2020).
18. McDaniel, J. R., Callahan, D. J. & Chilkoti, A. Drug delivery to solid tumors by elastin-

like polypeptides. *Advanced Drug Delivery Reviews* **62**, 1456–1467 (2010).

19. Janib, S. M. *et al.* A quantitative recipe for engineering protein polymer nanoparticles. *Polym. Chem.* **5**, 1614–1625 (2014).
20. Huang, Y. C., Dennis, R. G., Larkin, L. & Baar, K. Rapid formation of functional muscle in vitro using fibrin gels. *J. Appl. Physiol.* **98**, 706–713 (2005).
21. Eyrich, D. *et al.* Long-term stable fibrin gels for cartilage engineering. *Biomaterials* **28**, 55–65 (2007).
22. Janmey, P. A., Winer, J. P. & Weisel, J. W. Fibrin gels and their clinical and bioengineering applications. *Journal of the Royal Society Interface* **6**, 1–10 (2009).

IVAN UROSEV

Vogesenstrasse 69, 4056 Basel, CH | +41786675221 | iurosev527@gmail.com

Profile

Scientist with 6+ years of academic and industrial research experience, with a particular focus in molecular biology, protein engineering, and polymer chemistry. Lead the successful development of patentable therapeutic proteins for the clinical management of bleeding. Looking for opportunities to develop further in the field of biotechnology, and to work on projects that can impact patients in the clinic or aid researchers in the lab.

Technical Expertise

Molecular Biology

- Restriction cloning, PCR, Protein engineering, Gibson Assembly, Recombinant protein expression in E. Coli, Protein purification, Lyophilization of proteins, Relevant software (i.e. Snapgene, PyMol)

Polymer Chemistry

- Synthesis of natural and synthetic polymers, RAFT polymerization, GPC, NMR, IR, Mass spectrometry, DLS, synthesis of small molecule monomers

Other Key Expertise

- Mammalian cell culture (2D and 3D; human and mouse cell lines), Hematology, Coagulation, Confocal microscopy, Rheology, Scripting in MATLAB, Microsoft Office, GraphPad Prism, Adobe Illustrator, Manuscript preparation
- Strong communication skills (written/verbal), English (Native), German (B2), Serbian (Fluent)

Research Experience

Research Assistant & PhD Student | *UNIVERSITY OF BASEL AND ETH ZURICH, BASEL, SWITZERLAND* | May 2017 – Jul. 2021

- Engineered the first "smart" hemostatic intrinsically disordered proteins that could be delivered intravenously, were able to selectively integrate into blood clots, and which improved clot properties
- Lead this project from initial conception and design, through to hemostat production, in vitro characterization of hemostatic properties, investigation in 2D and 3D human cell cultures, and successful application in rat models of acute bleeding
- Submitted a patent on this technology, and received a Unitectra Proof-of-Concept grant (valued at 50 000 CHF) for its development and commercialization

Research Associate | Accucaps Inc., Strathroy, ON, Canada | May 2016 – Dec. 2016

- 6-month contract position with industrial producer of gel capsules for drug delivery
- Developed heuristics for predicting capsule properties based on rheological investigations of precursor materials
- Familiarized with concepts of GMP, industrial pharmaceutical production

Research Assistant & Master's Student | *McMaster University, Hamilton, ON, Canada* | Jan 2014 – May. 2016

- Completed this research-based Master's degree (involving 2+ years of in-lab work) with two first-author publications
- Developed a controlled radical polymerization method for the synthesis of "smart" synthetic polymers, which could be used to form hydrogels for tissue engineering and drug delivery applications
- Managed the laboratories mammalian cell culture facilities

Community-building Experience

Board Member | PhD Chemistry Community, *University of Basel* | Apr. 2018 – Jan. 2020

- Assisted in organizing outreach and social events for graduate students in the Department of Chemistry, such as intradepartmental seminars, ski weekends, and the annual summer party
- Chaired and assisted in organizing the departmental Christmas Symposium, with invited speakers from research institutions across Europe

Social Chair | Laboratory for Molecular Engineering of Synthetic Systems, *University of Basel* | Jan. 2018 – Jul. 2021

- Organized team-building events, such as hikes, trivia nights, an annual ping pong tournament, and the annual Christmas dinner

Education

PhD in Chemistry (Molecular Biology and Protein Engineering Focus) | May 2017 – Jul. 2021 | University of Basel, Basel, Switzerland

- Conducted in the laboratory of Prof. Dr. Michael A. Nash in the Department of Chemistry, and ETH Zurich, Department of Biosystems Science and Engineering

Master's in Biomedical Engineering | Jan. 2014 - May 2016 | McMaster University, Hamilton, ON, Canada

- Conducted in the laboratory of Prof. Dr. Todd R. Hoare in the Department of Chemical Engineering
- Won the School of Graduate Studies Entrance Scholarship (valued at $2000)

Bachelor's in Biology and Physiology | Sep. 2009 – Apr. 2013 | Western University, London, ON, Canada

- Achieved Dean's List Honours in the final year of study (grade average above 80%)

Publications & Patents

- **Ivan Urosev**, Joanan Lopez Morales, and Michael A. Nash. Phase Separation of Intrinsically Disordered Protein Polymers Mechanically Stiffens Fibrin Clots. *Advanced Functional Materials* 2020, 30 (51), 2005245.
- **Ivan Urosev** and Michael A. Nash (2020). Hemostatic Elastin-Like Polypeptides (European Patent Application No. 20191629.3). *European Patent Office*.

- **Ivan Urosev**, Helen Dorrington, Nicola Muzzin, Richard Alsop, Emilia Bakaic, Trevor Gilbert, Maikel Rheinstädter, and Todd Hoare. Injectable Poly(oligoethylene glycol methacrylate)-Based Hydrogels Fabricated from Highly Branched Precursor Polymers: Controlling Gel Properties by Precursor Polymer Morphology. *ACS Applied Polymer Materials* 2019, 1 (3), 369 – 380.
- Xudong Deng, Rana Attalla, Lukas P. Sadowski, Mengsu Chen, Michael J. Majcher, **Ivan Urosev**, Da-Chuan Yi, P. Ravi Selvaganapathy, Carlos D. M. Filipe, and Todd Hoare. Autonomously Self-Adhesive Hydrogels as Building Blocks for Additive Manufacturing. *Biomacromolecules* 2018, 19 (1), 62 – 70.
- **Ivan Urosev**, Emilia Bakaic, Richard Alsop, Maikel Rheinstädter, and Todd Hoare. Tuning the properties of injectable poly(Oligoethylene glycol methacrylate) hydrogels by controlling precursor polymer molecular weight. *Journal of Materials Chemistry B* 2016, 4, 6541 – 6551

Other Interests

- Neurology, astronomy, behavioural biology, physics, RNAi & CRISPR-Cas9
- Climbing, snowboarding, travel, music, reading

References

- Prof. Dr. Michael A. Nash, Assistant Professor, University of Basel, Department of Chemistry & ETH Zurich, Department of Biosystems Science and Engineering
  BPR 1096 / Mattenstrasse 24a, 4058 Basel, Switzerland
  michael.nash@unibas.ch | +41 61 207 38 44

- Dr. Rosario Vanella, Senior Scientist, University of Basel, Department of Chemistry & ETH Zurich, Department of Biosystems Science and Engineering
  BPR 1096 / Mattenstrasse 24a, 4058 Basel, Switzerland
  r.vanella@unibas.ch | +41 61 207 59 60

- Prof. Dr. Todd R. Hoare, Professor, McMaster University, Department of Chemical Engineering
  1280 Main St. W., Hamilton, ON, Canada, L8S 4L7
  hoaretr@mcmaster.ca | +1 905 912 03 69